VOLUME 3 (1957) No. 4

NUCLEAR PHYSICS

MONTHLY JOURNAL DEVOTED TO THE EXPERIMENTAL AND THEORETICAL STUDY OF ATOMIC NUCLEI, NUCLEAR FIELDS AND THE FUNDAMENTAL ASPECTS OF COSMIC RADIATION

EDITOR: L. ROSENFELD - MANCHESTER

G. ANDERSSON, P. A. TOVE, B. JUNG and I. B. SVENSSON, The isomeric transitions Tl^{197} and Tl^{195} 493

G. ANDERSSON and I. BERGSTRÖM, Note on the decay of Tl^{198m} 506

J. A. MCDONELL, R. STOCKENDAL, C. J. HERRLANDER and I. BERGSTRÖM, Levels in Pb^{202} and Tl^{202} populated from 3.62-h Pb^{202m} 513

G. ANDERSSON and I. BERGSTRÖM, Anomalous internal conversion ratios of E3 transitions in the region $Z=77$—82 541

L. G. ZASTAVENKO, A. L. LIUBIMOV, V. I. OGIEVITSKY and M. I. PODGORETSKY, On a possibility of k-meson investigation 549

E. M. BOWEY, Isotopic assignment of slow neutron resonances in germanium, rubidium, neodymium and tungsten 553

F. J. M. FARLEY and R. E. WHITE, Neutron alpha particle angular correlation in the reaction $^7Li(d,\alpha)$ and the ground state of ^5He 561

E. D. KLEMA and R. K. OSBORN, Empirical determination of nuclear shape factors and moments of inertia. 571

H. KOPPE, Zur Theorie der β-Wechselwirkung 585

A. PETERMANN, Invariance properties and identities between renormalization constants 592

S. ONEDA, Two-component theory of the neutrino and K-meson decays comprising two neutrinos 598

J. C. TAYLOR, Space-time reflections and isobaric spin 606

K. WILDERMUTH and K. BAUMANN, Some remarks on self-acceleration and similar effects in quantum field theory 612

Book Reviews 624

NORTH-HOLLAND PUBLISHING COMPANY - AMSTERDAM

June 1957

EDITORIAL BOARD

AUSTRIA:	B. Karlik (Vienna), H. Thirring (Vienna)
BELGIUM:	M. de Hemptinne (Louvain), J. Verhaeghe (Ghent)
CANADA:	G. Volkoff (Vancouver)
DENMARK:	C. Møller (Copenhagen), S. Rozental (Copenhagen)
EGYPT & ARAB COUNTRIES:	F. El Bedewi (Alexandria), M. G. Nooh (Cairo)
FINLAND:	L. Simons (Helsinki)
FRANCE	A. Berthelot (Saclay), S. Gorodetzky (Strasbourg), F. Joliot (Paris)
GERMANY (FED. REP.):	W. Gentner (Freiburg i. B.), J. H. D. Jensen (Heidelberg)
GERMANY (DEM. REP.):	G. Hertz (Leipzig)
GREAT BRITAIN:	S. Devons (Manchester)
HUNGARY:	L. Janossy (Budapest)
INDIA:	H. Bhabha (Bombay), B. Peters (Bombay), R. Ramanna (Trombay)
IRISH REPUBLIC:	J. McConnell (Maynooth)
ISRAEL:	G. Racah (Jerusalem)
ITALY:	E. Amaldi (Rome)
JAPAN:	S. Kikuchi (Tokyo), S. Tomonaga (Tokyo)
NETHERLANDS:	H. Brinkman (Groningen), S. R. de Groot (Leiden)
NORWAY:	E. Hylleraas (Oslo), A. Lundby (Oslo), H. Wergeland (Trondheim)
POLAND:	L. Infeld (Warsaw)
PORTUGAL:	J. M. Araújo (Porto), J. R. de Almeida Santos (Coimbra)
SOUTH AMERICA:	G. Beck (Saõ Paulo), J. Leite Lopes (Rio de Janeiro)
SPAIN:	J. M. Otero (Madrid), C. Sanchez del Rio (Madrid)
SWEDEN:	O. Klein (Stockholm), K. Siegbahn (Uppsala), I. Waller (Uppsala)
SWITZERLAND:	P. Huber (Basel), P. Scherrer (Zürich)
U.S.S.R.:	M. A. Markov (Moscow), I. S. Shapiro (Moscow), D. V. Skobeltzyn (Moscow)
YUGOSLAVIA:	I. Supek (Zagreb)
U.S.A. & MEXICO:	V. Weisskopf (Cambridge, Mass.)
AUSTRALIA & NEW ZEALAND:	H. Messel (Sydney), M. L. Oliphant (Canberra)

CONTRIBUTIONS may be sent to the Editor, Professor L. Rosenfeld, Dept. of Theoretical Physics, The University, Manchester, either directly, or preferably through the intermediary of one of the members of the Editorial Board of the country or region in which the author is working. They may be written in English, French or German.

NUCLEAR PHYSICS is published in monthly issues. The subscription price is fl 57.00; 114s; $ 15.00. Postfree.

SUBSCRIPTIONS should be sent to the publishers, **NORTH-HOLLAND PUBLISHING COMPANY**, P.O.Box 103, Amsterdam or to any subscription-agent. Subscriptions for U.S.A. are to be sent exclusively to **INTERSCIENCE PUBLISHERS, INC.**, 250 Fifth Avenue, New York 1, N.Y.

BOOKS FOR REVIEW should be sent to Professor Rosenfeld.

No part of this issue may be reproduced in any form, by print, photoprint, microfilm or any other means without written permission from the publisher. Reprints, photoprints or microfilms are obtainable at cost from the publisher.

Printed in the Netherlands

Nuclear Physics **3** (1957) 493—505; *North-Holland Publishing Co., Amsterdam*

THE ISOMERIC TRANSITIONS IN Tl^{197} AND Tl^{195}

G. ANDERSSON, P. A. TOVE, B. JUNG AND I. B. SVENSSON
The Gustaf Werner Institute for Nuclear Chemistry, University of Uppsala, Uppsala

Received 22 February 1957

Abstract: Internal conversion electrons from the isomeric transitions in Tl^{197} and Tl^{195} have been studied in high resolution β-spectrometers. The intensity ratios of the lines, when compared with recent theoretical values, were found to confirm the multipole assignment E3 for both transitions. The γ-energies were established as 222.45 ± 0.05 keV (Tl^{197m}) and 99.1 ± 0.1 keV (Tl^{195m}).

The half-lives of Tl^{197m} and Tl^{195m} have been measured as 0.55 ± 0.10 sec and 3.5 ± 0.4 sec, respectively, using rapid chemical techniques and a multichannel method of time analysis. Pulse height spectra of the short-lived activities were found to support the mass assignments.

1. Introduction

E3 transitions between the proton levels $h_{11/2}$ and $d_{5/2}$ may be expected to cause isomerism in odd-Z, even-N nuclei near the 82 proton shell closure. Isomers of this type are known to exist in Au^{197}, Au^{195}, Au^{193} [1]), and Ir^{191} [2]). In a recent communication from this institute [3]) the probable discovery of isomeric transitions also in Tl^{197} and Tl^{195} was announced.

The $K/\Sigma L$ conversion ratio of a 222 keV γ-ray, appearing in the decay of 42 min Pb^{197m} and converted in Tl, clearly indicated the multipole order E3 when compared with the value obtained from Rose's tables [4]). The experimentally found $(L_I + L_{II})/L_{III}$ ratio, however, was considerably smaller than expected. For the corresponding transition in Tl^{195}, where the low γ-ray energy — 99 keV — prevented the K line from being detected, the assignment E3 was mainly based on a similar reduction of $(L_I + L_{II})/L_{III}$ relative to the calculated value. These anomalous conversion intensities called for improved measurements of the electron spectra.

Further a determination of the half-lives was needed in order to establish the isomers more firmly. In fact, a 0.54 sec period had earlier been assigned to a 384 keV γ-ray in Tl^{197m} [5]). This was not quite contradictory to the findings reported in reference [3]), as 385 keV and 387 keV transitions of lower multipolarities had been shown to follow in cascade after the 222 keV γ-ray (cf. fig. 7). It remained to be proved, however, that the 0.54 sec half-life was characteristic also of the last-mentioned transition.

2. β-spectrometer Measurements

2.1. THE NUCLEUS Tl^{197m}

The K and L conversion lines of the 222 keV γ-ray in Tl^{197} were investigated in the ironfree double-focusing β-spectrometer [6]) of the Physics Department of this University.

June 1957

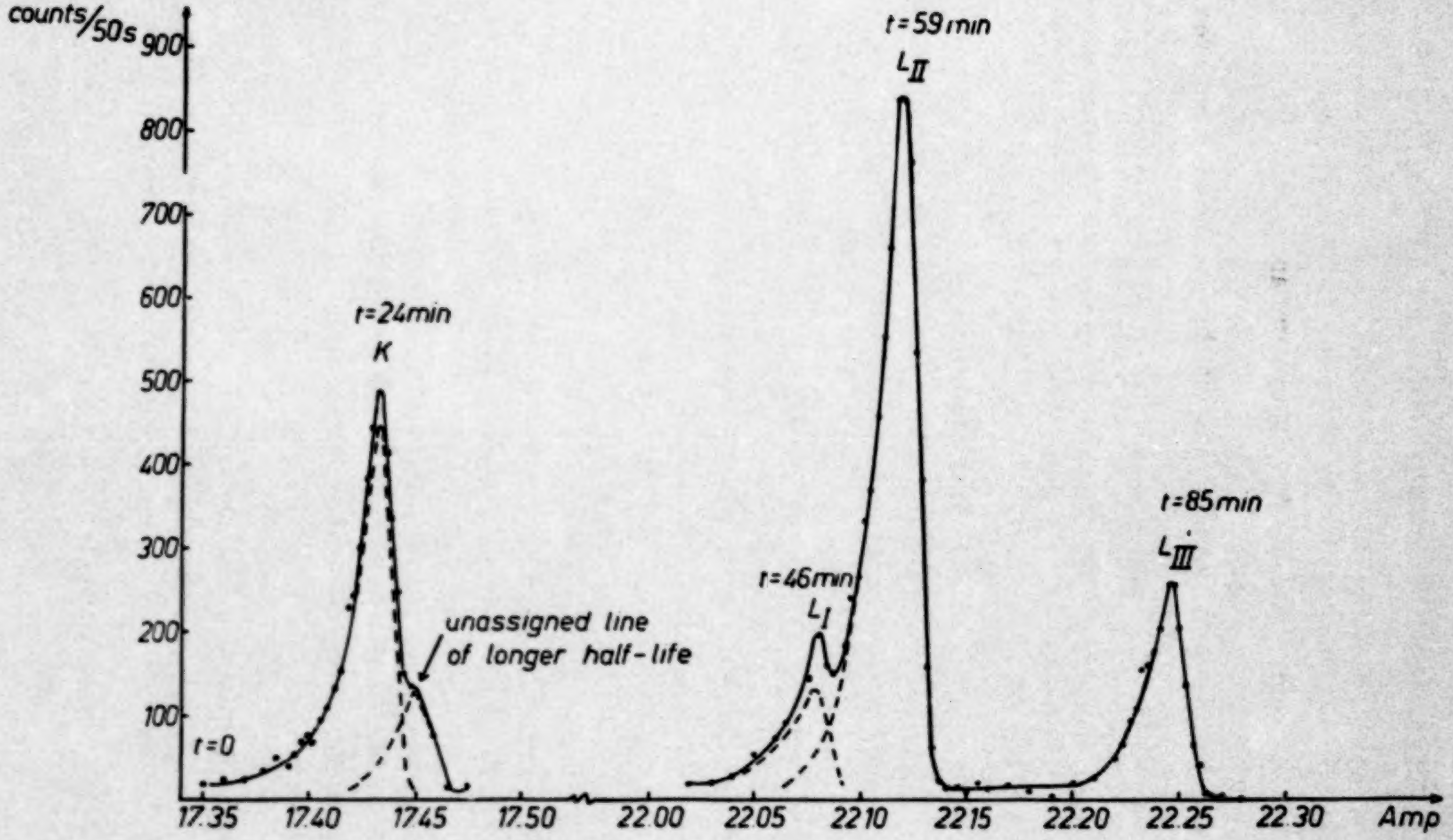

Fig. 1. Electron lines of the 222.5 keV γ-ray in Tl^{197}, measured in an ironfree double-focusing spectrometer. Counting time per point = 50 sec.

The source was obtained in the following way (cf. [3]). Natural Tl was irradiated in the synchro-cyclotron with protons of 95 MeV average energy, corresponding to maximal yield of 42 min Pb^{197m}. After chemical separation, using a few μg Pb carrier, the activity in the form of $PbCl_2$ was vacuum evaporated onto 0.18 mg/cm² Al foil. (The chemical procedure is described in sections 3.3 and 3.4).

With the source dimensions 0.5 by 8 mm and an estimated spectrometer transmission of about 1 ‰ the relative half-width at the L-lines was found to be 0.9 ‰. This was sufficient to permit the L_I line to be resolved with a fair accuracy from the much stronger L_{II} as indicated in fig. 1.

At the K-line the relative half-width was slightly more than 1 ‰ — even after the subtraction of an interfering line of longer half-life — evidently depending on a non-negligible thickness of the sample.

A careful analysis of the spectrum gave the results collected in table 1.

TABLE 1

Line	E_{e-} (keV)	E_γ (keV) (conv. Tl)	Electron intensity (arbitrary units)
K	136.931	222.451	0.556±0.028
L_I	207.108	222.452	0.223±0.022
L_{II}	207.758	222.453	1.843±0.074
L_I+L_{II}			2.066±0.041
L_{III}	209.795	222.448	0.856±0.026

As no suitable calibration line was available, the absolute electron energies were determined by adjusting the spectrometer constant to give a satisfactory agreement between γ-energies, calculated from the different lines using Tl electron binding energies. A consideration of possible sources of error finally led to the transition energy

$$E_\gamma = 222.45 \pm 0.05 \text{ keV}.$$

The electron line intensities in column 4 have been corrected for decay of the parent activity during the measurement, but the errors do not include the uncertainty in the half-life (42±2 min [3]). This was taken into account, however, in calculating the conversion ratios as

$$K/\Sigma L = 0.242 \pm 0.018 \quad (0.272 \pm 0.011),$$
$$(L_I+L_{II})/L_{III} = 2.43 \pm 0.15 \quad (3.98 \pm 0.14).$$

The figures given in parenthesis are the ratios for E3 originally obtained from Rose's tables [4]), with their estimated interpolation errors. Thus the results seemed to confirm the discrepancy mentioned in section 1. Several other E3 transitions in the same Z region were found to show a similar behaviour. A full discussion of this effect, leading to the conclusion that it could be caused neither by M4-admixture nor by the finite nuclear size, has been given elsewhere [7]). Recently, Rose announced a recalculation of his L_{III} conversion coefficients for E3 transitions [8]), which changed the theoretical ratios to

$$K/\Sigma L = 0.246 \pm 0.010 \text{ and } (L_I + L_{II})/L_{III} = 2.59 \pm 0.10,$$

in good agreement with the experimental values.

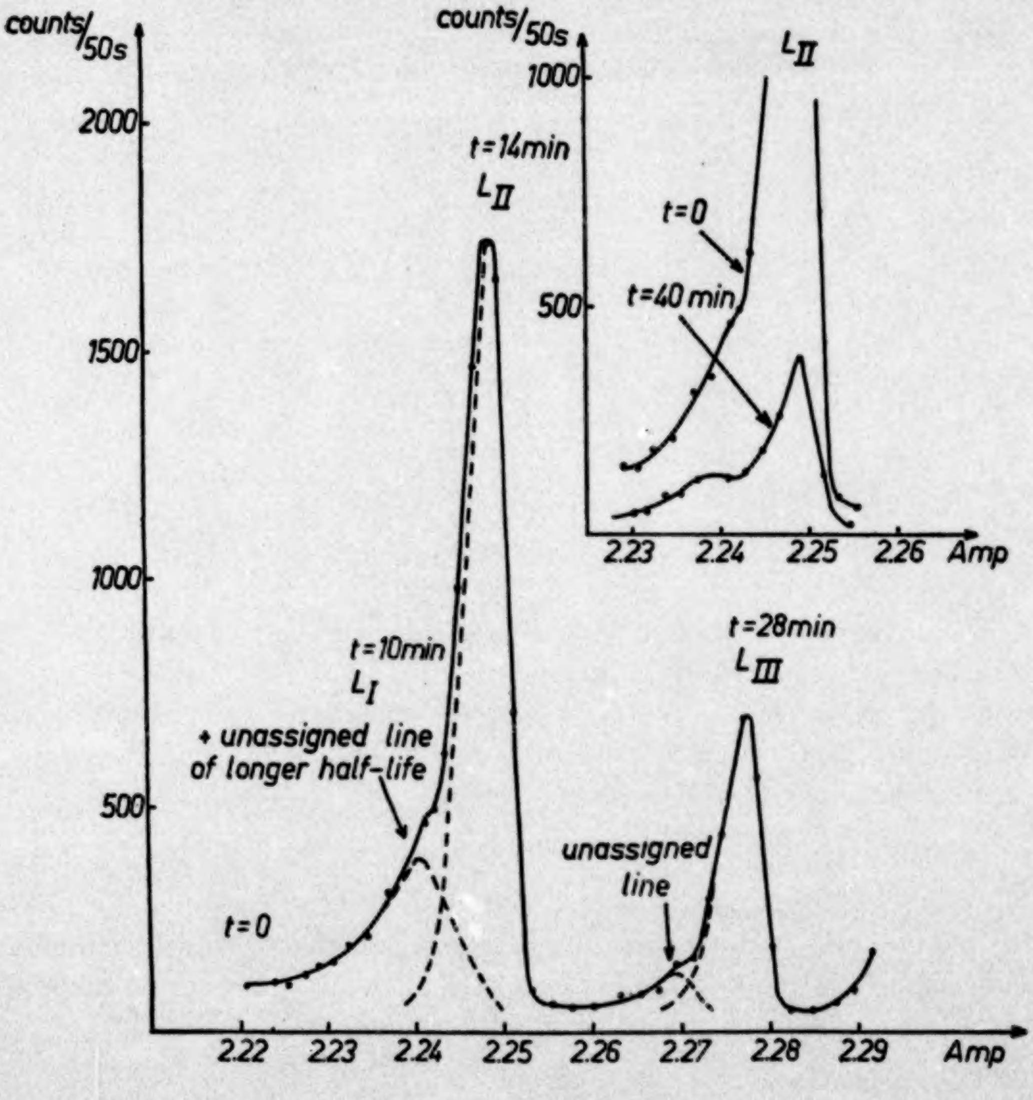

Fig. 2. Electron lines of the 99.1 keV γ-ray in Tl^{195}, measured in an iron yoke double-focusing spectrometer. Counting time per point = 50 sec. The inset illustrates the decay of the $L_I + L_{II}$ complex.

2.2. THE NUCLEUS Tl^{195m}

The L lines of the 99 keV transition in Tl^{195}, fed from the electron capture decay of 17 min Pb^{195m} [3]), were measured in the 18.5 cm double-focusing β-spectrometer of this institute [9]). The same method of sample preparation as in the case of Tl^{197m} was used, with the bombarding energy raised to about 120 MeV. A source width of 0.5 mm gave 2.2 $^0/_{00}$ relative half-width at a calculated solid angle of about 2 $^0/_{00}$.

Figure 2 shows the conversion electron spectrum. L_{III} could relatively easily be corrected for a parasite on the low energy side and was used as a line shape standard in an attempt to decompose the L_I+L_{II} complex. Unfortunately L_I turned out to be superimposed by a more long-lived (probably about 40 min) line of unknown origin (see the inset of figure 2). A detailed study of the decay of the complex was made impossible by the short parent half-life of the lines of interest (17±1 min). Thus only L_{II} and L_{III} could be accurately determined as appears in table 2.

TABLE 2

Line	E_{e^-} (keV)	E_γ (keV) (conv. Tl)	L_{II}/L_{III}
L_{II}	84.354	99.049	1.52±0.12
L_{III}	86.424	99.077	

The calculation of electron energies was performed using a calibration curve according to Arbman [10]). Taking the calibration uncertainty into account we give the energy as

$$E_\gamma = 99.1 \pm 0.1 \text{ keV}.$$

As to the comparison between the experimental and the theoretical conversion ratios a similar discussion applies as in the case of Tl^{197m}. The corrected theoretical L_{III} coefficient leads to $L_{II}/L_{III} = 1.42 \pm 0.04$.

3. Half-life Determinations

3.1. GENERAL CONSIDERATIONS

Assuming the assignment of a 0.54 sec activity to Tl^{197m} (cf. section 1) to be correct and taking into account the dependence of γ-decay lifetimes on energy and internal conversion [11]), a half-life of about 5 sec could be predicted for the 99.1 keV transition in Tl^{195}. This was considered measurable using rapid chemical techniques to separate Tl from its Pb parent and following the γ-decay with a scintillation counter connected to a multichannel time analyser. As it turned out, a refinement of the method even made possible a determination of the shorter-lived Tl^{197m}.

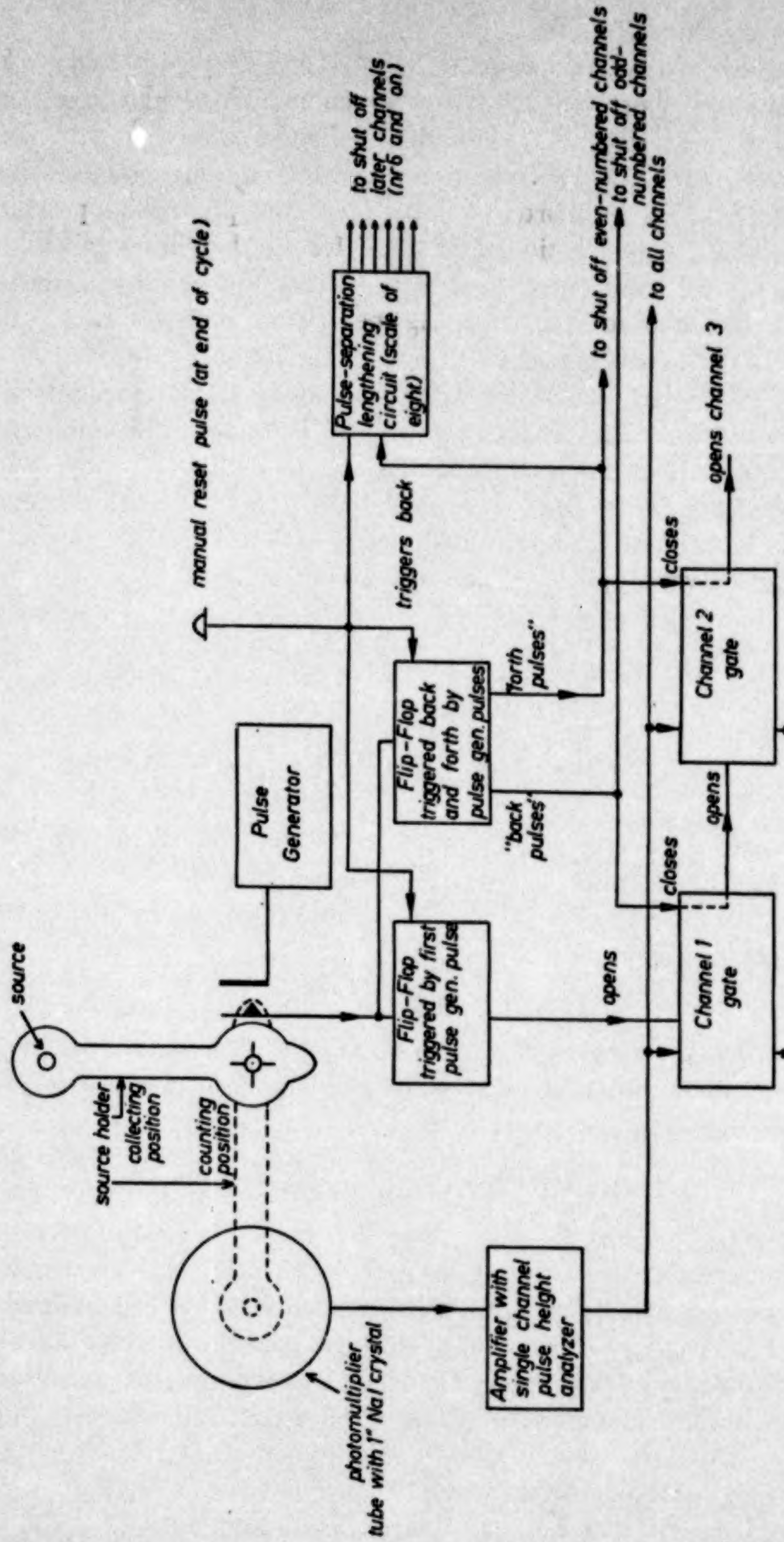
source
source holder
collecting position
counting position
photomultiplier tube with 1" NaI crystal
Amplifier with single channel pulse height analyzer
Pulse Generator
Flip-Flop triggered by first pulse gen. pulse
Flip-Flop triggered back and forth by pulse gen. pulses
manual reset pulse (at end of cycle)
triggers back
"back pulses"
"forth pulses"
Pulse-separation lengthening circuit (scale of eight)
to shut off later channels (nr 6 and on)
to shut off even-numbered channels
to shut off odd-numbered channels
to all channels
opens
closes
opens
closes
opens channel 3
Channel 1 gate
Channel 2 gate
Scaler
Scaler

Fig. 3. Functional diagram of the 20-channel time analysing system.

3.2. ELECTRONIC EQUIPMENT

To record the decays and in complementary experiments to study the energy spectra of the short-lived activities a combined time analyser — pulse height analyser system 12) was used.

In time analysis (see fig. 3) the pulses from the γ-counter are first passed through a single-channel kicksorter, set to select the photopeak pulses from the γ-ray under investigation. These are fed to the time analyser, consisting of 20 gated count channels, which are successively opened and shut by flip-flop circuits, each channel being open for a present time interval t_k, variable between 2 ms and 13 sec.

The process is controlled automatically by an independent pulse generator, giving pulses spaced t_k in time. Thus the first channel is opened by the first control pulse appearing after pressing a start button (in the actual experiments when the Tl source had been put in position) and is shut after the time t_k, simultaneously opening the second channel and so on. In this way the "channel sweep" proceeds through all the gates.

A scale-of-eight circuit, acting on the control pulses, can be used to increase the open time to $2 \times t_k$ for channels 6—10, $4 \times t_k$ for channels 11—15, and $8 \times t_k$ for channels 16—20. Thereby improved background statistics can be achieved.

The determination of t_k is made by feeding pulses of known frequency to the channel inputs, instead of pulses from the γ-counter.

In order to study the pulse height distribution of the short-lived activities, the equipment was rearranged to a 20-channel pulse-height analyser. In this operation the channel sweep, now with t_k very short (about 10 μs), is started by the pulse to be analysed. This pulse is also transformed into another pulse, having its length proportional to the height of the primary pulse. The trailing edge of the secondary pulse is fed to the inputs of the count channels and accepted in that channel which is open at the proper time. Thus the pulses accumulate as counts in the scalers of the various channels.

The rate of filling of the scalers was normally recorded by rapidly repeated photographing. Alternatively and more suitably for the shorter half-life, a gating system could be used which opened the pulse height analyser for a short time interval at a predetermined time T_d after putting the Tl source in position. The scaler readings were photographed and with the same source the procedure was repeated after a time, which should be long compared to the half-life concerned, in order to determine the background. By varying T_d it is possible to find the energy distributions and the approximate half-lives of the activities present.

3.3. BASIC CHEMICAL PROCEDURE

After irradiation, the Tl target was dissolved in concentrated HNO_3, containing about 5μg Pb^{2+} and 250 μg Fe^{3+} as carriers. In order to reduce Tl to the monovalent state the solution was boiled with H_2O_2 until excessive peroxide had disappeared. Fe and Pb were precipitated with NH_3, the rôle of the Fe being to carry down the more soluble lead hydroxide as co-precipitate. After centrifuging, the precipitate was dissolved in HNO_3, reprecipitated, and washed in water 3 times. Finally the hydroxides were dissolved in the smallest possible amount of HCl (about 10 drops of 0.1*N* acid).

3.4. THE NUCLEUS Tl^{195m}

A. Milking of Tl *from the* Pb *solution*

Use was made of the possibility of extracting $TlCl_3$ from an aqueous solution into ether. The Pb activity was kept in 6 *N* HCl. Three ether extractions were first made in order to get rid of the Fe carrier. (In preparing β-spectrometer sources, the remaining Pb solution was then evaporated to dryness on a tantalum strip fitting the vacuum evaporation device.)

The Tl formed in the decay of Pb most probably appears in the monovalent state. Therefore a drop of $KMnO_4$ solution was added immediately before each (about 3 ml) ether portion. After stirring with a glass rod for some seconds in order to bring the ether into intimate contact with the aqueous phase, that part of the ether phase which is formed first (nearest to the surface) was pipetted off and transferred to a test tube, which as fast as possible was put into counting position over the γ-detector and the analyser was started. The whole separation process was completed in some five seconds. In order to improve the ratio between short-lived and longer-lived activities in the ether fractions the Tl formed during the counting period was washed off with ether immediately before taking the next sample.

B. Measurements and results

The 99.1 keV isomeric transition is strongly converted ($\alpha_{\text{total}} = 155$ according to Rose [4]) with $\alpha_{M+N+\dots} = 0.3\ \alpha_L$), and for that reason the single channel energy selector was instead adjusted to 420 ± 50 keV in order to cover the two cascade transitions of 393 and 448 keV [3]).

About 20 Tl milkings were performed within the time limits set by the 17 min parent activity. The numbers of counts in the 20 channels were read after each run and those series showing the most favourable initial total count-to-background ratio were selected and combined to form the decay curve shown in fig. 4.

From this curve the half-life $T_{\frac{1}{2}} = 3.5 \pm 0.4$ sec was obtained. (The error limits are meant also to include systematic errors.)

In the pulse height analysis the same method of sampling was used. The counting rate in the 20 channels was recorded by photographing the scalers after 3, 6, 9, 12, and 24 seconds. The combined result of 14 runs in the energy interval 200—870 keV is illustrated in fig. 5.

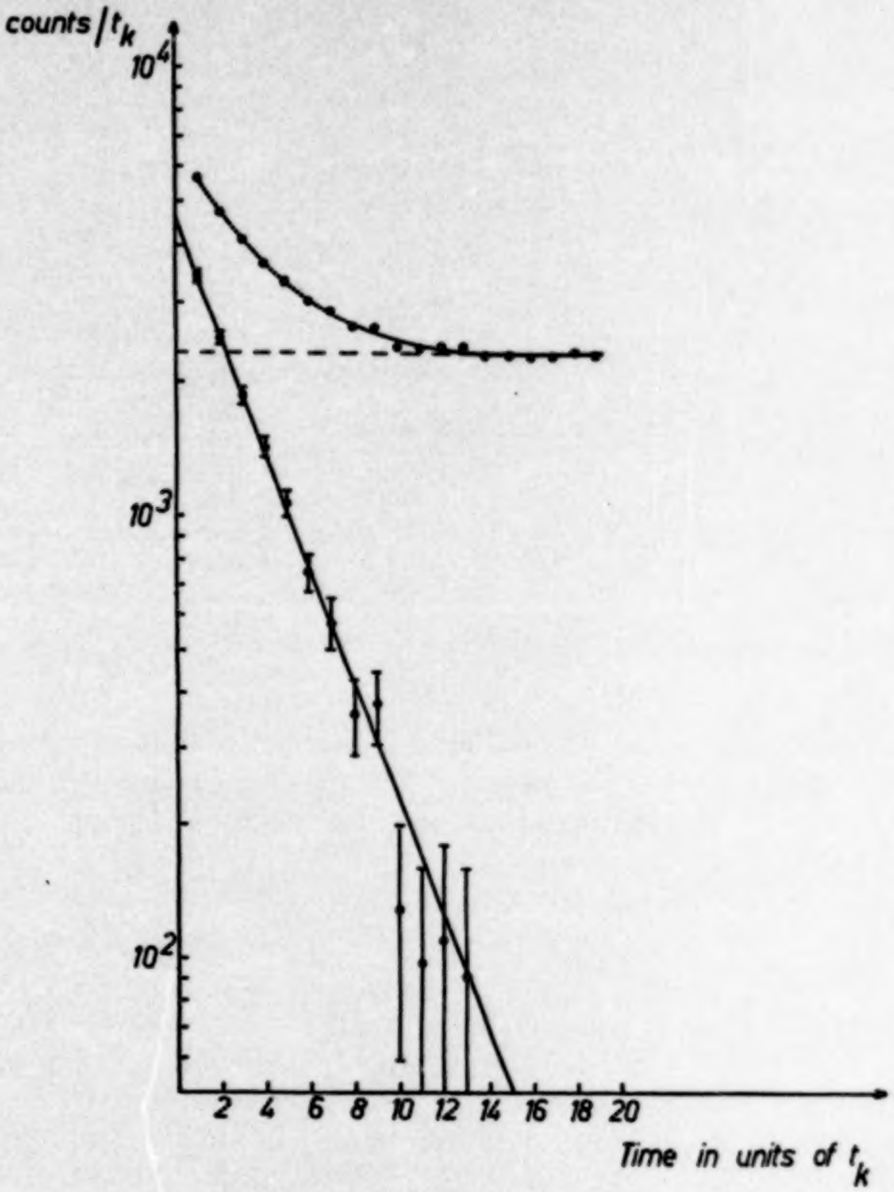

Fig. 4. Decay curve (including 13 runs) of the 393 keV and 448 keV γ-rays in Tl^{195}, assumed to be in cascade with the 99.1 keV E3 transition. $t_k = 1.51 \pm 0.01$ sec.

The presence of a short-lived photopeak with its center of gravity slightly above 400 keV is clearly indicated. From the measurements it was even possible to estimate the half-life as about 4 sec. This proves that the 3.5 sec period found in the time analysis was really due to a photopeak of the expected energy and not, for instance, to the Compton distribution of a γ-ray of higher energy.

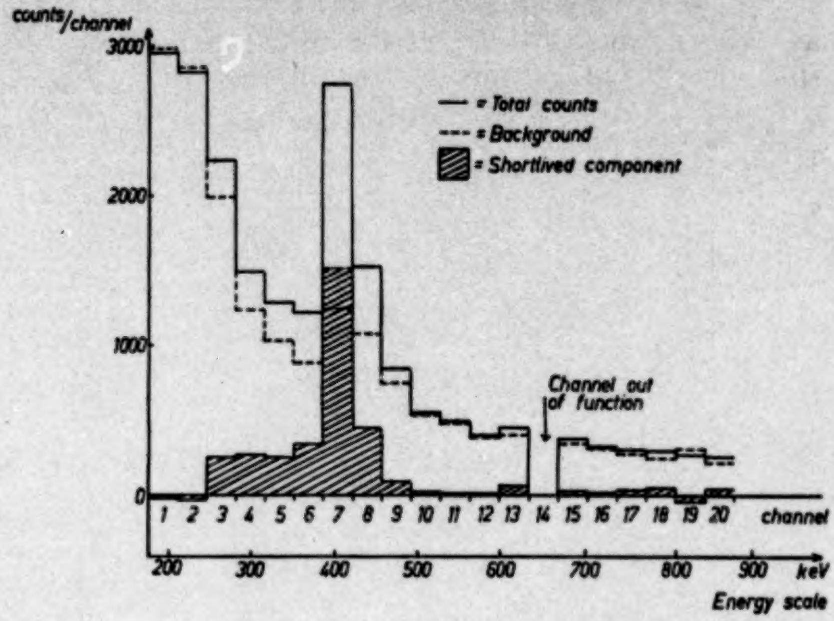

Fig. 5. Pulse height spectrum of the 3.5 sec activity, obtained by subtracting the background (calculated from the counting interval 12 sec—24 sec) from the total number of counts during the first three seconds.

3.5. THE NUCLEUS Tl^{197m}

A. Milking of Tl *from the* Pb *solution*

Attempts to use ether extraction also for Tl^{197m} failed because the separation time could not be decreased sufficiently in relation to the half-life of the isomeric state. Instead a new technique, involving ion exchange, was worked out.

The ion exchange resin (about 30 mg Dowex II, 200—400 mesh) was loaded with PO_4^{3-} ions. When the active Pb solution, containing also Fe^{3+} and Cl^- ions, was put on the top of the exchange column, the inactive ions were found to be trapped in the upper part of the resin (visible by a faint yellow-green discolouring), while the Pb accumulated immediately below this zone. The amount of resin was so chosen that the active layer was situated close to the bottom of the column.

The Tl formed in the decay of the radioactive Pb was eluted with water, continuously pressed through the column at a rate of about three drops a second. One drop at a time was collected on a paper pulp disc and rapidly moved to the γ-counter by means of a special sample changer, acting on a microswitch, which started the analyser as soon as the sample had reached counting position. It was estimated that 1—2 seconds escaped between the passage of the drop through the active layer and the start of the counting.

B. Measurements and results

As the total conversion coefficient of the 222.5 keV isomeric transition

($\alpha_{\mathrm{total}} = 2.26$) indicated a good possibility of detecting its γ-radiation, the single channel analyser was set at 222 ± 13 keV. The course of the experiment was mainly the one described for $\mathrm{Tl}^{195\mathrm{m}}$. Fig. 6 shows a resulting disintegration curve, where the slope of the background is ascribed to a small admixture of 3.5 sec $\mathrm{Tl}^{195\mathrm{m}}$.

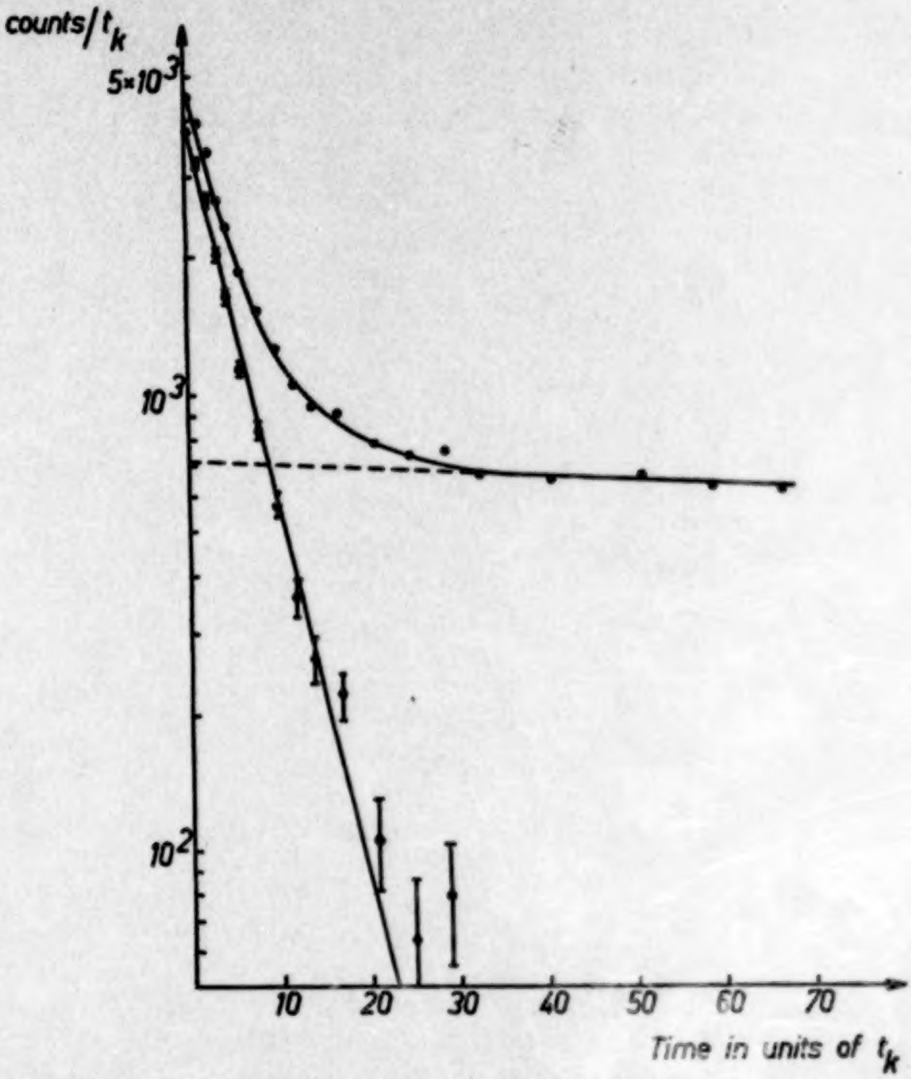

Fig. 6. Decay curve (including 41 runs) of the 222.5 keV γ-ray in Tl^{197}. $t_k = 0.150 \pm 0.001$ sec.

As a mean value of several determinations $T_{\frac{1}{2}} = 0.55 \pm 0.10$ sec was obtained.

In additional runs the energy channel was adjusted to accept the cascade transitions (385 and 387 keV). Within the error limits the same half-life was found.

Attempts to make a pulse height analysis of the 0.55 sec activity met with experimental difficulties, resulting in poor counting statistics. It can only be said that positive indications for a short-lived photopeak at 220 keV were found, but it was not possible to determine its half-life.

4. Discussion

The present investigation unambiguously confirms the E3 character of the 222.5 keV and 99.1 keV γ-rays. Their mass assignment and association with the measured half-lives, however, may need an amplifying discussion.

The 222.5 keV γ-ray was shown by Andersson *et al.* [3]) to be in coincidence with transitions of 385 and 387 keV energy. All three γ-rays were definitely converted in Tl and their strongest electron lines were found in β-spectra of mass 197 samples, electromagnetically separated. From the coincidence relation and the E3 multipolarity of the 222.5 keV γ-ray it can be concluded that this γ-ray is the cascade initiator. The present evidence for a 0.55 sec half-life associated with the γ-energies 222 and 385 keV taken together with the similar decay period of a 384 keV γ-ray found and ascribed to Tl^{197m} by Henrikson *et al.* form a strong support for the decay scheme of Pb^{197} shown in fig. 7.

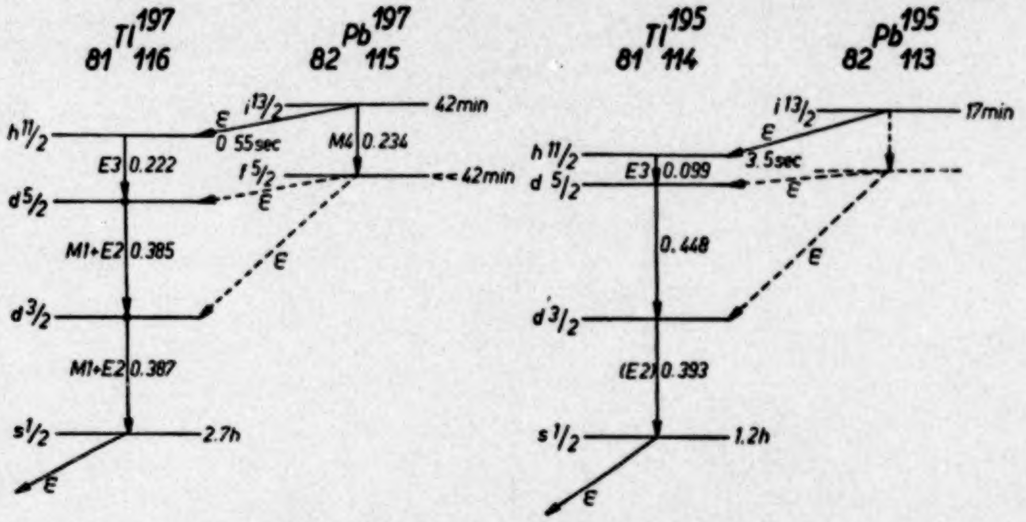

Fig. 7. Proposed decay schemes of Pb^{197} and Pb^{195}.

The assignment of 99 keV, 393 keV, and 448 keV γ-rays to the electron capture branch from Pb^{195m} was originally based partly on their 17 min half-life, which was also found in the decay curve of a mass 195 Pb sample, and partly on level systematics [3]). Recently, Jung *et al.* [13]) have demonstrated the presence of a broad photopeak with the proper half-life at about 400 keV in the γ-spectrum of a mass-separated Pb^{195} sample. For the mass assignment of the 99 keV γ-ray there is still only indirect proof. Its conversion in Tl, however, is confirmed by the present measurements (section 2.2). The 3.5 sec activity was shown by pulse height analysis to have a photopeak at about 400 keV, which is in agreement with the assumption that this half-life is due to the 99.1 keV E3 transition and thus characteristic also of the 448 keV and 393 keV γ-rays following it in cascade (fig. 7).

In principle it would have been possible to determine the parent half-lives from the Tl milkings described in sections 3.4 and 3.5. The sampling methods, however, were not sufficiently reproducible to allow any accuracy in this respect. It can only be stated, that the parent half-lives were short enough to exclude the possiblity of the 0.55 sec and 3.5 sec periods belonging to isotopes of lower elements, which could have been present in view of the bombarding energies used.

Knowing the energies as well as the half-lives of the E3 transitions one can calculate the comparative lifetimes [14]) as $\tau_\gamma \times A^2 \times E_\gamma{}^7$, where τ_γ is the γ-lifetime in sec and E_γ is the energy in MeV. This gives 1.9 for Tl^{197} and 2.0 for Tl^{195}. The theoretical value [11]) for a single proton transition of the $h_{11/2}-d_{5/2}$ type (statistical factor = 50/33) is 0.006. Thus the transition probabilities are reduced by factors of 320 and 330, respectively. Such large "hindrance factors" seem to be a common feature of E3 systematics in this Z region [7]). The similarity in comparative lifetimes of the 222.5 keV transition in Tl^{197} and the 99.1 keV transition in Tl^{195} forms a further argument for the proposed decay schemes (fig. 7), as the nuclear matrix elements for proton transitions of the same type in nuclei differing by two neutrons should be substantially equal.

We are greatly indebted to Prof. T. Svedberg for the working facilities given to us and for his continuous encouragement.

Our thanks are also due to Prof. K. Siegbahn for putting the ironfree double-focusing spectrometer at our disposal and to Drs. E. Sokolowski and C. Nordling for aid in handling the instrument.

Further we want to thank Dr. E. Arbman for the use of his β-spectrometer, Dr. G. Rudstam for valuable contributions in solving chemical problems, and Mr. S. Sundell for help with the electronic equipment.

The investigation was financially supported by the Swedish Atomic Energy Commission.

References

1) J. W. Mihelich and A. de-Shalit, Phys. Rev. **93** (1954) 135
2) J. W. Mihelich, M. McKeown and M. Goldhaber, Phys. Rev. **96** (1954) 1450
3) G. Andersson, E. Arbman and B. Jung, Arkiv Fysik **11** (1957) 297
4) M. E. Rose *et al.*, privately distributed tables
5) A. Henrikson, S. W. Breckon and J. S. Foster, Nuclear Science Abstracts **8** (1954) 24 B 76
6) K. Siegbahn and K. Edvarson, Nuclear Physics **1** (1956) 137
7) G. Andersson and I. Bergström, Nuclear Physics **3** (1957) 541
8) M. E. Rose, private communication
9) E. Arbman and N. Svartholm, Arkiv Fysik **10** (1956) 1
10) E. Arbman, private communication
11) S. A. Moszkowski in Beta- and Gamma-ray Spectroscopy, Ed. Kai Siegbahn (North-Holland Publishing Co., 1955) Ch. XIII
12) P. A. Tove, to be published; *cf.* P. A. Tove, Nuclear Instruments **1** (1957) 95
13) B. Jung, J. O. Burgman and G. Andersson, unpublished work
14) M. Goldhaber and A. W. Sunyar in Beta- and Gamma-ray Spectroscopy, Ed. Kai Siegbahn (North-Holland Publishing Co., 1955) Ch. XVI

Nuclear Physics **3** (1957) 506—512; *North-Holland Publishing Co., Amsterdam*

NOTE ON THE DECAY OF Tl^{198m}

G. ANDERSSON
The Gustaf Werner Institute for Nuclear Chemistry, Uppsala
and
I. BERGSTRÖM
Nobel Institute of Physics, Stockholm

Received 22 February 1957

Abstract: The energies and intensities of the conversion electrons of the 48 keV γ-ray emitted in the decay of 1.75 h Tl^{198m} have been measured in a high resolution spectrometer. The 48 keV γ-ray is converted in Hg, which leads to a revised level scheme of Tl^{198}, the levels being 7+ (543.1 keV) 3− (282.4 keV) and 2− (0 keV). The relative conversion intensities in the L and M subshells, respectively, agree perfectly with those obtained from the E2 conversion coefficients by Rose *et al.*

1. Introduction

Tl^{198m} was discovered by Bergström, Hill, and de Pasquali in 1953 [1]). In a study of activities produced in Hg (d, n) and Hg (d, 2n) reactions, using permanent magnet spectrometers for photographic recording, they found 2 h conversion lines corresponding to γ-rays of energies 260.7, 282.4, and 48.7 keV. It was definitely concluded that the former two γ-rays were converted in thallium and that the 261 keV γ-ray was responsible for an isomeric transition, presumably M4, while the multipolarity of the 282 keV γ-ray was mainly M1. The following level sequence was suggested: 9− (591.8 keV), 5+ (331.1 keV), 4+ (48.7 keV), and 3+ (0 keV).

Passell, Michel, and Bergström [2]) reinvestigated the decay of Tl^{198m} in a double focusing spectrometer. Intensity measurements confirmed the assignments of the 261 and 282 keV γ-rays. Because Tl^{198m} was produced in an Au^{197} (α, 3n) reaction it was also possible to study the conversion lines of the 48 keV transition without the disturbing lines present in the sources used by Bergström *et al.* Relative conversion intensities assigned the multipolarity E2 to the 48 keV γ-ray. In addition it was found that the transition intensities of the 48 and 261 keV γ-rays were 95 and 100 units, respectively, which strongly supported the decay scheme suggested by Bergström *et al.*, though the possibility of the 48 keV γ-ray being emitted from a level in mercury reached by capture was not excluded. Passell *et al.* preferred the following spin and parity assignments: 9+, 5−, 4− and 2−. Previous Berkely experiments [3]) suggested that the parent of the 2 h Tl^{198m} was a 25 min activity of Pb^{198}, which for this reason should have a high spin state. Andersson, Arbman, Bergström, and Wapstra[4]), however, investigated Pb^{198} without finding any high spin state or any indication of feeding to Tl^{198m}. It was concluded that in the Berkeley experiments the activity of mass number 197 probably was wrongly interpreted as being due to the mass number 198.

Knight and Baker[5]) have reported a large number of 2 h conversion lines converted in mercury and assigned to mass number 198 from excitation relations. This proves that there is indeed capture from the isomeric state in Tl^{198}.

Fisher and Knapp[6]) have performed coincidence measurements on some of the stronger 2 h lines converted in Hg^{198}. They conclude that there is about 60 % capture from the isomeric state in Tl^{198}. A spin as high as 9 for the isomeric state was not compatible with their experiments. They suggest the spin sequence: 7+, 3−, 2−, and 0−.

In view of the recent discoveries of isomeric states in Tl^{202} and Tl^{204} [7]) it is of interest to know whether the 48 keV γ-ray is converted in Tl or Hg. For this reason the present work is limited to a study of the 48 keV transition. By measuring the conversion lines with a high resolution and using good sources it should be possible to decide in which element this γ-ray is converted.

2. Experimental Procedure

Natural HgCl was bombarded with 30 MeV protons in the Uppsala synchrocyclotron. The HgCl was dissolved in 6 *N* HCl. A few μg Tl carrier was added and the thallium ions oxidized to Tl^{3+} with $KMnO_4$. Repeated ether extractions were carried out in order to separate $TlCl_3$ from the target solution. A few drops of water were added to the combined ether fractions, and the $TlCl_3$ transferred to the aqueous phase by evaporating the ether. After reduction with H_2O_2 in nitric acid solution the Tl activity was dried on a tantalum strip and evaporated as TlCl in vacuum onto an aluminium backing of thickness 0.18 mg/cm^2. The conversion lines were measured in a double focusing spectrometer (resolution set at about 2.5 $^0/_{00}$) constructed by Arbman and Svartholm[8]).

3. Results

3.1. ENERGIES OF CONVERSION LINES

Fig. 1 shows the conversion lines in the energy region 30−50 keV.

The 48 keV γ-ray has been assigned the multipolarity E2[2]). For this reason it should be converted mainly in the L_{II}, L_{III}, M_{II}, and M_{III} subshells. The resolution of the spectrometer and the quality of the source were such that it was possible to resolve not only the L_{II} and L_{III} lines but also L_I from L_{II} and even the M_{II} and M_{III} lines.

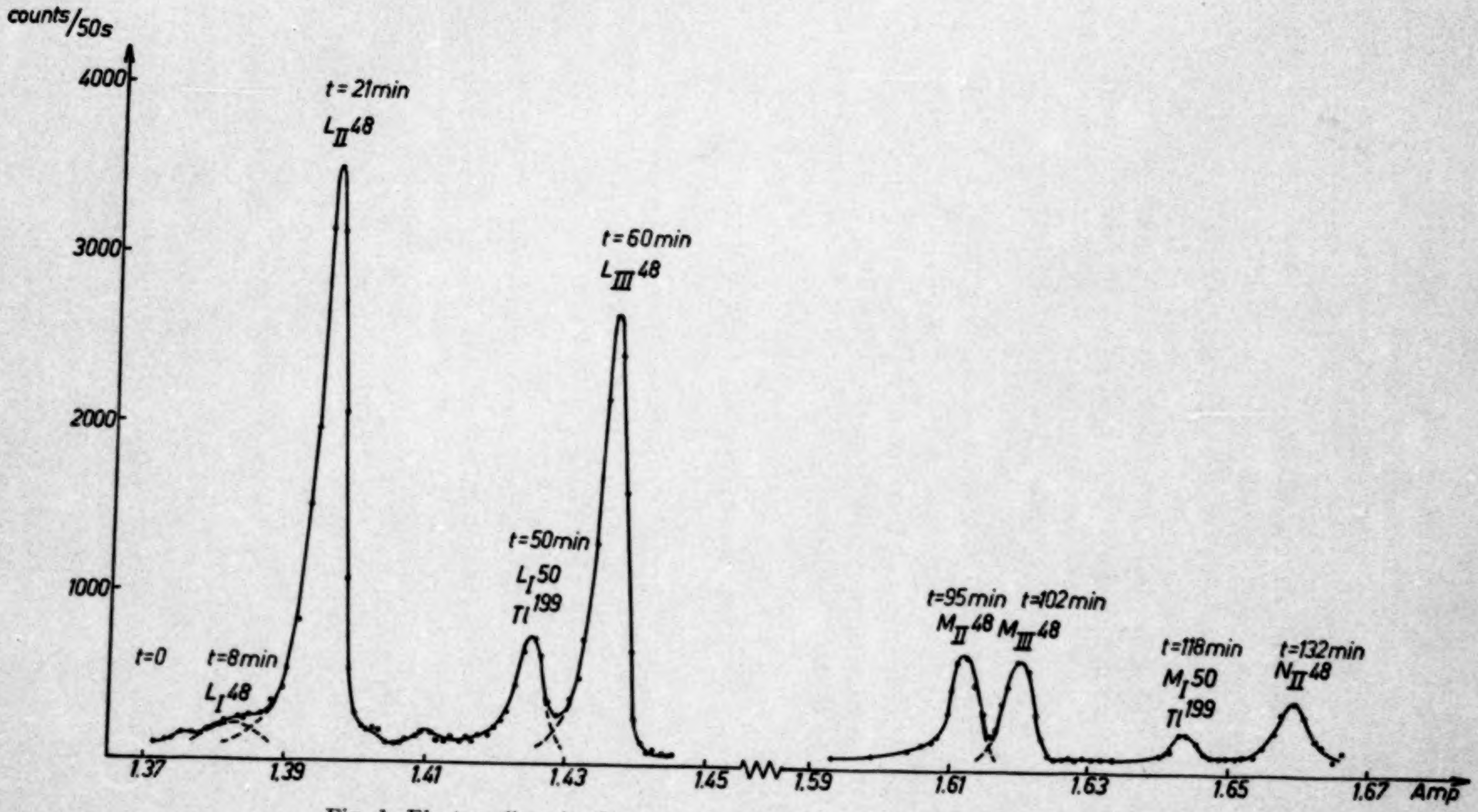

Fig. 1. Electron lines in the energy region 30—50 keV. Counting time per point = 50 sec

In the spectrometer used the coil current is measured accurately by means of a compensation method. The $B\varrho$ value is not a linear function of the current I:

$$B\varrho = K(B\varrho)\times I.$$

The calibration constant $K(B\varrho)$ has been determined by measuring conversion lines of known energies[9]). In the region 33–44 keV, $K(B\varrho)$ only changes 0.35 %. It is thus possible to determine energy differences within this energy region with high accuracy. The reliability of the calibration constant is demonstrated by the energy obtained for the 50 keV γ-ray converted in Hg^{199}. This γ-ray has been assigned the multipolarity M1[10]) and should be converted predominantly in the L_I and M_I subshells. As can be seen from table 1 the agreement between the energy values obtained from the L_I and M_I conversion lines is very satisfactory.

TABLE 1

Intensities and energies of conversion lines

Line	E_{e^-} (keV)	E_γ (Hg) (keV)	E_γ (Tl) (keV)	I_{e^-} †	Observed half life
L_I48	32.85	47.7	48.2	6	
$L_{II}48$	33.518	47.74	48.21	241	1.70 h
L_I50	34.936	49.78			≈6.3 h
$L_{III}48$	35.465	47.75	48.11	235	1.86 h
$M_{II}48$	44.456	47.74	47.87	71	
$M_{III}48$	44.918	47.77	47.87	70	
M_I50	46.185	49.75			
$N_{II}48$	47.11	47.78	47.83	49	

† half-life 1.75 h used [M. C. Michel and D. H. Templeton, Phys. Rev. **93** (1954) 1422]

From the energies of the conversion lines it can be unambiguously concluded that the 48 keV γ-ray is converted in mercury.

3.2. RELATIVE INTENSITIES OF THE CONVERSION LINES

Table 1 also includes the relative conversion intensities. The following intensity ratios are obtained:

$$L_I/L_{II} = 0.025\pm0.008 \ (0.023)$$
$$L_I/L_{III} = 0.026\pm0.008 \ (0.023)$$
$$(L_I+L_{II})/L_{III} = 1.05\pm0.08 \ (1.04)$$
$$M_{II}/M_{III} = 1.01\pm0.10 \ (0.94)$$
$$\Sigma L/\Sigma M = 3.43 \pm 0.25 \ (2.31).$$

The values given in brackets are the ratios for an E2 transition calculated from the theoretical conversion coefficients of Rose *et al.* [11]). Except for the last value the agreement between theory and experiment is very good. The discrepancy in the case of $\Sigma L/\Sigma M$ is explained by the fact that the influence of screening has been neglected in the computation of M shell conversion coefficients. Rose has pointed out [11]) that screening may cause a reduction by as much as a factor of two. In the actual case our measurements suggest a reduction factor of 1.5.

It might be expected that the experimental $(L_I+L_{II})/L_{III}$ ratio should be lower than the theoretical value, because the finite size of the nucleus (which should influence K, L_I and L_{II} about equally but leave L_{III} approximately unchanged) was not taken into account in the calculations. A comparison between Rose's K conversion coefficients [11]) and those of Sliv and Band [12]) indicates, however, that for E2 transitions of low energy the finite nuclear size effect is probably unimportant, which is in accordance with our results.

From the L_I/L_{III} ratio it can be concluded that the maximum amount of M1 admixture is 5 %.

4. Discussion of the Decay of Tl^{198m}

The fact that the 48 keV γ-ray is converted in Hg means that there are only two γ-rays of energies 260.7 and 282.4 keV [1]) emitted in cascade from a high spin state in Tl^{198}. Recent atomic beam experiments by Brink *et al.* [13]) suggest that the isomeric state in Tl^{198} has the spin 7. The 261 keV γ-ray is definitely an M4 transition [2]) and is therefore emitted between levels of spin 7 and 3. The transition intensities of the 261 and 282 keV γ-rays must be the same, because they are emitted in cascade. Using the K conversion tables of Sliv and Band [12]) and the electron intensities measured by Passell *et al.* [2]) one obtains the value 0.23 for the K conversion coefficient of the 282 keV γ-ray. This suggests an M1 transition (theoretical value 0.39) with possible E2 admixture and means that the ground state spin of Tl^{198} is 2. (It may be of interest in this connection to notice that Brink *et al.* [13]) confirm the spin 2 for the Tl^{204} ground state.) The parity is probably negative (combination of the 81st proton and the 117th neutron in their lowest states, which have different parity), giving the isomeric state positive parity and the intermediate state negative parity. A level scheme, based on these considerations, is shown in fig. 2.

The position of the 48 keV transition in the decay is still uncertain. Pending further investigation of the E. C. branch from Tl^{198m} only a few remarks will be made. Fisher and Knapp [6]) arrive at the spin 6 for the level in Hg^{198} which is fed from Tl^{198m}, by assigning E2 or M2 multipolarity to the 637 and 588 keV γ-rays, shown by them to be in coincidence with the well established 412 keV E2 transition to the ground state. The conversion electron data of Knight and Baker [5]), however, would rather suggest M1 character for these two γ-rays.

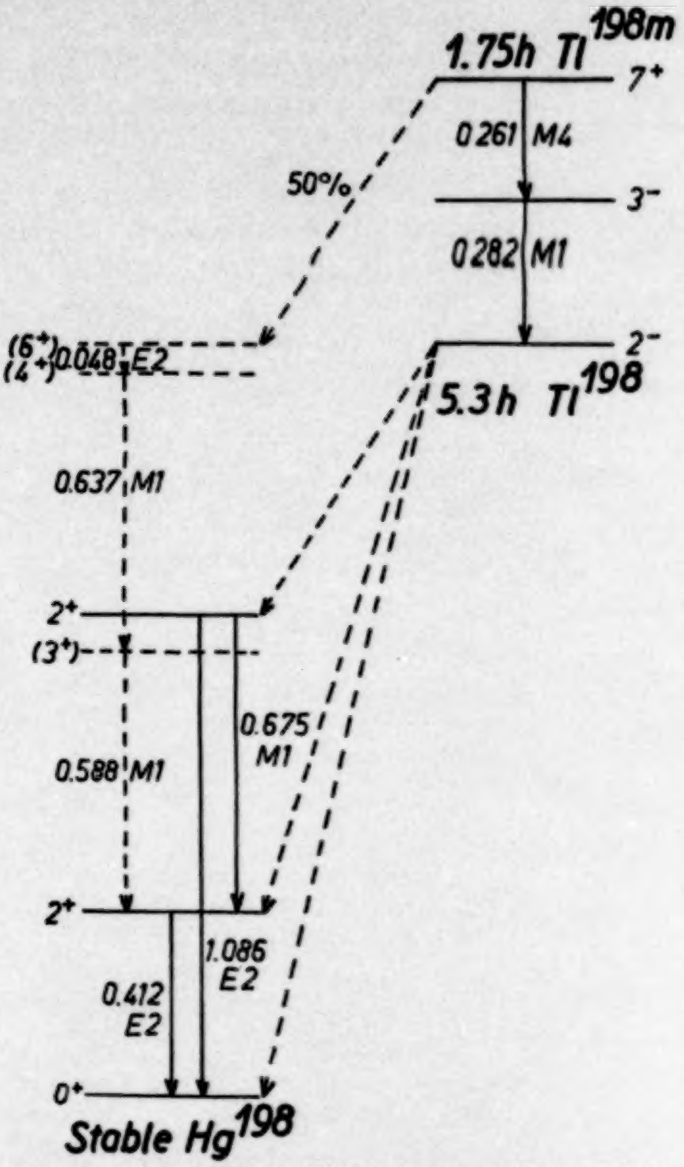
1.75h Tl198m
7+
0.261 M4
50%
3-
0.282 M1
2-
5.3h Tl198
(6+)
(4+)
0.048 E2
0.637 M1
2+
(3+)
0.675 M1
0.588 M1
2+
1.086 E2
0.412 E2
0+
Stable Hg198

Fig. 2. Revised level scheme of Tl^{198}. A tentative level scheme of Hg^{198} is indicated.

As further a branching ratio E.C./I.T. ≈ 1 has been reported [6]) and the intensity of the 48 keV transition is very nearly equal to that of the isomeric transition [2]), the level scheme of Hg^{198} indicated in fig. 2 does not disagree with the experimental findings. In this way the spin 6 for the capture level would be retained. A spin value of 7 or 8, however, cannot be excluded. It should be stressed that this part of the level scheme is very tentative and incomplete.

The similarities of the isomeric decays in Tl^{198m}, Tl^{202m}, and Tl^{204m} are discussed in a paper by McDonell *et al.* [7]).

References

1) I. Bergström, R. D. Hill and G. de Pasquali, Phys. Rev. **92** (1953) 918
2) T. O. Passell, M. C. Michel and I. Bergström, Phys. Rev. **95** (1954) 999
3) H. M. Neumann and I. Perlman, Phys. Rev. **78** (1950) 191
4) G. Andersson, E. Arbman, I. Bergström and A. H. Wapstra, Phil. Mag. **46** (1955) 70
5) J. D. Knight and E. W. Baker, Phys. Rev. **100** (1955) 1334
6) P. S. Fisher and V. Knapp, Proc. Phys. Soc. A **69** (1956) 541
7) J. A. McDonell, R. Stockendal, C. J. Herrlander and I. Bergström. Nuclear Physics **3** (1957) 513
8) E. Arbman and N. Svartholm, Arkiv Fysik **10** (1956) 1
9) E. Arbman, personal communication.
10) M. Goldhaber and R. D. Hill, Revs. Modern Phys. **24** (1952) 179
11) M. E. Rose *et al.*, privately distributed tables
12) L. Sliv and J. Band, privately distributed tables
13) G. O. Brink, J. C. Hubbs, W. A. Nierenberg and J. L. Worcester, Bull. Am. Phys. Soc. **1**, no. 7 (1956) 343

Nuclear Physics **3** (1957) 513—540; *North-Holland Publishing Co., Amsterdam*

LEVELS IN Pb^{202} AND Tl^{202} POPULATED FROM 3.62-h Pb^{202m}

J. A. McDONELL[†], R. STOCKENDAL, C. J. HERRLANDER AND I. BERGSTRÖM
Nobel Institute of Physics, Stockholm

Received 22 February 1957

Abstract: Using beta spectroscopic techniques, conversion electrons of transitions following the decay of 3.62-h Pb^{202m} have been investigated. The previously suggested level sequence in Pb^{202} is unambiguously supported by our results: 0+ (0 keV), 2+ (961.4 keV), 4+ (1383.5 keV), 5− (2041.1 keV) and 9− (2170.7 keV). From the 9− state two gamma rays of multipolarity E4 (129.3 keV) and E5 (787.2 keV) are emitted. In addition, a very weak E5 transition of energy 547.2 keV between the 9− state and a second 4+ state (1623.8 keV) was observed, as well as an M1 transition of energy 240.3 keV between the two 4+ states. The succession of the 422.1 keV and 961.4 keV transitions was determined by comparing their relative intensities in the decay of Pb^{202m} and Bi^{202}. Except for the 5− level, the similarity between levels in Pb^{202} and Pb^{204} is very striking.

The 9− state in Pb^{202} was found to be deexcited also by electron capture (9.7 %) to levels in Tl^{202}. The following level sequence is suggested for the Tl branch: 2− (0 keV), 4− (490.4 keV), 7+ (950.2 keV), 6+ (1099.1 keV) and 8+ (1340.1 keV). The 8+ state is deexcited by an M1 transition of energy 389.9 keV, and also by a 241.1 keV E2 transition followed by a 148.9 keV M1 transition. The isomeric 7+ state is deexcited by a 459.8 keV E3 transition and a 490.4 keV E2 transition in cascade. The succession of the 389.9, 459.8 and 490.4 keV transitions is suggested from coincidence measurements. A gamma ray of energy 335.6 keV and multipolarity M1 (?) may be emitted from an 8+ or 9+ (1675.7 keV) level to the 8+ (1340.1 keV) level. In addition, some weak conversion lines were found, to which no definite assignment could be given.

CONTENTS

1. INTRODUCTION 514
2. EXPERIMENTAL PROCEDURES 514
3. ENERGIES OF CONVERSION LINES; IDENTIFICATION OF GAMMA RAYS 515
4. INTENSITIES OF CONVERSION LINES; CONVERSION RATIOS 524
5. LEVELS IN Pb^{202}; MULTIPOLARITIES OF GAMMA RAYS 524
6. LEVELS IN Tl^{202} 530
    6.1. Multipolarities of gamma rays 530
    6.2. Discussion of additional information relevant for the construction of the level scheme of Tl^{202} 534

[†] On leave of absence from the University of Melbourne, Australia.

a) Spins and parities of the ground state and the "capture state" in Tl^{202} 534
b) Order of emission of gamma rays 534
c) Discussion of the isomeric decay in Tl^{202} 536
7. ELECTRON CAPTURE FEEDING FROM Pb^{202m} 537
8. TRANSITION PROBABILITIES 538

1. Introduction

The isomer Pb^{202m} was discovered by Maeder and Wapstra [1]) in 1954. It has been studied further by the Amsterdam [2, 3]) and Stockholm [4, 5]) groups. Our preliminary measurements [4]) showed that the 2+, 4+ and 9− levels in Pb^{202} and Pb^{204} were of about equal energy. Recently a second very weak E5 transition to another 4+ state was found [6]) in the decay of Pb^{204m}. As a similar transition may take place in Pb^{202m}, a more accurate investigation of the decay of Pb^{202m}, concentrated mainly on previously unassigned lines, was undertaken. The present theoretical interest in levels of nuclei around $N = 126$, $Z = 82$ also emphasized the importance of more accurate information of the decay of Pb^{202m}. This nucleide no doubt presents one of the most outstanding cases of nuclear isomerism.

2. Experimental Procedures

Targets of spectroscopically pure thallium were bombarded with 23-MeV deutrons in the Nobel Institute cyclotron and the lead activities separated and deposited as beta-spectrometer sources using techniques which have been described elsewhere [6]). The conversion-electron spectra were observed both in a double-focusing spectrometer [7]) (with resolutions varying from 0.15 to 0.35 %) and in a permanent magnet semi-circular spectrometer for photographic recording [8]).

Some measurements of conversion lines were carried out on a bismuth sample containing Bi^{202}, produced by bombarding lead with 70-MeV protons in the synchrocyclotron of the Gustaf Werner Institute, Uppsala. The separation of the active bismuth from the target material and the preparation of the beta spectrometer source has been described in a previous work [9]).

Preliminary electron-electron coincidence measurements were performed in a double long-lens spectrometer [10]) adapted for the purpose with a coincidence circuit with a resolving time $2\tau = 0.15 \mu s$. As the relative half-width for this instrument is about 2 %, it was impossible to resolve several of the line groups. The measurements were carried out by focusing the actual lines or line groups in the spectrometer channels. The genuine, as well as the accidental counting rates were measured. The latter were obtained by introducing into one of the channels a time delay, long compared to the resolving time of the coincidence circuit.

3. Energies of Conversion Lines; Identification of Gamma Rays

Tables 1, 2 and 3 give the values of the gamma energies which were found from the conversion lines. Each of these lines has been observed on more than one occasion in the double-focusing spectrometer and in the permanent magnet spectrometer, and has been shown to decay with a half-life of approximately 4 hours. Fig. 1 shows a small part of the conversion-line spectrum measured in the double-focusing spectrometer. The energy accuracy of the conversion lines should be better than 5 : 10^4 except for the very weakest lines. This means that one can unambiguously determine, from the energy difference between the K and L lines, whether the gamma ray concerned is converted in Pb or Tl. At low energies it is even possible to assign the conversion lines on the basis of the energy differences between the L lines. In the case of the 129.3 keV gamma ray, the energy

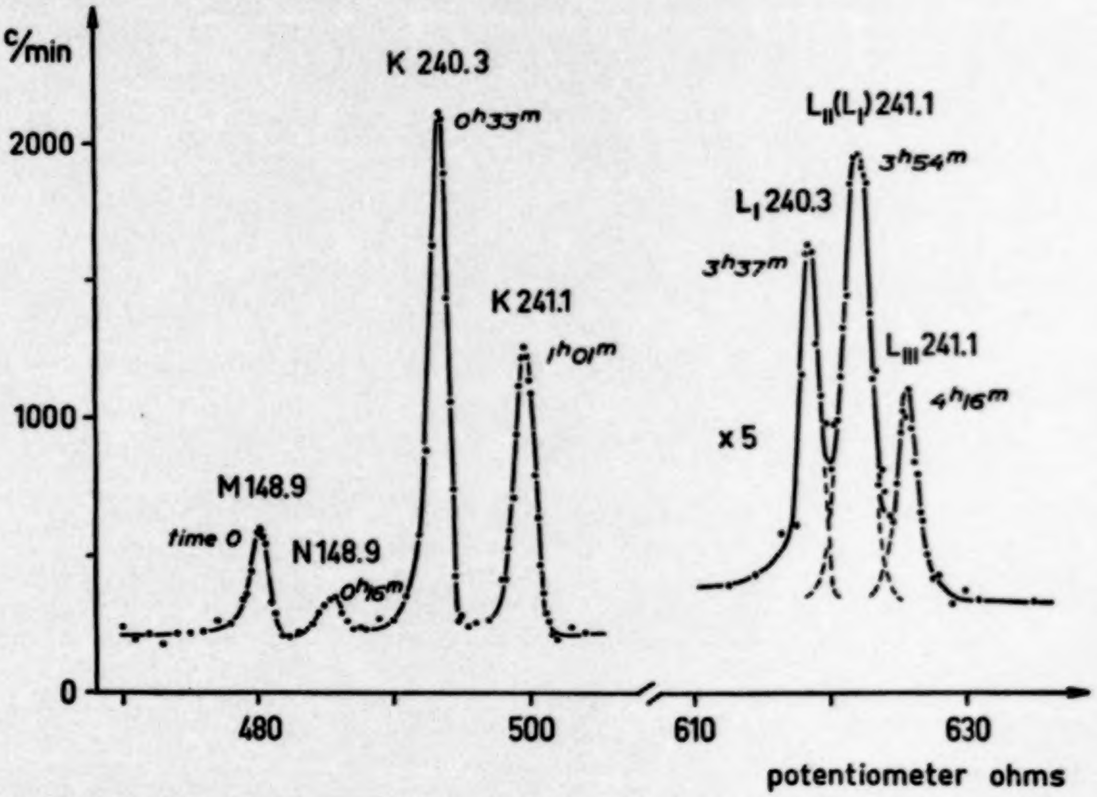

Fig. 1. Part of the conversion-electron spectrum, measured with 0.3 % resolution in a double-focusing spectrometer. On account of difficulties in making decay-corrections of the background, which is due to activities with various half-lives, the time at which a line peak was measured is given in figs. 1, 2, 4 and 5.

difference between the two L lines (cf. fig. 2) is found to be 2.19±0.05 keV, which is to be compared with the energy differences of 2.17 keV and 2.04 keV between the L_{II}- and L_{III}-binding energies in Pb and Tl respectively and the differences of 2.83 keV and 2.69 keV between the L_I- and L_{III}-binding energies in the same elements. Thus the lines are identified as being the L_{II} and L_{III} lines of a high multipole electric transition, converted in Pb. This assignment was later supported by the position and intensity of its weak K line.

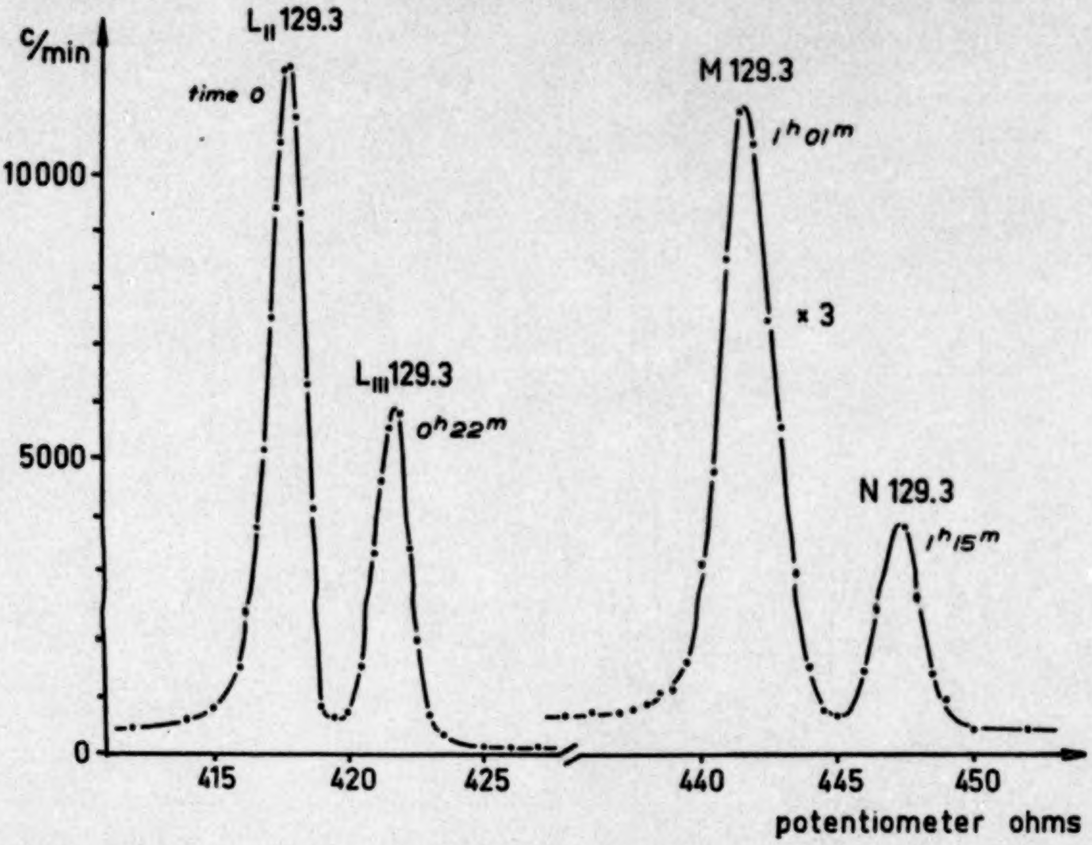

Fig. 2. Conversion lines of the 129.3 keV transition in Pb^{202m} measured with 0.3 % resolution in a double-focusing spectrometer. The measured energy difference between the two L peaks identifies these as L_{II} and L_{III} lines of a high multipole electric radiation converted in Pb.

It will be noted that, due to the energy accuracy, the L-conversion lines are assigned as predominantly L_I or L_{II} lines, depending on which one gives the better fit with the gamma ray energy as determined from the K line. In this way, although the L lines cannot always be resolved, we can often make a sufficiently accurate assessment of the relative L intensities to distinguish between electric and magnetic transitions. In the case of the 422.1 keV transition other evidences suggest that it is of multipolarity E2, so that for this transition one expects the L_I and L_{II} intensities to be approximately equal. This is borne out by the fact that the addition to the

TABLE 1

Gamma transitions in the decay of Pb^{202m}
(converted in Pb)

E_γ (keV) adopted value	E_γ (keV) values calculated from conversion lines	Relative conversion line intensity (K 787.2 = 100)	K/L	$\frac{L_I+L_{II}}{L_{III}}$	Multi-polarity	Multipolarity assignment based on
129.3	129.33 [K]; 129.29 [L_{II}]; 129.31 [L_{III}]; 129.5 [M_{II})]; 129.4 [M_{III}]; 129.3 [M_{IV}, M_V]; 129.3 [N_{II}].	690±50 (ΣL)	< 0.008	1.88±0.12	E4	1) K/L. 2) $(L_I+L_{II})/L_{III}$ 3) $L_I \ll L_{II}$ 4) cascade relation 5) half-life
240.3	240.3, 240.3, 240.4 [K]; 240.0, 240.1 [L_I]; 240.4, 239.9 [M_I].	4.0±0.3 (K)	5.0±0.6		M1	1) K/L 2) cascade relation
422.1	422.0, 422.0, 422.2 [K]; 422.1, 422.0 [L_IL_{II}]; 422.1, 422.1 [L_{III}]; 422.1 [M_{II}]; 422.3 [N_{II}].	66±5 (K)	2.6±0.3	5.6±0.8	E2	1) K/L 2) $(L_I+L_{II})/L_{III}$ 3) $L_I \approx L_{II}$ 4) cascade relation 5) half-life 6) angular correlation
547.2	547.4 [K]; 547.1, 547.2, 547.1 [$L_{II}(L_I)$]; 547.2, 547.3 [L_{III}]; 547.0, 547.2 [M_{II}]; 547.2 [N_{II}].	1.1±0.1 (ΣL)	$0.8\pm^{0.1}_{0.3}$	6.0±1.5	E5	1) K/L 2) $(L_I+L_{II})/L_{III}$ 3) cascade relation 4) half-life
657.6	657.7, 657.7, 657.4, 657.5 [K]; 657.7, 657.5 [L_I].	4.4±0.4(K)	5.5±0.7		E1	1) K/L 2) $L_{II} \ll L_I$ 2) cascade relation
787.2	787.2, 787.2, 787.2 [K]; 787.3 [$L_{II}(L_I)$].	100 (K)	1.18±0.10	≈ 10 †	E5	1) K/L 2) L_I/L_{II} 3) cascade relation 4) half-life
961.4	961.2, 961.6 [K]; 961.4 [$L_I(L_{II})$].	13±1 (K)	5.0±0.7	≈ 15 †	E2	1) K/L 2) cascade relation 3) angular correlation

† value estimated from the photographic film shown in fig. 3

TABLE 2
Gamma transitions in the decay of Pb^{202m}
(converted in Tl)

E_γ (keV) adopted value	E_γ (ke V) values calculated from conversion lines	Relative conversion line intensity (K 787.2 = 100)	K/L	$\frac{L_I+L_{II}}{L_{III}}$	Multi-polarity	Multipolarity assignment based on
148.9	149.0, 148.6 [K]; 148.4, 149.3 [L_I]; 149.0 [M_I]; 149.0 [N_I].	17±3 (K)	6.1±1.2		M1	1) K/L 2) $L_{III} \ll L_I$ 3) cascade relation
241.1	241.2, 241.4 [K]; 241.2, 240.9 [$L_{II}(L_I)$]; 241.1, 241.0 [L_{III}]; 241.0 [$M_{II}M_{III}$]; 241.0 [N_{II}].	2.5±0.2(K)	1.3±0.2	2.5±0.3	E2	1) K/L 2) $(L_I+L_{II})/L_{III}$ 3) cascade relation
335.6	335.6, 334.7 [K]; 335.6, 335.6 [L_I];	1.3±0.1 (K)	≈ 5		E1? M1?	K/L
389.9	389.9, 390.0, 389.8 [K]; 389.5, 389.6 [L_I].	28±3 (K)	6±3		M1	1) K/L 2) cascade relation
459.8	459.8, 459.7 [K]; 459.6, 459.6, 459.7, 459.9 [$L_{II}(L_I)$]; 460.4 [L_{III}]; 459.8, 459.8, 460.2 [M_{II}]; 459.5, 460.2 [N_{II}].	9±1 (ΣL)	< 1.7	5.1±0.5	E3	1) K/L 2) $(L_I+L_{II})/L_{III}$ 3) cascade relation 4) half-life
490.4	490.4 [K]; 490.3, 490.4, 490.8 [L_IL_{II}]; 490.5 [M_IM_{II}].	1.7±0.2(ΣL)	3.5±1.0	8±2	E2	1) K/L 2) $(L_I+L_{II})/L_{III}$ 3) cascade relation

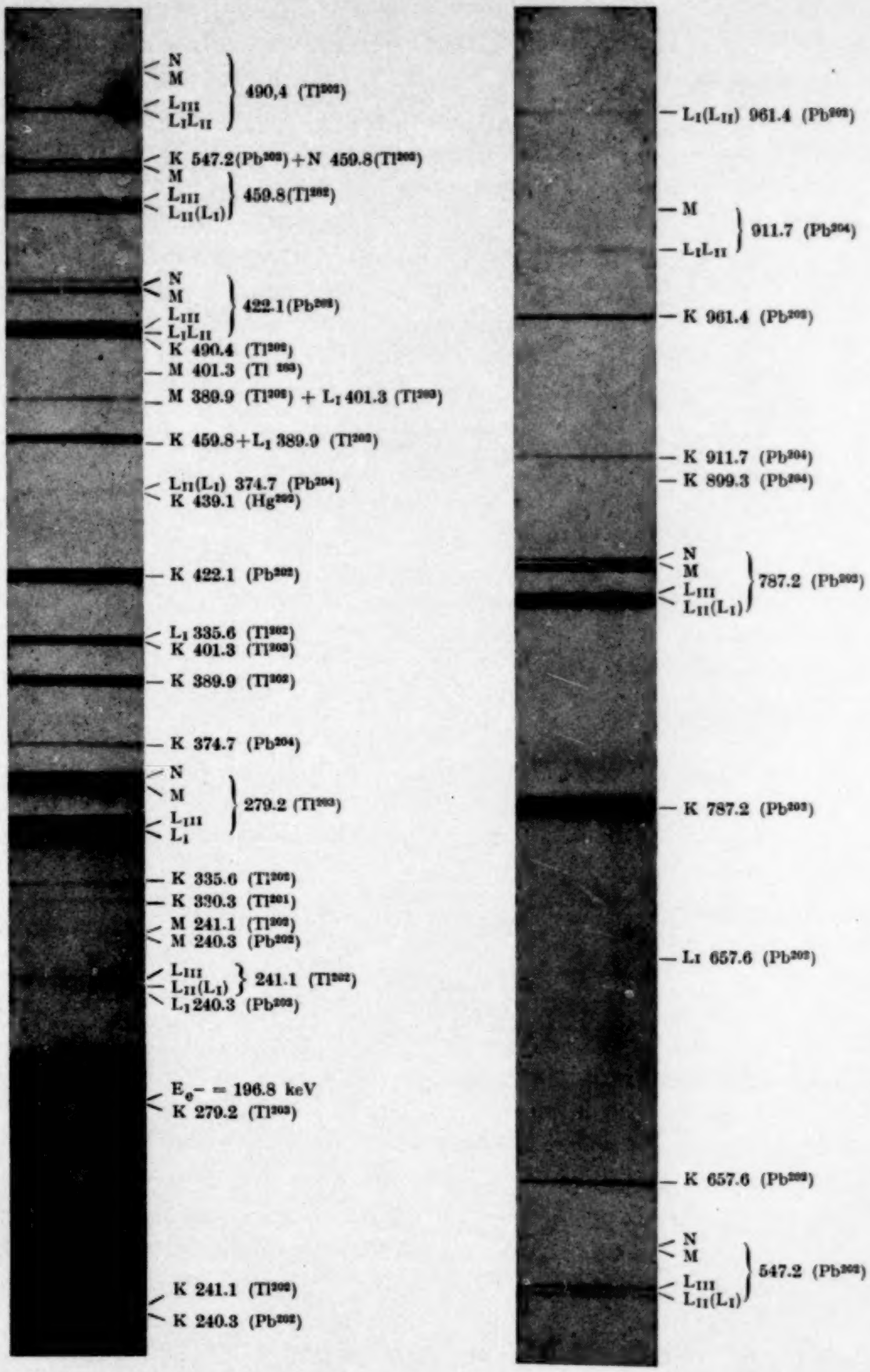

Fig. 3. Beta ray spectrum of Pb^{202m} recorded from a 6.7 hours' exposure in a permanent magnet spectrometer. The region L 459.8—N 547.2 is taken from a preceding exposure.

conversion line energy of the mean of the L_I- and L_{II}-binding energies gives a gamma energy in excellent agreement with that determined from other conversion lines of the transition. This L line is therefore denoted L_IL_{II} in table 1 and in figs. 3 and 4. In other similar cases, where, according to the multipolarity assignment, the L_I/L_{II} ratio [11]) should be different from 1, the gamma ray energy was obtained by adding to the L-conversion line energy a weighted mean value of the L_I- and L_{II}-binding energies. Such lines are denoted L_I, $L_I(L_{II})$ etc. in fig. 3 and in tables 1 and 2.

TABLE 3

Unassigned conversion lines in the decay of Pb^{202m}.

Electron energy (keV)	Relative intensity (K 787.2 = 100)	Possible assignment
196.8	2.64	K 282.2 (Tl) or K 284.8 (Pb) [L_I212.1 (Tl) or L_I 212.7 (Pb)]
204.2	0.12	K 289.7 (Tl) or K 292.0 (Pb)
208.6	0.54	K 294.1 (Tl) or K 296.6 (Pb) [M_I212.8 (Tl) or M_I 212.5 (Pb)]
211.5	0.17	K 297.0 (Tl) or K 299.5 (Pb) [N_I212.4 (Tl) or N_I 212.4 (Pb)]
516.6	0.25	K 602.1 (Tl) or K 604.6 (Pb)
524.5	0.051	K 610.0 (Tl) or K 612.5 (Pb)
527.6	0.17	K 613.1 (Tl) or K 615.6 (Pb)

Fig. 3 shows a film obtained in the permanent magnet beta spectrometer. In addition to Pb^{202} and Tl^{202} lines, there are also present the conversion lines of gamma rays emitted from the decays of 9.4-h Pb^{201} (only the strong K 330.3 line detectable), 52-h Pb^{203} and 67.5-min Pb^{204m}. Because of the large number of conversion lines, there is a great probability of overlapping. In the following, cases will be discussed where such overlapping of conversion lines made the assignment difficult.

An electron line of energy 304.4 keV is identified as a K line from the absence of any strong line having an energy in the vicinity of 232 keV. There are, in fact, some weak conversion lines in this region, but none of them is within one keV of the energy of any K line which would correspond to the 304.4 keV line, if it were the L line of a gamma ray converted in Tl or Pb. The 304.4 keV line is so strong (cf. table 2: 389.9 K) that, if it were an L line, the gamma ray would need to have a higher multipolarity than 2^5-pole for its K line to remain undetected in our spectra. If the 304.4 keV line is a K line, its corresponding L line should be in the vicinity of either 375 keV or 377 keV, depending on whether it is converted in Tl or Pb. A line of energy 374.3 keV is observed, but by the presence of other lines, it is identified as being (at least partly) the K line of a 460 keV gamma ray, converted in Tl. A line of 377 keV would be clearly resolvable from the

374.3 keV line, since the momentum difference between two such lines is 0.45 %. No such line is seen, and hence it is assumed that we have two gamma rays, both converted in Tl, of energies such that the K line of one ($E_\gamma = 459.8$ keV) is almost coincident with the L line of the other ($E_\gamma = 389.9$ keV). The identification of these lines is supported by other conversion lines of these gamma rays (cf. table 2).

One group of conversion lines is identified as the L, M and N lines of a 490.4 keV gamma ray (cf. fig. 3). The corresponding K line would have a position very close to the 422.1 L group, but was not seen in measurements at 0.3 % resolution. For this reason the 422.1 L group was measured at 0.16 % resolution. As can be seen from fig. 4, there is a conversion line very close to the 422.1 L_I and L_{II} lines, which is interpreted as the K line of a 490.4 keV gamma ray converted in Tl.

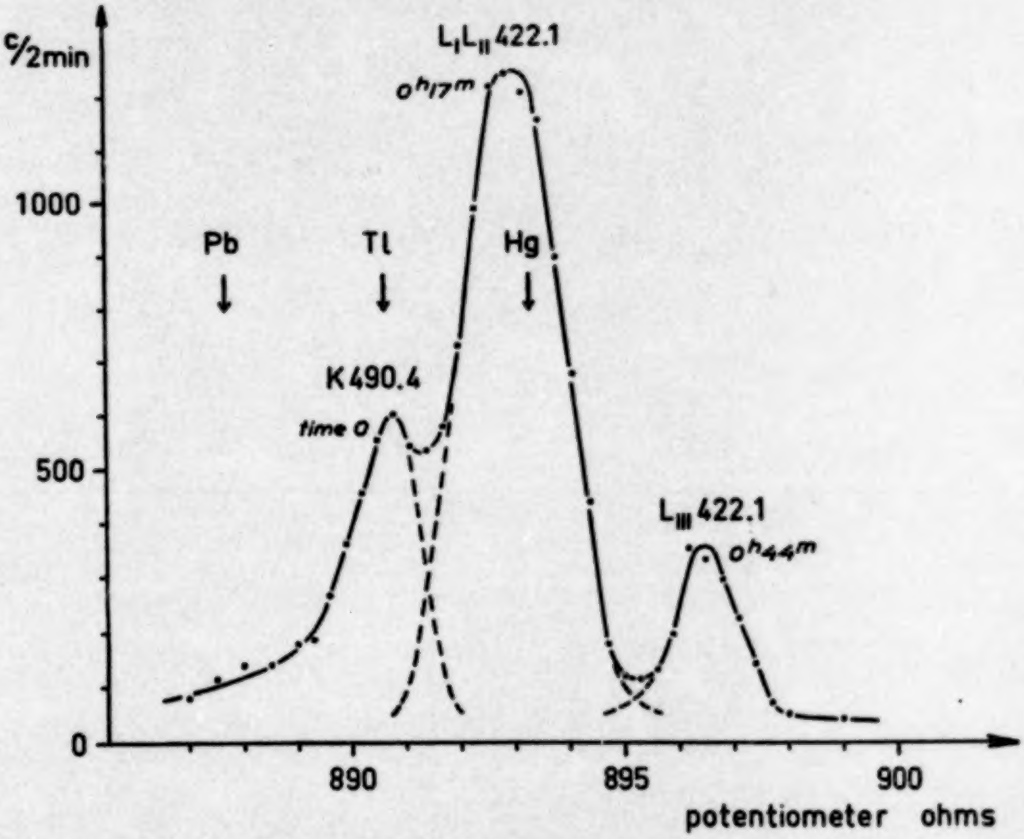

Fig. 4. The (K 490.4, L 422.1) group as measured at 0.16 % resolution in a double-focusing spectrometer. As indicated by the arrows, the location of K 490.4 shows that the 490.4 keV transition is converted in Tl.

The 547.2 keV transition was first discovered from its L-, M- and N-conversion lines (cf. figs. 3 and 5). The 547.2 L_{III} line and the K line of the 622.2 keV transition of 67.5-min Pb^{204m} partly overlap. The multipole

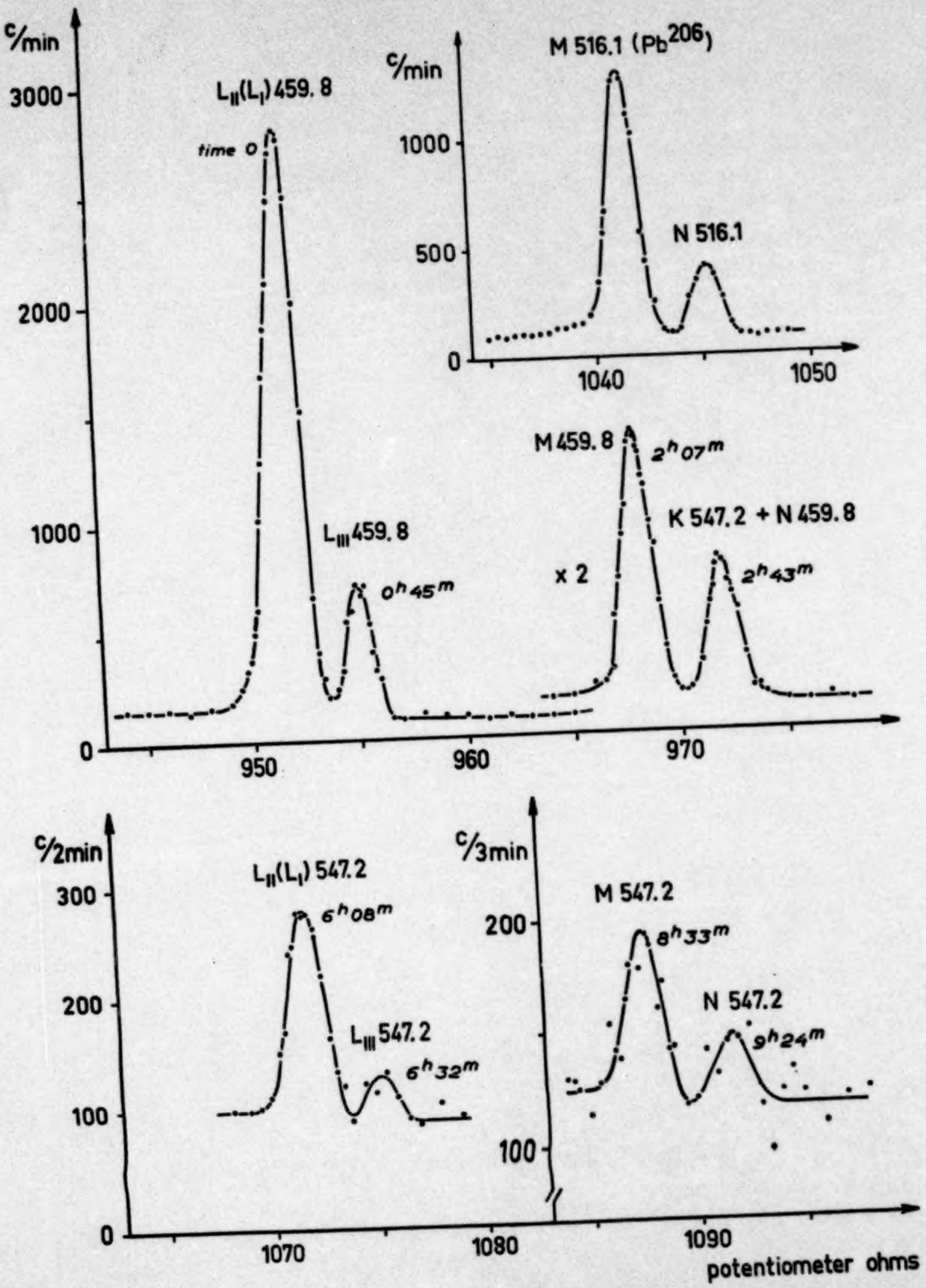

Fig. 5. Conversion-electron lines of the 459.8 keV E3 and 547.2 keV E5 transitions as measured in a double-focusing spectrometer at 0.16 % resolution. The existence of K 547.2 is proved from a comparison between the M/N ratio of the 459.8 group (Tl^{202}) and that of the 516.1 (E3) group (Pb^{206}, from the decay of 6–d Bi^{206}) shown in the inset.

order of the 547.2 keV gamma ray was assumed to be high, since no strong K line was found. If this gamma ray were converted in Pb, its energy should differ by less than 0.5 keV from the N line of the 459.8 keV E3 transition, which means that these lines could not be resolved in our measurements. However, the M and N lines of this transition were measured in the double-focusing spectrometer at 0.16 % resolution, and were compared to the M and N lines of the 516 keV E3 transition in Pb^{206}, which had been measured in a previous investigation [12]), (cf. fig. 5). The M/N ratios of these two E3 transitions should be nearly the same, but were here found to be 1.7 ± 0.2 and 4.3 ± 0.4 respectively. This proves that there is a line superimposed on the N 459.8 line, and it is interpreted as the K line of the 547.2 keV gamma ray converted in Pb. The K/L ratio of this transition could also be calculated and indicates a high multipole order (cf. table 1). (Coincidence measurements confirmed that the gamma ray is converted in Pb (cf. table 8)).

In previous investigations a gamma ray of energy 401.3 keV converted in Tl has been reported [3, 4, 5]). This energy is identical with that of the gamma ray known to occur in the decay of 52-h Pb^{203}. This 52-h activity is always present in our sources. The assignment of a gamma ray of the same energy to the decay of Pb^{202m} was presumably made on the basis of an apparent anomaly between the relative intensities of the conversion lines of Pb^{203} as they occur in these sources and as they occur in sources of Pb^{203} prepared in other ways. However, we have made a careful measurement of the decay of the K 401.3 line and found no indication of any 3.6-h component superimposed on the 52-h decay. Thus we do not include any gamma ray of this energy amongst those following the decay of Pb^{202m}.

Table 3 includes those electron lines, for which no definite assignments could be made. Since no energy correspondences were found, they are all suggested to be K lines.

The conversion lines of electron energies 196.8, 208.6 and 211.5 keV (cf. table 3) might be identified as L_I, M and N lines respectively of a gamma ray of about 212 keV, converted in Tl or Pb. As no corresponding L_{III} line is observed, the multipolarity of the transition would be M1 or M2. The K line, which would have a position in or close to the M 129.3 group, is not observed in a photographic spectrum with the $(M_I + M_{II})$, M_{III} and $(M_{IV} + M_V)$ lines well resolved. The expected intensity of K 212 is, however, so low that the line may be superimposed on one of the M lines and thus remain undetected. With the available data it is impossible to make definite conclusions about the 212 keV transition. Its existence seems doubtful, however, on account of the value $L/M = 5$, which seems abnormally high.

4. Intensities of Conversion Lines; Conversion Ratios

Tables 1, 2 and 3 include the relative intensities of some K-conversion lines, (or L-conversion lines in those cases, where the K lines are either very weak or not directly measurable due to overlapping), K/L ratios, $(L_I + L_{II})/L_{III}$ ratios, and the multipolarities assigned to the gamma rays. The multipolarity assignments are all consistent with the measured conversion ratios, but are not assigned solely on this basis. Indeed there are only a few cases in which the measured conversion ratios are sufficiently significant to exclude all but one possible multipolarity. However, other factors support the assignments shown in the tables. Firstly, there are the accurate measurements of the L-line energies, as discussed in section 3. Secondly, taking transition intensities into account, it is found that a consistent decay scheme can be deduced only if the multipolarities shown in the tables are adopted. Thirdly, gamma transition probabilities discussed in section 8 give in some cases definite multipole order.

5. Levels in Pb^{202}; Multipolarities of Gamma Rays

Fig. 6 shows the level scheme of Pb^{202}. The levels of 961.4 keV (2+), 1383.6 keV (4+), 2041.1 keV (5−), and 2170.4 keV (9−) have been suggested (with slightly different energy values) in previous investigations [2, 3, 4, 5]). The 2041.1 keV level suggestion is strongly supported by the energy sum:

129.3+657.6 = 786.9 (cf. energy of cross-over gamma ray = 787.2 keV). In addition, a new level is suggested by the energy sum of two weak transitions:

$$547.2+240.3 = 787.5 \text{ (cf. } 787.2 \text{ keV).}$$

Previous measurements gave no experimental proof for the succession of the 961.4 and 422.1 keV transitions. For this reason the ratios K 422.1/K 961.4 obtained from the decays of Pb^{202m} and Bi^{202} were compared. From table 1 it is seen that in the decay of Pb^{202m} the ratio of the intensities of the two conversion lines K 422.1/K 961.4 is 5.1±0.5. However, in the decay of Bi^{202} this ratio is found to be 3.9±0.4, indicating that the 961.4 keV transition has a greater relative intensity in the latter decay, due to feeding from higher levels. This shows that the 961.4 keV transition is emitted after the 422.1 keV transition.

Further support for the suggested level scheme is obtained by considerations of transition intensities. The transition intensity I, defined by

$$I = I_K + I_L + I_M + I_N + \ldots + I_\gamma,$$

(where the quantities on the right hand side of the equation are the contributions to the transition intensity, which arise from K, L, M, N, ...

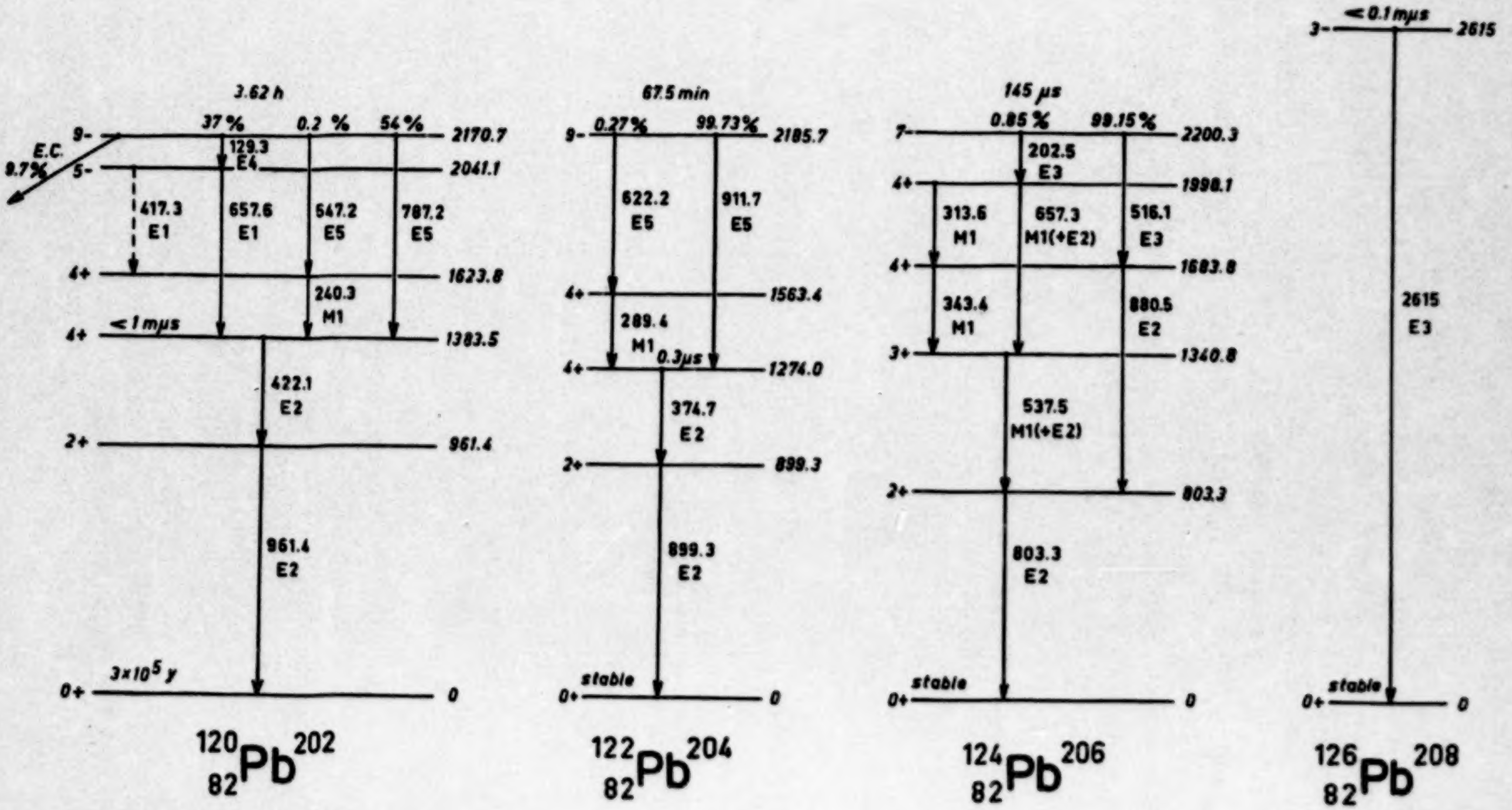
3.62 h
37 %
0.2 %
54 %
E.C.
9.7%
9-
5-
4+
4+
2+
0+
2170.7
2041.1
1623.8
1383.5
961.4
0
129.3
E4
417.3
E1
657.6
E1
547.2
E5
787.2
E5
240.3
M1
<1 mμs
422.1
E2
961.4
E2
3×10⁵ y
120 82 Pb 202
67.5 min
0.27%
99.73%
9-
4+
4+
2+
0+
2185.7
1563.4
1274.0
899.3
0
622.2
E5
911.7
E5
289.4
M1
0.3μs
374.7
E2
899.3
E2
stable
122 82 Pb 204
145 μs
0.85 %
99.15 %
7-
4+
4+
3+
2+
0+
2200.3
1998.1
1683.8
1340.8
803.3
0
202.5
E3
313.6
M1
657.3
M1(+E2)
516.1
E3
343.4
M1
880.5
E2
537.5
M1(+E2)
803.3
E2
stable
124 82 Pb 206
<0.1 mμs
3-
0+
2615
0
2615
E3
stable
126 82 Pb 208

Fig. 6. Decay schemes of Pb^{202m} and, for comparison, the decay schemes of Pb^{204m} [6]), Pb^{206m} [30]), and Pb^{208m} [21]). The Tl branch of Pb^{202m} is shown in fig. 7. Transition intensities as calculated from conversion-line intensities are given in percent per disintegration at the head of some of the transitions. The weak 417.3 keV E1 transition in Pb^{202m} (K-line intensity estimated at about 0.1 % of the intensity of the neighbouring K 422.1) was not observed in the measurements. As can be seen above, the level schemes of the neutron-deficient isomers show a striking similarity. The levels probably represent neutron-excited states, because in Pb^{208} the first excited state is as high as 2.6 MeV.

conversion and gamma ray emission, respectively), can be written

$$I = I_K[1+1.3/(K/L)+1/\alpha_K].$$

The values of I were calculated by use of the relative K-conversion intensities I_K ($I_K(787.2) = 100$), the theoretical values [13]) of the K-conversion coefficient α_K and the experimental values of the conversion ratio K/L (cf. table 1). In those cases, where the K-line intensity could not be directly measured, the value I_K was calculated from the measured L-line intensity (cf. table 1) and the theoretical [11]) value of K/L. A discussion of the transition intensities is therefore intimately connected with the multipolarity assignments of the transitions. The transition intensities based on the adopted multipolarities are given in table 4.

TABLE 4

Transition intensities in the decay of Pb^{202m} (Pb branch)

E_γ (keV)	Multi-polarity	Relative transition intensities (adopted from conversion line intensities with K 787.2 = 100)				
129.3	E4		990±70	980±60 adopted value	2425±110 sum	2335±100 mean value of total transition intensity
657.6	E1	965±90	Sum: 971±90			
417.3 †	E1	6.0±1.1††				
547.2	E5		5.2±0.5	5±1 adopted value		
240.3	M1	11.2±0.9	Diff.: 5.2±0.5			
417.3 †	E1	6.0±1.1††				
787.2	E5			1440±90		
422.1	E2				2300±170	
961.4	E2				2280±180	

† Possible E1 transition between the 2041.1 and 1623.8 keV levels, (see section 5).

†† The intensity value obtained as the difference between the intensities of the 240.3 and 547.2 keV transitions (cf. decay scheme of fig. 6).

Multipolarity assignments and transition intensities will be discussed below in the order convenient for the construction of the level scheme.

γ(961.4): The measured K/L ratio 5.0±0.7 does not decide between the multipolarities M2 and E2 [theoretical values [11]): 5.4 (M2) and 4.9 (E2)]. However, from the photographic spectrum, the intensity ratio $(L_I+L_{II})/L_{III}$ is estimated at about 15, which should be compared to the theoretical values [11]) of 76 and 17 for M2 and E2 respectively. Hence the E2 assignment seems quite definite for this transition. This assignment is also supported by the fact that the transition takes place from a state, which is believed to be the first excited state (2+) of the even-even nucleus

Pb^{202}. The E2 assignment gives rise to a transition intensity $I = 2280 \pm 180$ for this transition.

γ(422.1): The values $K/L = 2.6 \pm 0.3$ and $(L_I + L_{II})/L_{III} = 5.6 \pm 0.8$ found for this transition are consistent only with an E2 assignment (theoretical values [11]): 2.6 and 4.8 respectively). This assignment is also supported by the measured energy value of the $L_I L_{II}$ line (see section 3). Within the experimental errors, an E2 assignment of the 422.1 keV transition gives the same transition intensity ($I = 2300 \pm 170$) as was adopted for the 961.4 keV transition ($I = 2280 \pm 180$), which is also required by the level scheme. Angular correlation measurements by Wiedling [14]) suggest the spin combination 0, 2, 2 or 0, 2, 4. In our experiments there is no evidence for a ground-state transition from the 1383.5 keV level. For these reasons the assignments 2+ and 4+ for the first two excited states seem to be well established.

γ(787.2): For this transition the conversion ratio $K/L = 1.18 \pm 0.10$ was found. The only theoretical values [11]) of K/L which can be considered for this energy are 1.4 (E5) and 2.0 (E4). An E5 assignment seems therefore probable for this transition. The ratio $(L_I + L_{II})/L_{III}$, estimated at about 10 from the photographic film, is in agreement with this assignment [theoretical value [11]): 10.9 (E5)]. The E5 assignment is supported by the lifetime of the isomeric state, (see section 8). This assignment suggests the spin 9− for the 2170.7 keV state, and gives rise to an intensity $I = 1440 \pm 90$ for the 787.2 keV transition.

An estimate of a possible M6 admixture in the 787.2 keV E5 transition can be made by comparing its experimentally found K-conversion coefficient with the theoretical K-conversion coefficients [13]) for E5 and M6 transitions of this energy. By taking the total transition intensity in the Pb branch as the average of the intensities of the 961.4 and 422.1 keV transitions, one finds $I_{tot} = 2290 \pm 130$ (cf. table 4). Subtraction of the sum $I = 985 \pm 60$ of the transition intensities of the (129.3−657.6) and (547.2−240.3) cascades gives: $I_{787.2} = 1305 \pm 150$. By use of this equation (cf. the formula for I) and the values of I_K (787.2) and K/L (787.2) from table 1, the experimental value of the K-conversion coefficient is found to be $\alpha_{787.2} = 0.091 \pm 0.014$. Thus, from a comparison between the value $0.105 (= 0.091 + 0.014)$ and the theoretical values [13]) 0.082 and 0.874 for E5 and M6, respectively, the upper limit of M6 admixture in the 787.2 keV E5 transition is found to be about 3 %.

γ(129.3): As discussed in section 3, the L-conversion lines of the 129.3 keV transition were interpreted as L_{II} and L_{III} lines, suggesting an electric transition of high multipole order. This is also confirmed by the intensity ratios of the conversion lines. On the basis of its $(L_I + L_{II})/L_{III}$ ratio. 1.88 ± 0.12, the 129.3 keV transition is of multipolarity E4 or E5 [cf.

theoretical values [11]) : 1.9 (E4) and 2.0 (E5)]. These are also the only multipolarities, which are consistent with the measured value $K/L < 0.008$ (theoretical values [11]) : < 0.01 for E4 and E5). From life-time considerations, however, the E4 assignment is more probable, (see section 8). The value of I for the 129.3 keV transition is found to be 990 ± 70 for both the E4 and E5 assignment. As will be shown below, the consideration of transition intensities also supports the E4 assignment for the 129.3 keV transition, (cf. table 5).

The possible admixture of M5 radiation in the 129.3 keV E4 transition cannot be estimated from a calculation of the conversion coefficient on account of the strongly dominating conversion electron intensity in this case. However, from a comparison between the experimental value of $(L_I+L_{II})/L_{III} = 1.88 \pm 0.12$ and the theoretical values [11]) 1.91 (E4) and 0.29 (M5), the upper limit of M5 admixture was found to be about 9 %.

γ(657.6): If the cross-over suggested by the energy sum $129.3+657.6 = 786.9$ keV does occur, and if the multipolarity of the 129.3 keV transition is E4 or E5, conservation of parity and angular momentum requires the 657.6 keV transition to have multipolarity E1 or M1, respectively. Either of these assignments would fit the value $K/L = 5.5 \pm 0.7$, which was found for this transition [cf. theoretical values [11]) : 6.4 (E1) and 6.0 (M1)]. The energy of its L-conversion line suggests that it is an L_I line, and while this fact confirms the low multipolarity, it does not distinguish between the E1 and M1 possibilities. However, the E1 assignment is adopted, since I(657.6) has calculated values of 965 ± 90 or 110 ± 10 for the E1 or M1 assignments, respectively (cf. $I(129.3) = 990 \pm 70$), and it is clear that the measurements are all consistent with a 129.3 keV (E4)$-$657.6 keV (E1) cascade, (cf. table 5). The 2041.1 keV state is therefore suggested to have spin and parity 5$-$.

TABLE 5

129.3$-$657.6 cascade

E_γ (keV)	Relative transition intensities	
129.3	990 ± 70 (E4)	990 ± 70 (E5)
657.6	965 ± 90 (E1)	110 ± 10 (M1)

γ(547.2): The values $K/L = 0.8^{+0.1}_{-0.3}$ (see section 3) and $(L_I+L_{II})/L_{III} = 6.0 \pm 1.5$ for this transition suggest the multipolarity E5 or E4, [theoretical K/L values [11]): 0.64 (E5) and 1.0 (E4), and theoretical $(L_I + L_{II})/L_{III}$ values [11]): 7.1 (E5) and 7.2 (E4)]. From life-time consideration, however, the E5 assignment is preferable (see section 8). The intensity I of the 547.2

keV transition is found to be 5.2±0.5 if the multipolarity is E5, and 13.8±1.4 if it is E4. As will be shown below, a comparison with the intensity of the 240.3 keV transition supports the assignment E5 to the 547.2 keV transition, (cf. table 6).

$\underline{\gamma(240.3)}$: The energy sum $547.2+240.3 = 787.5$ keV strongly suggests the 547.2 and 240.3 keV transitions to be emitted in cascade from the 9− level. If the 547.2 keV transition has the multipolarity E5 or E4, conservation of parity and angular momentum requires the 240.3 keV transition to be of multipolarity M1 or E1. Either of these transitions is suggested also by the measured K/L ratio 5.0±0.6 for this transition [cf. theoretical values [11]): 5.8 (M1) and 5.7 (E1)]. To decide which multipolarity should be chosen, transition intensities can be considered. The transition intensity of the 240.3 keV transition is found to be 11.2±0.9 or 102±10 for the M1 or E1 assignments, respectively.

TABLE 6

547.2−240.3 cascade

E_γ (keV)	Relative transition intensities	
547.2	13.8±1.4 (E4)	5.2±0.5 (E5)
240.3	102±10 (E1)	11.2±0.9 (M1)

Both of these values are higher than expected from the possible intensities of the 547.2 keV transition (cf. table 6). This might be understood by introducing a transition of 417.3 keV from the 2041.1 keV level to the 1623.8 keV level. If the E5−M1 sequence is accepted, the K-line intensity of this 417.3 keV transition (E1) would be about 0.1 % of the K 422.1 intensity. These two lines are too close to allow such a high intensity difference to be detected in these experiments. On the other hand, if the E4−E1 combination is chosen, the K 417.3 (M1) intensity would be about 15 % of K 422.1 and thus be possible to detect. As no K line corresponding to the 417.3 keV transition is observed, the cascade $\gamma(547.2)-\gamma(240.3)$ is consistent with the E5−M1 assignments. The spin and parity of the intermediate state should then be 4+.

In this way a total intensity of 2425±110 is found for the transitions from the 9− level to the lower 4+ level, and, if the decay scheme is correct, the same I value is expected to be found for each of the 422.1 and 961.4 keV transitions. Within the experimental errors, this is in fact also the case (cf. table 4).

$\gamma-\gamma$ coincidence measurements on the strongest transitions in Pb^{202} were carried out by the Amsterdam group [2]) and by Åström and Johansson[15]) and support the suggested level scheme. The 547.2 keV transition was investigated by us in electron-electron coincidence measurements (see subsection 6.2.b). As can be seen from table 8, the coincidence experiments support the position of the 547.2 keV transition in the level scheme (see fig. 6).

It can therefore be concluded that the level energies and assignments suggested for Pb^{202} are well established (cf. decay scheme of fig. 6). It cannot be excluded that some of the weak unassigned lines in table 3 are due to transitions in Pb^{202}, and thus may be able to give additional information about levels in Pb^{202}. These transitions are, however, relatively weak. Even if the lines (assumed to be K lines) are due to E1 transitions, the transition intensities are found to be smaller than 50 units. An exceptional case is the 196.8 keV electron line, which would be due to an E1 transition with an intensity of 135 units. Under all circumstances, however, these transitions cannot give any notable contribution to the total transition intensity.

As can be seen from fig. 6, there is a striking similarity between the level schemes of Pb^{202m}, Pb^{204m} and Pb^{206m}. Their levels probably represent neutron-excited states, because in Pb^{208} the first excited state is as high as 2.6 MeV.

6. Levels in Tl^{202}

6.1. MULTIPOLARITIES OF GAMMA RAYS

From the energies of the gamma rays converted in Tl (see table 2) little information can be obtained about the levels in Tl^{202}. Even if the unassigned conversion lines (see table 3) are assumed to be K or L lines of transitions in Tl^{202}, no cross-over transitions are indicated except for the cascade suggested by the sum relation

$$241.1+148.9 = 390.0 \quad (\text{cf. } E_\gamma = 389.9 \text{ keV}).$$

Because of the scarcity of sum relations, it seems plausible to assume that several gamma rays are emitted in succession without any cross-over transitions. The absence of such transitions indicates successively decreasing angular momentum of the levels. If this be a correct interpretation, several transitions with the same intensity must exist. Below, an attempt to assign multipolarities to the gamma rays is made in order that the transition intensities may be calculated. It should be pointed out that in a few cases the internal-conversion data cannot directly decide between two multipolarity suggestions. However, in the last part of this section some requirements which must be fulfilled by levels in Tl^{202} populated from the 9− state in Pb^{202}, will be discussed. These requirements lead to unambiguous multipolarity assignments.

$\gamma(459.8)$: As mentioned in section 3, the conversion lines K 459.8 and L 389.9 overlap. It is therefore not possible to obtain a K/L value of the 459.8 keV transition directly. However, an upper limit can be obtained from the intensity relations below (cf. table 2):

$$I_K\,(389.9) = 28 \pm 3$$
$$I_K\,(459.8) + I_L\,(389.9) = 17 \pm 2$$
$$I_L\,(459.8) = 9 \pm 1.$$

As K/L (389.9) cannot take a higher value than 6.3 [11]), it follows that K/L (459.8) < 1.7. This value suggests the multipolarities E3, E4, E5 or M5, [theoretical values [11]): 1.4 (E3), 0.7 (E4), 0.4 (E5) and 1.5 (M5)]. The experimental value of $(L_I + L_{II})/L_{III} = 5.1 \pm 0.5$ rules out M5, as the theoretical values [11]) are 6.5 (E3), 5.2 (E4), 5.2 (E5) and 1.9 (M5). Further, as will be seen in section 8, life-time considerations exclude all multipolarity assignments apart from E3 and M3. A difficulty with an E3 assignment for the 459.8 keV transition is the low experimental $(L_I + L_{II})/L_{III}$ ratio. It has recently been shown by Andersson and Bergström [16]) that the experimental $(L_I + L_{II})/L_{III}$ values for $Z = 77-82$ vary smoothly with energy, but are considerably lower than the theoretical values of Rose *et al.* [11]). The value 5.1 for the $(L_I + L_{II})/L_{III}$ ratio of the 459.8 keV transition fits the empirical $(L_I + L_{II})/L_{III}$ curve for E3 transitions very well. No similar deviations were found for other multipolarities. In particular, it was shown that experimental and theoretical K/L values agree well. The multipolarity E3 for the 459.8 keV transition can therefore be accepted with confidence. The theoretical value K/L (459.8) = 1.4, combined with the value $I_L(459.8) = 9 \pm 1$, gives $I_K(459.8) = 13 \pm 1$ and a transition intensity $I = 230 \pm 15$ for the 459.8 keV transition.

$\gamma(389.9)$: By use of the intensity relations above, the value K/L (389.9) = $= 6 \pm 3$ can be calculated, suggesting an M1, E1 or M2 transition, [theoretical values [11]): 6.0 (M1), 6.1 (E1) and 4.5 (M2)]. For these multipolarities the transition intensities are 210 ± 25, 2200 ± 250 and 90 ± 10, respectively. Inclusion of the cross-over transition intensity (see below) gives the values 240 ± 25, 2230 ± 250 and 120 ± 10, respectively. The first value is almost identical with the value 230 ± 15 of the 459.8 keV transition. Thus, if the 459.8 and 389.9 keV transitions be emitted in cascade, the latter transition must have a multipolarity M1. As will be shown later in this section, there are strong reasons for believing this to be the case.

$\gamma(241.1)$: The measured intensity ratios $K/L = 1.3 \pm 0.2$ and $(L_I + L_{II})/$ $/L_{III} = 2.5 \pm 0.3$ suggest an E2 transition (theoretical values [11]): K/L = 1.3 and $(L_I + L_{II})/L_{III} = 2.5$). The possible admixture of M1 should be less than about 0.2 %. It is therefore assumed that this transition takes place with an angular momentum change of 2 units. The transition intensity for an E2 assignment is 29 ± 3.

γ(148.9): As mentioned above, the energy sum 241.1+148.9 = 390.0 keV strongly suggests the 241.1 and 148.9 keV transitions to be emitted in cascade from the same level as the 389.9 keV transition. The absence of an L_{III}-conversion line suggests a low multipole order for the 148.9 keV transition. This is confirmed by the measured value K/L = 6.1±1.2, which indicates an E1 or M1 transition, [theoretical values [11]): 5.5 (E1) and 5.9 (M1)]. Since the assignment for the 389.9 keV transition is taken to be M1, and that for the 241.1 keV transition E2, conservation of parity excludes the multipolarity E1 for the 148.9 keV transition. The transition intensity is found to be 27±3 for an M1 assignment (140±15 for E1), which is about the same as was found above for the 241.1 keV transition (29±3). Hence, there is no evidence for any additional feeding to the intermediate level from which either the 241.1 or 148.9 keV transition takes place.

γ(490.4): The measured value of K/L = 3.5±1.0 suggests the multipolarity to be E2, M2 or M3 for this transition, [theoretical values [11]): 3.2 (E2), 4.7 (M2) and 3.4 (M3)], but only E2 and M3 are in agreement with the experimental value $(L_I+L_{II})/L_{III} = 8\pm2$, [theoretical values [11]): 6.2 (E2), 29 (M2) and 8.3 (M3)]. The transition intensity is found to be 260±35 for the multipolarity E2 and 17±3 for M3. As will be shown below, it must be assumed that the 490.4 keV transition is emitted after the 459.8 keV transition, and must, for this reason, have a transition intensity of at least 200 units. Only the E2 assignment fulfils this requirement.

TABLE 7

Transition intensities in the decay of Pb^{202m} (Tl branch)

E_γ (keV)	Multi-polarity	Relative transition intensities (adopted from conversion line intensities, with K 787.2 = 100)			
335.6	E1 M1	71±6 6.6±0.5			
389.9	M1	210±25		sum: 240±25	245±20 mean value of total transition intensity
241.1 148.9	E2 M1	29±3 27±3	mean value: 28±3		
459.8	E3	230±15			
490.4	E2	260±35			

γ(335.6): There is no accurate information about the conversion intensities of the 335.6 keV transition. Its K/L ratio ≈ 5 indicates the multipolarity M1 or E1. Even if no definite multipolarity assignment for this gamma ray can be made, it should be noticed that its transition intensity must under all circumstances be smaller than 77 units, (see table 7). This information will be used later.

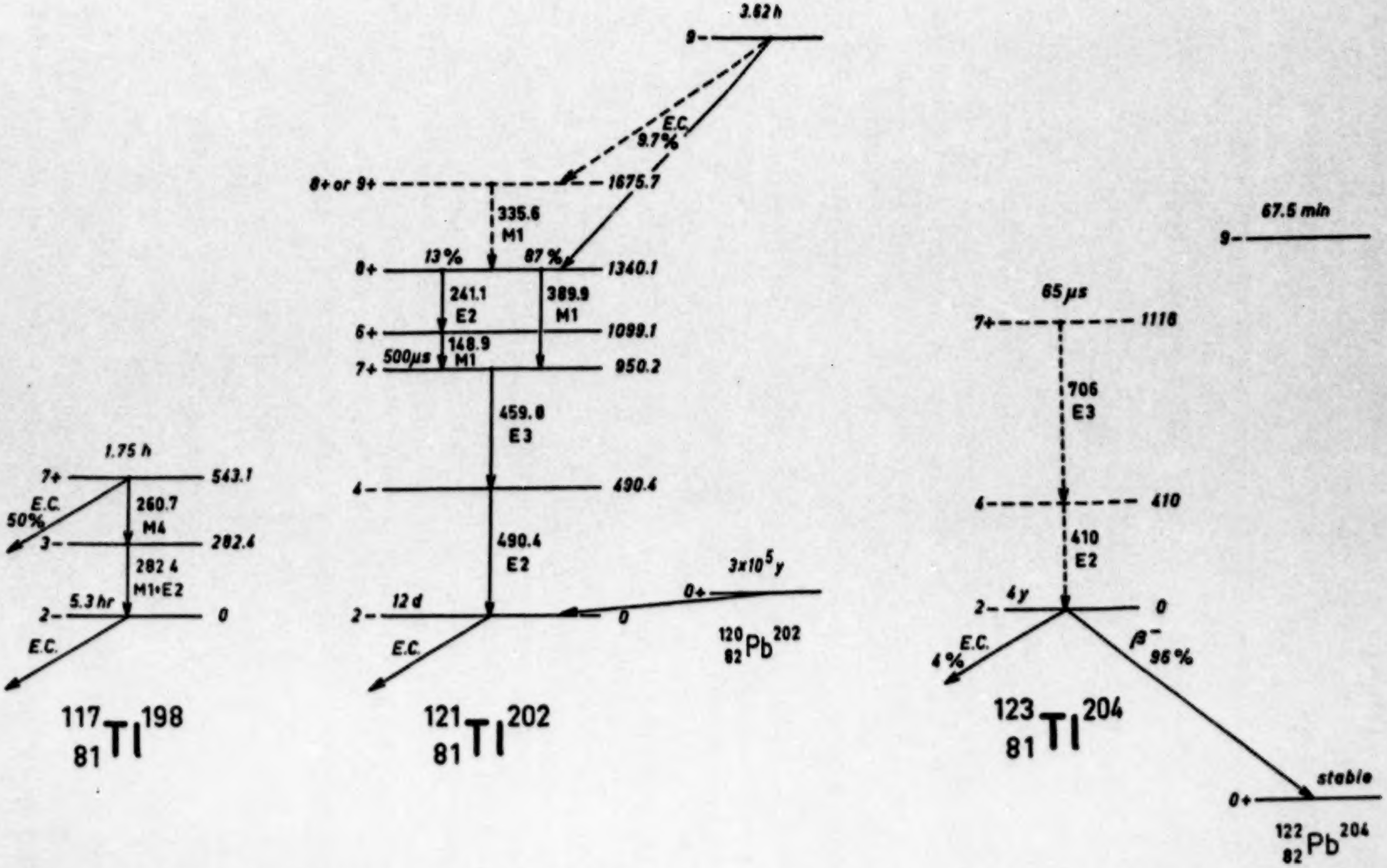
3.62 h
9-
E.C.
9.7%
8+ or 9+
1675.7
335.6
M1
13%
87%
8+
1340.1
241.1
E2
389.9
M1
6+
1099.1
148.9
M1
500μs
7+
950.2
459.8
E3
4-
490.4
490.4
E2
12 d
2-
0
E.C.
0+
3x10⁵y
120 82 Pb 202
121 81 Tl 202
1.75 h
7+
543.1
E.C.
50%
260.7
M4
3-
282.4
282 4
M1+E2
5.3 hr
2-
0
E.C.
117 81 Tl 198
67.5 min
9-
65 μs
7+
1118
706
E3
4-
410
410
E2
4y
2-
0
E.C.
4%
β⁻
96%
123 81 Tl 204
stable
0+
122 82 Pb 204

Fig. 7. Levels in Tl^{202} reached in the decay of 3.62-h Pb^{202m}. The position of the 335.6 keV transition is uncertain. Transition intensities, as calculated from the intensities of the conversion lines, are given in per cent for some of the transitions. For comparison, the experimentally found level scheme of Tl^{198m} 19) is given and also a proposed level scheme of Tl^{204m} (cf. subsection 6.2.c).

Other possible gamma rays: The unassigned conversion lines, given in table 3, may also be due to transitions in Tl^{202}. Their transition intensities should all be smaller than 50 units, except for one case where $I \leqq 135$ units, (see end of section 5).

The transition intensities based on the adopted multipolarities of the transitions in Tl^{202} are given in table 7. As can be seen in the table, the total transition intensity is found to be 245±20, in the Tl branch of Pb^{202m}.

6.2. DISCUSSION OF ADDITIONAL INFORMATION RELEVANT TO THE CONSTRUCTION OF THE LEVEL SCHEME OF Tl^{202}

a) *Spins and parities of the ground state and the "capture state" in* Tl^{202}

It seems plausible to assume that the ground state of Tl^{202} should have spin and parity 2— or 3— ($s_{\frac{1}{2}}$ proton, $f_{5/2}$ neutron). Measurements have shown that Tl^{200} 17) and Tl^{204} 18) have 2— ground states, and that the ground state of Tl^{198} 19) has spin 2. Kramer *et al.*20) suggested 1— or 2— for the ground state of Tl^{202}. However, the alternative 1— seems impossible for reasons discussed below in section 7. A 2— ground state in Tl^{202} is therefore adopted.

The levels in Tl^{202} which are reached by electron capture from the 9— state in Pb^{202} should have spins 8, 9 or 10 only. Hence, in the Tl branch of Pb^{202m} there should be found a cascade of gamma rays "carrying away" an angular momentum of at least 6 units. This is in fact also the case, since this requirement is fulfilled by the 389.9 (M1), 459.8 (E3) and 490.4 (E2) gamma rays, suggested to be emitted from a state with spin 8.

Huizenga and Stevens21) observed L and M capture from the 0+ ground state in Pb^{202} ($T_{\frac{1}{2}} = 3 \times 10^5$ y) to the ground state of Tl^{202}, and suggests a capture-decay energy of 80±60 keV. The energy difference between the 9— (2170.7 keV) state in Pb^{202} and the ground state of Tl^{202} is therefore (2250±60) keV. Thus the energy sum (389.9+459.8+490.4 = 1340.1) keV gives rise to a decay energy of (910±60) keV for the capture transition from the 9— state in Pb^{202} to the state with spin 8 in Tl^{202}. As the partial capture half-life is about 40 hours (see section 7), the log *ft* value is found 22) to be 6.5. This suggests a first forbidden capture transition, which assigns positive parity to the state with spin 8. Although the classification of β-transitions according to *ft*-values is not so reliable for heavy nuclei as for light nuclei, it seems to give a consistent result in this case, because positive parity of the spin 8 state is also required by the multipolarity assignments M1, E3 and E2 of the 389.9, 459.8 and 490.4 keV transitions.

b) *Order of emission of gamma rays*

Electron-electron coincidence measurements are not complete. As can be seen from table 8, however, the available data definitely show that the

TABLE 8

Electron-electron coincidence measurements

Pair number	Conversion line focused in		Coincidence counting-rates			
	Channel I	Channel II	a Total coincidences = c_{tot} (c/min)	b Measured accidental coincidences = c_{acc} (c/min)	c Measured genuine coincidences = $c_{tot}-c_{acc}$ (c/min)	d Calculated genuine coincidences (c/min)
1	389.9 K	547.2 L	5.0±0.5	4.9±0.5	0.1±0.7	0[1]
2	389.9 K	490.4 K 422.1 L	17.8±1.1	17.4±1.1	0.4±1.5	0[1], 35[2]
3	389.9 K	459.8 K 389.9 L	7.3±0.6	5.8±0.5	1.5±0.8	0[1], 83[2]
4	389.9 L 459.8 K	389.9 L 459.8 K	3.9±0.5	2.0±0.4	1.9±0.7	0[1], 27[2]
5	490.4 K 422.1 L	547.2 L	1.0±0.2	0.4±0.2	0.6±0.3	1[1]
6	490.4 K 422.1 L	422.1K	9.8±0.7	7.1±0.6	2.7±0.9	0[1]
7	422.1 K	787.2 K	73 ±3	12 ±2	61 ±4	70[1]

[1] As expected from the level schemes of figs. 6 and 7.

[2] Expected coincidence rate if the 389.9 keV transition had a position below the isomeric level in Tl^{202}.

Because of possible systematic errors no coincidence effect is considered as significant, unless the ratio between the measured genuine and accidental coincidence counting-rates (columns c and b respectively) exceeds about 1. It was found that the measured accidental coincidence counting-rates (column b) agreed fairly well with the expected ones. For this reason, and in view of the satisfactory agreement between the measured and expected genuine coincidence counting-rates (see columns c and d) in a case in which a strong coincidence effect is expected (pair 7), it is fairly certain that the results obtained for pairs 2, 3 and 4 indicate that no prompt coincidences occur between the 389.9 keV transition and either the 459.8 or the 490.4 keV transition. Thus we conclude that the order of emission of the 389.9, 459.8 and 490.4 keV gamma rays is that given in fig. 7. Delayed coincidence measurements between the 787.2 and 422.1 K-conversion lines showed that the half-life of the lower 4+ state in Pb^{202} must be less than 5×10^{-8} sec. Wertheim and Pound [23] have found that this half life should be less than 10^{-9} sec.

389.9 keV transition is not in coincidence with either the 459.8 or the 490.4 keV transition. From this result, combined with the fact that only the 459.8 keV E3 gamma ray can be directly emitted from the 500 μs isomeric state in Tl^{202} (see sections 6.2. c and 8), it can be unambiguously concluded that gamma rays are emitted from the 8+ level in the following order: 389.9 keV (M1), 459.8 keV (E3) and 490.4 keV (E2).

The most probable order of the 241.1 keV (E2) and the 148.9 keV (M1) gamma rays is shown in the level scheme of fig. 7. The opposite order of these gamma rays and spin suggestions for the intermediate state other than 6+ leads to incompatibilities with capture and gamma transition probabilities.

Due to the lack of sum relations, the 335.6 keV gamma ray has been given the position shown in fig. 7. It should then be emitted from an 8+ or a 9+ state. Negative parity is excluded, because this assignment would lead to an allowed capture transition, which would very probably give rise to a much stronger transition intensity that than observed.

The unassigned lines (see table 3 and subsection 6.1) may also be due to gamma transitions from 8+, 9+ or 10+ states to the lowest 8+ state. It is hoped that these uncertain questions will be solved by using a faster coincidence circuit.

c) *Discussion of the isomeric decay in* Tl^{202}

Vegors and Axel [24]) found two isomers of half-lives 530±50 μs ($E_\gamma =$ $= 485\pm20$ keV) and 65±5 μs ($E_{\gamma1} = 410\pm15$ keV, $E_{\gamma2} = 706\pm20$ keV), when natural Tl was irradiated with 20 MeV gamma rays. Tove [25] and Åström [26]) showed by two different methods that, in the decay of electromagnetically separated Pb^{202m}, a state with a half-life of about 500 μs is present. It is therefore very probable that the 530 μs activity observed by Vegors and Axel is due to the isomeric state in Tl^{202}. This conclusion is emphasized by the fact that Vegors and Axel did not observe the strong 389.9 keV transition. The energy 485 keV of the observed photo peak is in agreement with the unresolved photopeaks of the 459.8 and 490.4 keV transitions.

A speculation on the origin of the 65-μs activity observed by Vegors and Axel should be of interest. The abundance of the isotopes in natural Tl is 29.5 % Tl^{203} and 70.5 % Tl^{205}. Since the 530-μs activity, according to our interpretation, is obtained in a (γ, n) reaction in Tl^{203}, it seems very probable that the 65-μs activity arises from a (γ, n) reaction in Tl^{205}. The production of metastable states in Tl^{203} and Tl^{205} by (γ, γ) reactions can be excluded because of the fact that the $d_{3/2} \rightarrow s_{\frac{1}{2}}$ transitions of energies 279 and 205 keV in Tl^{203} and Tl^{205}, respectively, did not appear in the experiment of Vegors and Axel.

The half-life 65 μs and a gamma ray energy of 706 keV may suggest a slow E3 transition. The isomeric levels in both Tl^{198m} [19]) and Tl^{202m} are 7+ levels. If this is the case also for Tl^{204}, the level scheme shown in fig. 7 can be deduced, (ground state 2− ascertained [18])). It can then be seen that the distance between the 7+ and 2− levels increases with increasing mass number.

7. Electron-capture feeding from Pb^{202m}

An estimate of the capture branching-ratio X_{EC} from the 9− Pb^{202} level to the Tl branch can be made from a comparison between the total transition intensities in the Pb and Tl branches, (see tables 4 and 7). As the mean values of these transition intensities are 2335 ± 100 and 245 ± 20, respectively one finds

$$X_{EC} = (9.5 \pm 1.0)\,\%.$$

The branching ratio can also be obtained from a knowledge of the decay of the ground state of Tl^{202} to Hg^{202}. This is a 12-day electron-capture decay with only one E2 gamma ray of 439.1 keV emitted [27]). Kramer *et al.* [20]) found 63 % electron capture to the 0+ ground state of Hg^{202} and 37 % to the 2+ state. The most recent measurements [28]), however, give an upper limit of 10 % to the electron-capture feeding to the 0+ ground state, supporting the 2− assignment of the Tl^{202} ground state, (see subsection 6.2.a). The value 0.54−0.75 MeV, deduced by Kramer *et al.* [20]) for the energy difference between the ground states of Tl^{202} and Hg^{202}, is also in disagreement with the value of about 1.4 MeV, found by interpolation between the values 2.46 MeV [17]) and 0.34 MeV [18]) of the corresponding energy differences for the mass numbers 200 and 204, respectively. From a total transition energy of about 1.4 MeV, the capture feeding to the Hg^{202} ground state would be expected to be a few percent only [22]). In our calculations of the capture branching-ratio from the Pb^{202} 9− level, it has therefore been assumed that the Tl^{202} ground state decays with 100 % electron capture to the Hg^{202} 2+ level.

If, in the decay of Pb^{202m}, the conversion lines $K(787.2)_{Pb^{202}}$ and $K(439.1)_{Hg^{202}}$ are observed at times t_1 and t_2, respectively, (where $t = 0$ is the time of the final chemical separation of the source), it can be shown that the ratio of the intensities of these lines is given by

$$\frac{I_K(787.2)}{I_K(439.1)} = k \cdot \frac{1-X_{EC}}{X_{EC}} \cdot \frac{\lambda_2-\lambda_1}{\lambda_2} \cdot \frac{e^{-\lambda_1 t_1}}{e^{-\lambda_1 t_2}-e^{-\lambda_2 t_2}} \cdot \frac{[1+1.3/(K/L)+1/\alpha_K]_{439.1}}{[1+1.3/(K/L)+1/\alpha_K]_{787.2}}$$

where

k = ratio of intensity of the 787.2 keV transition to the total transition intensity from the Pb^{202} 9− level (EC excluded),

α_K = K-conversion coefficient [13]),
λ_1 = total decay constant of the Pb^{202} 9− level,
λ_2 = total decay constant of the Tl^{202} ground state,
X_{EC} = capture branching-ratio.

As a result of four different measurements of the intensities of the two conversion lines, the following values were obtained for the branching ratio: 9.8, 10.1, 9.3 and 10.5 % giving an average value of

$$X_{EC} = (9.9 \pm 0.6)\%.$$

This value is in fair agreement with the value $(9.5 \pm 1.0)\%$ obtained above in a different way, and supports the assumption made above that the electron-capture feeding to the 0+ ground state of Hg^{202} is small ($< 10\%$).

8. Transition Probabilities

Valuable information about multipolarities of gamma rays can in some cases be obtained from life-time considerations. A comparison is therefore made between the experimental and theoretical values of the transition probabilities P of the isomeric transitions found in the decay of Pb^{202m}. The experimental values are obtained from the observed half-lives $T_{\frac{1}{2}}$, the total conversion coefficient α and the gamma-branching ratio X by use of the expression $P = X \ln 2/[T_{\frac{1}{2}}(1+\alpha)]$, whereas the theoretical values are found from the theory of Weisskopf [29]) for transitions of a single proton. The statistical factor S, is set equal to 1, and the value $r = 1.20 \times 10^{-13} A^{1/3}$ cm is used for the nuclear radius. Although the use of this theory here may be questionable, because the isomeric transitions in Pb^{202m} are probably not due to a single proton (see section 5), it is likely to give the right order of magnitude. Experience has shown that for $Z \approx 82$ this is generally the case, especially for high multipolarities. Furthermore, it may be interesting to study, for different transitions, the relative deviation between experimental values of transition probabilities and theoretical values for single proton transitions ($S = 1$). These deviations are given by a deviation factor (ratio of theoretical value to experimental value) in table 9, in addition to the experimental and theoretical values of the transition probabilities.

The experimental values of P for the 129.3, 547.2 and 787.2 keV transitions were calculated by use of the value $T_{\frac{1}{2}} = 3.62 \pm 0.04$ h for the half-life of the Pb^{202m} 9− level. This half-life was measured by Åström [26]). The value of P for the 422.1 keV transition was calculated by use of the value $T_{\frac{1}{2}} \leqq 1$ mμs for the lower 4+ level in Pb^{202}. This value was obtained by Wertheim and Pound [23]). For the 459.8 keV transition in Tl^{202} the value $T_{\frac{1}{2}} = 475 \pm 20$ μs, measured by Tove [25]), was used in the calculation of P, (see subsection 6.2.c).

The fair agreement between the experimental and theoretical values of P shown in table 9 supports the multipolarity assignments of these transitions (cf. sections 5 and 6), because any other choice of multipole order would give rise to a deviation of at least a factor 10^5 between the theoretical transition probabilities for a single proton ($S = 1$) and the experimental value.

TABLE 9

Transition probabilities of isomeric transitions in the decay of Pb^{202m}

E_γ (keV)	Multipolarity (spin change)	Transition probability		Deviation factor (theor. v./exp. v.)
		Exp. value	Theor. value (single proton, $S = 1$, $r_0 = 1.20 \times 10^{-13}$)	
129.3	E4 $(9- \rightarrow 5-)$	6.2×10^{-8}	1.6×10^{-7}	2.6
422.1	E2 $(4+ \rightarrow 2+)$	6.5×10^{8}	1.2×10^{9}	1.8
459.8	E3 $(7+ \rightarrow 4-)$	1.3×10^{3}	6.3×10^{3}	4.8
547.2	E5 $(9- \rightarrow 4+)$	5.9×10^{-8}	1.5×10^{-7}	2.5
787.2	E5 $(9- \rightarrow 4+)$	2.4×10^{-5}	8.4×10^{-6}	0.35

The present investigation has been carried out at the Nobel Institute of Physics, Stockholm. We would like to thank Dr. H. Atterling and his cyclotron crew for the numerous bombardments necessary in these experiments, and Dr. T. Gerholm, Physics Dept. of the University of Uppsala, for placing his double lens spectrometer at our disposal. One of us (J. A. McDonell) wishes to thank the Head of the Institute, Professor Manne Siegbahn, and other members of the Institute for their hospitality during his stay in Sweden.

References

1) D. Maeder and A. H. Wapstra, Phys. Rev. **93** (1954) 1433
2) D. Maeder, A. H. Wapstra, G. J. Nijgh and L. Th. M. Ornstein, Physica **20** (1954) 521
3) G. J. Nijgh, thesis (G. van Soest, Amsterdam, 1955)
4) I. Bergström and A. H. Wapstra, Phil. Mag. **46** (1955) 61
5) K. E. Bergkvist, I. Bergström, C. J. Herrlander, S. Hultberg, H. Slätis, E. Sokolowski, A. H. Wapstra and T. Wiedling, Phil. Mag. **46** (1955) 65
6) C. J. Herrlander, R. Stockendal, J. A. McDonell and I. Bergström, Nuclear Physics **1** (1956) 643
7) A. Hedgran, N. Svartholm and K. Siegbahn, Proc. Phys. Soc. A **63** (1950) 960
8) H. Slätis, Arkiv Fysik **6** (1953) 415
9) R. Stockendal, J. A. McDonell, M. Schmorak and I. Bergström, Arkiv Fysik **11** (1956) 165
10) T. R. Gerholm, Rev. Sci. Instr. **26** (1955) 1069
11) M. E. Rose, G. H. Goertzel and C. Swift, privately circulated tables
12) M. Schmorak, R. Stockendal, J. A. McDonell, I. Bergström and T. R. Gerholm, Nuclear Physics **2** (1956/57) 193

13) L. A. Sliv and I. M. Band, published by Academy of Sciences of the USSR (Moscow-Leningrad, 1956)
14) T. Wiedling, thesis (Almqvist and Wiksells Boktryckeri AB, Uppsala, 1956)
15) B. Åström and B. Johansson, Nobel Institute of Physics, Stockholm, private communication
16) G. Andersson and I. Bergström, Nuclear Physics **3** (1957) 541
17) C. J. Herrlander and T. R. Gerholm, Nuclear Physics **3** (1957) 161
18) E. der Mateosian and A. Smith, Phys. Rev. **88** (1952) 1186;
T. Yuasa, J. Laberrigue-Frolow and L. Feuvrais, Comptes rendus **238** (1954) 1500;
G. O. Brink, J. C. Hubbs, W. A. Nierenberg and J. L. Worcester, Bull. Am. Phys. Soc. **1** (1956) 343
19) G. Andersson and I. Bergström, Nuclear Physics **3** (1957) 506
20) P. Kramer, H. C. Hamers and G. Meijer, Physica **22** (1956) 208
21) J. R. Huizenga and C. M. Stevens, Phys. Rev. **96** (1954) 548
22) S. A. Moszkowski, Phys. Rev. **82** (1951) 35
23) G. K. Wertheim and R. V. Pound, Phys. Rev. **102** (1956) 185
24) S. H. Vegors and P. Axel, Phys. Rev. **101** (1956) 1067
25) P. A. Tove, Gustaf Werner Institute for Nuclear Chemistry, Uppsala, private communication
26) B. Åström, Nobel Institute of Physics, Stockholm, to be published in Arkiv för Fysik
27) I. Bergström, R. D. Hill and G. de Pasquali, Phys. Rev. **92** (1953) 918
28) A. H. Wapstra, Instituut voor Kernphysisch Onderzoek, Amsterdam, private communication
29) S. A. Moszkowski, Beta- and Gamma-ray Spectroscopy, Ed. K. Siegbahn (North-Holland Publishing Co., Amsterdam, 1955) Ch. XIII
30) D. E. Alburger and M. H. L. Pryce, Phys. Rev. **95** (1954) 1482
31) L. G. Elliott, R. L. Graham, J. Walker and J. L. Wolfson, Phys. Rev. **93** (1954) 356

Nuclear Physics **3** (1957) 541—548; *North-Holland Publishing Co., Amsterdam*

ANOMALOUS INTERNAL CONVERSION RATIOS OF E3 TRANSITIONS IN THE REGION $Z = 77-82$

G. ANDERSSON

The Gustaf Werner Institute for Nuclear Chemistry, Uppsala

and

I. BERGSTRÖM

Nobel Institute of Physics, Stockholm

Received 28 January 1957

Abstract: A systematic disagreement between experimental and theoretical L conversion ratios has been observed for E3 transitions in Pb, Tl, Au and Ir. It is shown that multipole mixing cannot explain the discrepancies and that a nuclear size effect seems very improbable.

1. Introduction

Work in progress [1]) to systematize the knowledge of metastable states in the region $Z = 77-82$ has revealed a peculiar trend in the internal conversion intensities of transitions, assigned the multipolarity E3. While the experimental K/ΣL ratios as a rule seem to agree reasonably well with the point charge calculations of Rose [2]), considerable discrepancies exist for $(L_I+L_{II})/L_{III}$, the experimental values being much lower than the theoretical ones.

This inconsistency has already been pointed out for an isolated case by Andersson *et al.* [3]). The purpose of the present paper is to compile all available data on E3 transitions in the above-mentioned Z-region and to discuss some possibilities of explaining the anomalies found. It should be remarked that E2, E4, E5, and M4 transitions in the same Z-region do not exhibit such large deviations from the theoretical conversion ratios, as far as can be judged from a preliminary survey.

2. Evidence of the Discrepancy

In table 1 the relevant experimental data are listed together with theoretical E3 conversion ratios, calculated by interpolation from Rose's tables [2]). The 2.62 MeV E3 transition in Pb^{208} has not been included, because its high energy makes it less interesting in this connection.

The measurements are of a varying accuracy. It should be emphasized, however, that in all cases the L_I+L_{II} group is well resolved from the L_{III} line. (In one case, that of Tl^{197}, L_I was even resolved from L_{II}.) Thus the errors in $(L_I+L_{II})/L_{III}$ should be rather small, probably about ±10 %,

TABLE 1

Nucleide	E_γ (keV)	k	K/L			$(L_I+L_{II})/L_{III}$			Remarks
			Exp.	Theor. E3	Exp./Theor.	Exp.	Theor. E3	Exp./Theor.	
$_{82}Pb^{206}$	516.1	1.01	$1.50 \pm 0.08^{a,b}$)	1.65	0.909 ± 0.054	6.0 ± 0.3^{b})	7.69	0.780 ± 0.042	Exp. K/ΣL is a mean value obtained from ref. a and b.
$_{81}Tl^{202}$	459.8	0.900	—	1.38	—	5.0 ± 0.5^{c})	6.79	0.737 ± 0.077	K/ΣL not measurable [c])
$_{81}Tl^{197}$	222.5	0.435	0.242 ± 0.018^{d}	0.273	0.887 ± 0.071	2.43 ± 0.15^{d})	3.98	0.610 ± 0.041	
$_{82}Pb^{208}$	202.5	0.396	$0.140^{a} \pm 0.014$	0.191	0.732 ± 0.076	$2.28^{a}) \pm 0.23$	3.95	0.577 ± 0.060	Uncertainty in exp. values estimated from ref. a.
$_{79}Au^{197}$	130	0.254	0.114 [e])	0.0532	2.14	1.32^{e}) 2.5^{f})	2.97	0.445 0.843	$L_I/L_{II} \leqq 0.1$ [j])
$_{81}Tl^{195}$	99.1	0.194	—	0.00516	—	1.52 ± 0.12^{d})	2.67	0.590 ± 0.050	Refers to L_{II}/L_{III}
$_{77}Ir^{192}$	58.0	0.114	—		—	1.1^{g})	2.24	0.491	
$_{79}Au^{195}$	56.9 56.5	0.111	—		—	1.05^{e}) 1.0^{h})	2.29	0.459 0.437	$L_I/L_{II} \leqq 0.1$ [j])
$_{77}Ir^{191}$	41.7	0.081	—		—	0.80^{i})	1.92	0.416	$L_I/L_{II} \leqq 0.1$ [j])
$_{79}Au^{193}$	31.9	0.062	—		—	0.65^{h})	1.98	0.328	

a) D. E. Alburger and M. H. L. Pryce, Phys. Rev. **95** (1954) 1482
b) Treatment of data from M. Schmorak, R. Stockendal, J. A. McDonell, I. Bergström and T. R. Gerholm, Nuclear Physics **2** (1956/57)193
c) J. A. McDonell, R. Stockendal, C. J. Herrlander and I. Bergström, in course of publication
d) G. Andersson, P. A. Tove, B. Jung, and I. B. Svensson, Nuclear Physics **3** (1957) 493
e) R. Joly, J. Brunner, J. Halter and O. Huber, Helv. Phys. Acta **28** (1955) 403
f) J. W. Mihelich and A. de-Shalit, Phys. Rev. **91** (1953) 78
g) J. P. Mize, M. E. Bunker and J. W. Starner, Phys. Rev. **96** (1954) 444
h) L. P. Gillon, K. Gopalakrishnan, A. de-Shalit and J. W. Mihelich, Phys. Rev. **93** (1954) 124
i) J. B. Swan and R. D. Hill, Phys. Rev. **88** (1952) 831
j) H. Slätis, private communication

even where no error limits are given in the references cited. The $(L_I+L_{II})/L_{III}$ ratio of the Au^{197} transition forms an exception in this respect. The two widely differing values reported and the fact that the $K/\Sigma L$ ratio of the same transition fits poorly into the general picture (cf. below) call for a remeasurement of the conversion intensities.

Some care has been taken in interpolating the theoretical conversion coefficients to the proper *Z*-values and transition energies. The interpolation uncertainty in the individual coefficients is believed to be less than ± 2 %. The Au^{197} transition happens to fall in an energy region where the K conversion coefficients follow a strongly non-linear course when plotted against energy in a log-log diagram, and the values given by Rose are too sparse to allow an interpolation with sufficient accuracy. In this case (and also in calculating the M4 K conversion coefficient for the same transition; cf. section 3.1) Sliv's more detailed tables [4]) were used. Though the finite size of the nucleus has been taken into account by Sliv, the two sets of K conversion coefficients were found to coincide almost exactly in the neighbourhood of the energy region of interest.

The columns 6 and 9 of table 1 give the ratios between experimental and theoretical values. In fig. 1 these ratios are plotted as functions of the transition energy, expressed in mc^2 units $(= k)$. Unfortunately the experimental material on $K/\Sigma L$ is not very extensive, but the three most reliable points clearly indicate a different behaviour from that of $(L_I+L_{II})/L_{III}$, which is indeed very striking.

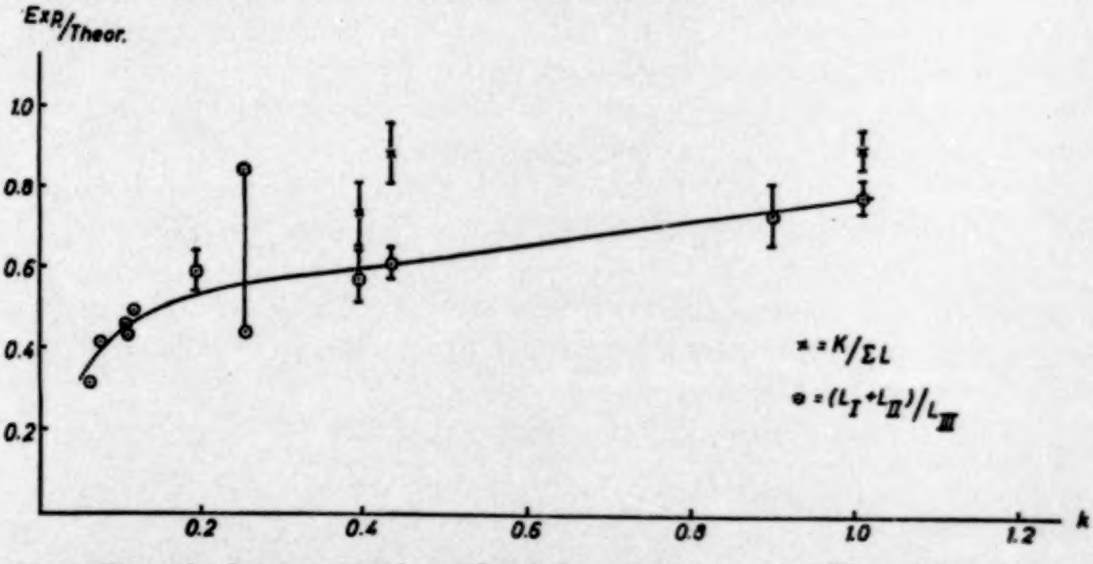

Fig. 1. The ratios between experimental and theoretical values of $K/\Sigma L$ and $(L_I+L_{II})/L_{III}$ as functions of energy. (The $K/\Sigma L$ point for Au^{197} has not been included.)

3. Discussion

3.1. THE POSSIBILITY OF MULTIPOLE MIXING

A small admixture of M4 into the E3 transitions would explain the observed lowering of $(L_I+L_{II})/L_{III}$. On this assumption, however, the same amount of mixing should show up in the other conversion ratios. In order to investigate if this is consistent with experimental facts, we have calculated the hypothetical admixtures [5]) from the $(L_I+L_{II})/L_{III}$ and $K/\Sigma L$ ratios where this could be done and in one case also from the L_I/L_{II} ratio. The results are shown in table 2. Because of the importance of the uncertainty limits to this discussion, they are given as maximum errors.

TABLE 2

Nucleide	*k*	M4 admixture from		
		$K/\Sigma L$	$(L_I+L_{II})/L_{III}$	L_I/L_{II}
Pb^{206}	1.01	-0.0098 ± 0.0105	0.0273 ± 0.0143	
Tl^{197}	0.435	-0.0020 ± 0.0027	0.0175 ± 0.0056	0.0006 ± 0.0011
Pb^{206}	0.396	-0.0037 ± 0.0015	0.0165 ± 0.0071	
Au^{197}	0.254	0.021	0.0074	

In the first three cases the definite positive effects obtained from $(L_I+L_{II})/L_{III}$ find no correspondence in the $K/\Sigma L$ data, which even show a marked tendency towards negative values. It is perhaps still more significant that the admixture indicated by the L_I/L_{II} ratio of the Tl^{197} transition is zero within the limits of error. Thus it may be concluded that in these three cases M4 admixture alone cannot explain the discrepancies between experimental and theoretical conversion ratios.

The fourth transition (that of Au^{197}) shows quite different characteristics. As mentioned above, however, the reliability of the measurements has to be doubted in this case.

A further argument in the discussion of possible multipole mixing may be obtained from a survey of the transition probabilities. For a single proton these are given by [6])

$$P(\mathrm{E3}) = 1.1\times10^{2}\times A^{2}\times E^{7}\times S$$
$$P(\mathrm{M4}) = 1.5\times10^{-4}\times A^{2}\times E^{9}\times S$$

with E_γ in MeV.

Thus for $E_\gamma = 0.5$ and 0.05 the M4 admixture should in this case only be of the order 10^{-7} and 10^{-9} respectively. It would be possible to explain the large (1−2 %) values of M4-mixing suggested by the intensity ratio $(L_I+L_{II})/L_{III}$, only if the E3 transitions were exceptionally slow. We define an E3 hindrance factor F in the following way:

$$P(\mathrm{E3}) = 110 \times A^2 \times E^7_\gamma / F,$$

which gives

$$F = \tau_\gamma \times A^2 \times E^7_\gamma / 0.0091,$$

where τ_γ is the γ lifetime.

$\tau_\gamma \times A^2 \times E^7_\gamma$ has been defined as the "comparative lifetime" 7) for a gamma transition. For a single proton transition this quantity is a constant6) which in the case of an E3 transition has the value 0.0091. However, if the experimental values of E_γ, A and τ_γ are used it is very often found that the comparative lifetime deviates appreciably from the constant value, which is suggested from the simple model of a single proton transition. The hindrance factor F is a measure of this deviation and gives the ratio between the matrix elements of a single proton transition (the statistical factor $S = 1$) and that of the observed transition.

TABLE 3

Nucleide	E_γ (MeV)	$T_{1/2}$ obs. (sec)	α_{total} (Rose)	τ_γ (sec)	F	spin change
$_{82}$Pb^{206}	0.5161	120×10^{-6} a,b)	0.0912	190×10^{-6}	8	7− → 4+
$_{81}$Tl^{202}	0.4598	475×10^{-6} b)	0.122	770×10^{-6}	14	7+ → 4−
$_{81}$Tl^{197}	0.2225	0.76 c)	2.08	3.4	390	11/2− → 5/2+
$_{82}$Pb^{206}	0.2025	—	3.47	0.37 d)	24	7− → 4+
$_{79}$Au^{197}	0.130	7.4 e)	24.7	270	730	11/2− → 5/2+
$_{81}$Tl^{195}	0.0991	3.5 c)	126	640	250	11/2− → 5/2+
$_{77}$Ir^{192}	0.0580	85 f)	1770	220000	1950	?
$_{79}$Au^{195}	0.0567	31 e)	2560	120000	900	11/2− → 5/2+
$_{77}$Ir^{191}	0.0417	4.9 e)	13300	94000	83	11/2− → 5/2+
$_{79}$Au^{193}	0.0319	3.9 e)	69399	390000	54	11/2− → 5/2+

a) B. Åström, private communication
b) P. A. Tove, private communication
c) G. Andersson, P. A. Tove, B. Jung and I. B. Svensson, Nuclear Physics **3** (1957) 493
d) Calculated from τ_γ of 0.5161 MeV, Pb^{206} and relative conversion line intensities given by D. E. Alburger and M. H. L. Pryce, Phys. Rev. **92** (1953) 514
e) V. K. Fischer, Phys. Rev. **99** (1955) 764
f) N. Hole, Arkiv Mat. Astron. Fysik A **36** (1948) no. 9

From table 3 it can be concluded that although F is large, it is not sufficiently large to account for a few percent M4 mixing. However, it is more significant to observe that F is not a smooth function of energy, as would be required if the amount of M4 admixture were only due to exceptionally slow E3 transitions. It cannot be excluded of course that in addition the

M4 transition probability is enhanced, but it seems hard to understand how a combined slowing down of E3 transitions and speeding up of M4 transitions could result in a multipole mixing varying so smoothly with energy as suggested by $(L_I+L_{II})/L_{III}$ (cf. fig. 1).

For these reasons it seems unlikely that M4 admixture is responsible for the low values of $(L_I+L_{II})/L_{III}$.

3.2. FINITE NUCLEAR SIZE EFFECTS

It was first shown by Wapstra and Nijgh [8]) that the K conversion coefficients of M1 transitions in heavy nuclei are low by about 40 % relative to Rose's values [2]). A better agreement between theory and experiment is obtained if the finite size of the nucleus is considered, which has been done in Sliv's calculations [4]).

There is strong experimental evidence that the L_I conversion coefficients are reduced to about the same extent as the K coefficients [8]). The L_{II} as well as the L_{III} subshells were originally expected to be much less influenced by nuclear size effects, an argument being that these are both p electrons [9]). As to L_{II}, however, this expectation was not compatible with some experimental data [8, 9, 10]). In fact there seems to be theoretical support for a difference between L_{II} and L_{III}, caused by their different angular momenta (1/2 and 3/2, respectively)[11]). An indication of the behaviour of the corresponding wave functions is given in a paper by Brysk and Rose on orbital capture [12]). Thus at present it seems likely that the finite nuclear size effect is always negligible for the L_{III} shell, while K, L_I and L_{II} are influenced about equally.

If this were true also of E3 transitions it would qualitatively explain the trends in conversion ratios illustrated in section 2. Assuming that this is the case and that the transitions are of a pure E3 character we can write the experimental conversion coefficients (cf. ref. [13])):

$$\alpha^*_K = f \cdot \alpha_K; \quad \alpha^*_{L_I} = g \cdot \alpha_{L_I}; \quad \alpha^*_{L_I} = h \cdot \alpha_{L_{II}} \text{ and } \alpha^*_{L_{III}} = \alpha_{L_{III}},$$

where α_K, α_{L_I} etc. refer to Rose's values. If absolute values of the α^*'s are not available, a knowledge of the relative intensities of all four conversion lines of a transition is required to determine f, g and h independently. So far only Tl^{197} offers this possibility [14]). The correction factors in this case were found to be equal within the error limits (see table 4). Thus it was considered justified, lacking sufficient experimental material, to assume g and h to be equal also for the other transitions, when this was necessary in order to perform the calculations. Table 4 shows the results.

As a consequence of the way of calculation, the correction factors as a function of transition energy will follow very nearly the course of the $(L_I+L_{II})/L_{III}$ curve in fig. 1.

A very remarkable fact in view of these indications of a nuclear size effect — apart from the magnitude of the corrections — is that for all energies and Z-values concerned, the point charge K shell coefficients of Rose [2]) almost exactly coincide with Sliv's values [4]), calculated with the finite nuclear size taken into account. This would rather suggest a correction to the L_{III} coefficients and thus strongly speaks against the explanation suggested above.

TABLE 4

Nucleide	k	l	g	h	Remarks
Pb^{204}	1.01	0.73±0.06	0.78±0.05	0.78±0.05	g put = h
Tl^{202}	0.900		0.74±0.15	0.74±0.15	g put = h
Tl^{197}	0.435	0.61±0.07	0.66±0.07	0.61±0.04	
Pb^{206}	0.396	0.49±0.07	0.58±0.06	0.58±0.06	g put = h
Au^{197}	0.254	1.57	0.64	0.64	g put = h
Tl^{195}	0.194			0.59±0.05	
Ir^{192}	0.114		0.49	0.49	g put = h
Au^{195}	0.111		0.45	0.45	g put = h
Ir^{191}	0.081		0.42	0.42	g put = h
Au^{193}	0.062		0.33	0.33	g put = h

Recently, however, Church and Weneser [15]) (cf. also ref. [16])) have pointed out that the interaction between atomic electrons and the nuclear charge and current distribution gives rise to additional matrix elements, which are not considered in Sliv's treatment. Of special interest in the present connection is their statement that the different shells may be differently influenced, that is, conversion ratios may be very sensitive to this new effect. The calculations by Church and Weneser were restricted to M1 transitions, which also in this case are expected to be most strongly affected. Awaiting further calculations, however, it is very hard to see why E3 conversion ratios should be influenced to the extent needed. We only wanted to mention this possibility, as for the present no plausible explanation of the anomalies is available.

References

1) I. Bergström and G. Andersson, to be published
2) M. E. Rose *et al.*, privately distributed tables
3) G. Andersson, E. Arbman and B. Jung, Arkiv Fysik **11** (1957) 297
4) L. Sliv and J. Band, privately distributed tables
5) See for instance E. L. Church and J. E. Monahan, Phys. Rev. **98** (1955) 718

6) S. A. Moszkowski, Beta- and Gamma-ray Spectroscopy, Ed. Kai Siegbahn (North-Holland Publishing Co., 1955) Ch. XIII
7) M. Goldhaber and A. W. Sunyar, Beta- and Gamma-ray Spectroscopy, Ed. Kai Siegbahn (North-Holland Publishing Co., 1955) Ch. XVI (II)
8) A. H. Wapstra and G. J. Nijgh, Nuclear Physics **1** (1956) 245
9) E. Sokolowski, K. Edvarson and K. Siegbahn, Nuclear Physics **1** (1956) 160
10) C. Nordling, K. Siegbahn, E. Sokolowski and A. H. Wapstra, Nuclear Physics **1** (1956) 326
11) M. E. Rose, private communication
12) H. Brysk and M. E. Rose, ORNL-1830 (1955)
13) J. W. Mihelich, T. J. Ward and K. P. Jacob, Phys. Rev. **103** (1956) 1285
14) G. Andersson, P. A. Tove, B. Jung, and I. B. Svensson, Nuclear Physics **3** (1957) 493
15) E. L. Church and J. Weneser, Phys. Rev. **104** (1956) 1382
16) G. Kramer, Z. Physik **146** (1956) 187

Note added in proof:

During the course of the work a stimulating contact was held with Dr. M. E. Rose. After the completion of this paper we received from him the information that a coding error in the computations, affecting only the L_{III} conversion coefficients of E3 transitions, had been discovered. The revised values given by Dr. Rose lead to a good agreement between theoretical and experimental conversion ratios (cf. ref. 14)). This will be more extensively discussed in a forthcoming paper 1)). The present investigation shows on one hand that the internal conversion coefficients computed by M. E. Rose and L. Sliv and their collaborators constitute a powerful tool for the multipolarity assignment of γ-rays and notably for the detection of multipole mixing. On the other hand the importance of a systematic treatment of data in order to establish discrepancies between theory and experiment is emphasized.

Nuclear Physics **3** (1957) 549—552; *North-Holland Publishing Co., Amsterdam*

ON A POSSIBILITY OF K-MESON INVESTIGATION

L. G. ZASTAVENKO, A. L. LIUBIMOV, V. I. OGIEVITSKY
AND M. I. PODGORETSKY
Joint Institute of Nuclear Research, U.S.S.R.

Received 7 February 1957

Abstract: Assuming θ and τ-mesons to be different particles, one should expect the neutral τ-meson life-time to be considerably greater than 10^{-10} sec. This can be used in some experiments to determine the differences between θ and τ-particles. In the present paper two experiments of this kind are proposed.

1. Introduction

At present the existence of several schemes of charged K-meson decay has been established. In some cases, namely, in the decay into two or three π-mesons, the decay products appear to be in states with different space parity. It would be reasonable to consider these decays to correspond to different particles, θ and τ. In this case an essential difficulty arises, however, since the main properties of θ and τ-mesons (mass value, lifetime, characteristics of nuclear interactions) appear to be identical within the limits of experimental errors. On the other hand the assumption that θ and τ-mesons correspond to alternative decay modes of the same particle implies violation of parity conservation [1]). It may also be assumed that θ and τ-mesons are different states of the same particle, distinguished by their parity, just as π^+, π^0, and π^--mesons are different charge states of a pion. Such a point of view was developed in ref. [2]).

2. The Lifetimes of Neutral K-Mesons

A choice between the above-mentioned possibilities is of great importance. In solving this problem it is natural to attempt to detect some differences in the properties of θ and τ-mesons; for this purpose more accurate lifetime measurements would be a suitable type of experiment.

Indeed, under some assumptions one can obtain different lifetimes, (see, e.g., ref. [3, 4])). The difference expected is, however, rather small for charged θ and τ-mesons.

However, the situation changes essentially if we consider the neutral isobaric partners of θ and τ-particles. In fact, if θ^0 and τ^0-mesons have different parities we can expect a sharp difference in their lifetimes to occur. The lifetime of the odd K^0-meson (τ^0) may considerably exceed the lifetime of the even one (θ^0) †. This may prove to be the most effective method of investigation of the problem under consideration as well as of some other related problems ††.

In principle, the lifetime of θ^0 and τ^0-mesons can be determined by means of direct measurements as in the case of their charged partners. However, such measurements in practice are very complicated due to the difficulty of τ^0-meson identification ††† and due to difficulties in creating monoenergetic beams of sufficient intensity, etc. Under such conditions one must apply various indirect methods. In particular, the possibility of using the differences in the time development of the Gell-Mann-Pais-Piccioni process for θ^0 and τ^0-mesons 7, 9) seems to us very attractive. Indeed, in the case of τ^0-mesons both components are long-lived, whereas for the θ^0-particles only the component with odd charge parity appears to be long-lived; the component θ_1^0 decays very quickly ($t \approx 10^{-10}$ sec). Therefore at distances from the site of production which are large relative to the decay path of τ^0-mesons, the ratio between the number of mesons of various types changes sharply. Only θ_2^0-particles remain from the parent θ^0-mesons while the number of τ^0-mesons remains practically the same.

The principle outlined above can be taken as a basis for some interconnected experiments. Two experiments of such a type are proposed below.

3. First Proposed Experiment

One of the experiments consists in measuring the ratio $K^+_{\pi 3}/K^+_{\pi 2}$ for K^+-mesons obtained by charge exchange scattering from K^0-mesons. As is well known, this ratio has appeared so far to be the same within the limits of experimental errors in a number of experiments conducted under various conditions (see, e.g., ref 10)).

In the experiment under consideration θ^0 and τ^0-mesons should undergo charge exchange scattering in a layer of matter during a period $t \approx 10^{-9}$ sec after generation. Then if θ and τ are distinct particles, the ratio $K^+_{\pi 3}/K^+_{\pi 2}$

---

† From Gell-Mann's and Pais's assumptions 5)) that the change of the isobaric spin is equal to $\frac{1}{2}$ in decay we can derive for the probabilities of τ^0 and τ^+-decay into three π-mesons the inequality $w(\tau^0 \rightarrow 3\pi) \leq \frac{1}{2} w(\tau^+ \rightarrow 3\pi)$. An analogous result was obtained by Schwinger on the basis of the strong $\pi - K$ coupling assumption 4)). (See also the papers by Dalitz 6)) and Snow 7)).)

†† If, say, θ^0 and τ^0-mesons appear to be different particles the question arises whether the one transforms into the other by nuclear interactions. The difference in the lifetimes can be used also for the solution of this question.

††† Though a number of the so-called "anomalous V^0-decays" can be best explained as decays into three π-mesons, the existence of τ^0 particles has not so far been reliably enough established experimentally. Apparently this is due not only to the difficulty of the τ^0-meson identification but also to the fact that the ratio of the decays $\tau^0 \rightarrow (\pi^0\pi^+\pi^-)/\theta^0 \rightarrow (\pi^+\pi^-)$ is less than the ratio of the decays $\tau^+ \rightarrow (\pi^+\pi^+\pi^-)/\theta^+ \rightarrow (\pi^+\pi^0)$ (at least under usual conditions of observation where the registration probability of the process $\theta^0 \rightarrow (\pi^+\pi^-)$ is large).

may change since according to the reasons presented above, the amount of τ^0-mesons remains almost the same †.

The change of this ratio should be a direct proof of a distinction between θ and τ-particles.

Simultaneously other ratios such as $K^+_{\mu 2}/K^+_{\pi 3}$ should also change.

A simultaneous measurement of such ratios would allow one to determine the probabilities of the various alternative decay schemes of θ^+ and τ^+-mesons and also the true ratio of the number of these particles (which evidently may not coincide with the ratio of the number of $K^+_{\pi 2}$ and $K^+_{\pi 3}$ decays).

As a source of the neutral K-mesons one can use either nuclear reactions, involving particles of sufficiently high energy or charge exchange of the K^+-meson beam in a layer of matter.

4. Second Proposed Experiment

Another experiment consists in measuring the ratio between the numbers of decays ††

$$K^0 \rightarrow \pi^- + \mu^+ + \nu \quad \text{and} \quad K^0 \rightarrow \pi^+ + \mu^- + \nu$$

or

$$K^0 \rightarrow \pi^- + e^+ + \nu \quad \text{and} \quad K^0 \rightarrow \pi^+ + e^- + \nu .$$

It should be noted that in order to determine the aforementioned ratios it is not necessary to completely identify the decay products; it should be quite sufficient to measure the ratio

$$\frac{\mu^+}{\mu^-} \left(\text{or } \frac{e^+}{e^-} \right) .$$

At the same time the conditions for observing the particles of both signs should be identical. Further, to be more definite we shall consider the value μ^+/μ^-. If $\theta^0 \equiv \tau^0$ then the long-lived neutral particles observed in ref. [11]) must be identical with the odd charge parity component $\theta_2{}^0$ which decays into $\pi^-\mu^+\nu$ and $\pi^+\mu^-\nu$ with equal probabilities. Therefore the relation

$$\frac{\mu^+}{\mu^-} = 1$$

must hold.

If $\tau^0 \not\equiv \theta^0$ then at great distances both τ^0-mesons and θ^0-particles will hit the detector. One can expect the τ^0-mesons mainly to decay into $(\pi^-\mu^+\nu)$ and not into $(\pi^+\mu^-\nu)$. Moreover, under some theoretical assumptions the decay into $(\pi^+\mu^-\nu)$ is in general impossible [4, 13]). This will lead to a change in the ratio μ^+/μ^-. If equal numbers of τ^0 and θ^0-mesons are always produced [2]), then the ratio μ^+/μ^- may be as high as 5.

---

† It is worth noting that this experiment may be useful even if the Gell-Mann-Pais-Piccioni scheme is not correct.

†† These ratios were already considered in ref. [12, 13]) but only with respect to θ^0-particle decay and without any connection with the problem of the existence of two neutral K-mesons.

Thus if it be found experimentally that $\mu^+/\mu^- \neq 1$ this should signify the existence of two different types of neutral particles †. Conversely equality of this ratio to unity will be an argument for $\tau^0 \equiv \theta^0$.

If it turns out that $\mu^+/\mu^- \neq 1$ further more specific experiments can be arranged. There is the possibility, for instance, of measuring this ratio at larger distances in order to detect the expected difference in the lifetimes of θ_2^0 and τ^0. Another possible experiment is connected with placing a thick absorber before the indicator. θ_2^0-particles contain θ^0-mesons as a component and therefore they are strongly absorbed by nuclei. On the contrary τ^0-mesons may only be scattered by nuclei. Therefore they are absorbed more slowly. Consequently after passing through the absorber the ratio between the numbers of τ^0-mesons and θ_2^0-particles may sharply change and this should lead to a change of μ^+/μ^-.

---

† Possible existence of the decays $(\mu^+\mu^-)$ and $(\mu^\mp e^\pm)$ does not alter this conclusion. One can expect, however, the probabilities of these decays to be small [4]).

References

1) T. D. Lee and C. N. Yang, Phys. Rev. **104** (1956) 254
2) T. D. Lee and C. N. Yang, Phys. Rev. **102** (1956) 290
3) P. R. Bludman, Phys. Rev. **102** (1956) 1420
4) J. Schwinger, Phys. Rev. **104** (1956) 1164
5) M. Gell-Mann and A. Pais, Proceedings of 1954 Glasgow Conference, p. 342
6) R. N. Dalitz, Proc. Phys. Soc. A **69** (1956) 527
7) G. A. Snow, Phys. Rev. **103** (1956) 1111
8) M. Gell-Mann and A. Pais, Phys. Rev. **97** (1955) 1387
9) A. Pais and O. Piccioni, Phys. Rev. **100** (1955) 1487
10) T. F. Hoang, M. F. Kaplan, and G. Yekutieli, Phys. Rev. **102** (1956) 1185
11) K. Lande, E. T. Booth, J. Impeduglea, L. M. Lederman and W. Chinowsky, Phys. Rev. **103** (1956) 1901
12) Ya. B. Zeldovich, JETP **30** (1956) 1169
13) S. B. Treiman and B. G. Sachs, Phys. Rev. **103** (1956) 1545

Nuclear Physics **3** (1957) 553—560; *North-Holland Publishing Co., Amsterdam*

ISOTOPIC ASSIGNMENT OF SLOW NEUTRON RESONANCES IN GERMANIUM, RUBIDIUM, NEODYMIUM AND TUNGSTEN

ELEANOR M. BOWEY
Atomic Energy Research Establishment,
Nuclear Physics Division, Harwell near Didcot (*Berks.*)

Received 20 February 1957

The uses of a scintillation detector in time-of-flight experiments with the 15 MeV Linear accelerator at Harwell are described more fully elsewhere [1]). The detector measured the yield of gamma rays due to neutron capture in a sample placed in the neutron beam, and it was shown that even when only very small samples of the capturing material are available this provides a sensitive method for the detection of neutron resonances.

In order to make a detailed determination of resonance parameters, it is necessary to know the isotopic assignment of the resonances. For the determination of the positions of resonances in small samples the capture gamma ray detector is particularly suitable, since it gives rise to positive peaks in a yield curve rather than small dips as in a transmission experiment.

In the measurements described below the isotopic samples were all mounted in thin walled aluminium cans 1″ in diameter. The neutron beam was collimated and had a diameter of 1″ at the sample position. The sample was suspended normal to the axis of the beam in the centre of a 2″ diameter hole through a 6″ cubical aluminium box, containing a mixture of B_4C chips and water. Sodium iodide crystal detectors were recessed into the faces of this cube not traversed by the neutron beam so that these surrounded the sample. The minimum thickness of B_4C + water shielding between the sample and the crystal was $\frac{3}{4}$ inch. The whole assembly was surrounded by lead shielding to reduce the background, with an outer shield of boron and wax (see fig. 1).

The output of the photomultipliers (up to four in number — E.M.I. type 6260) were connected in parallel to the input of the main amplifier, and thence through a discriminator to the timing channels. The bias level of the discriminator was set to correspond to an energy dissipation of about 100 keV in the crystals. In this condition the detector responds not only to gamma rays due to neutron capture in the sample, but also to those due to neutron capture in the B_4C from neutrons scattered by the sample. Thus scattering resonances can also be identified, though with a lower efficiency than for the detection of capture resonances. The probability of detection of a neutron captured in the sample is of the order of 30 %, and the background counting rate is sufficiently low to enable even weak resonances to be identified quickly with such small samples. In most cases the counting time per isotope was only 1$\frac{1}{2}$—2 hours. The resolution of the apparatus was 0.17 μsec/metre; and the neutron burst had a duration of ≈ 1 μsec, the timing channels being 2 μsec wide. The recurrence frequency of the spectrometer is 400 cycles/sec.

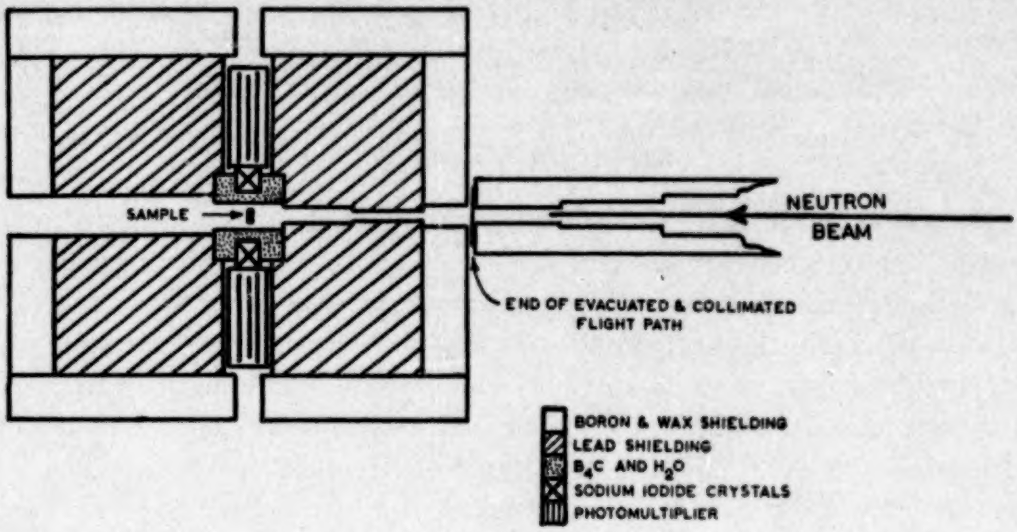

Fig. 1

The separated isotopes of the elements Germanium, Rubidium, Neodymium and Tungsten have been studied, and the results are shown as gamma ray yield curves. In every case the yield is defined as the number of counts recorded in a given channel times the delay in μsec of that channel per 50 000 monitor counts. The multiplication by delay time is to eliminate the effect of the neutron spectrum from the accelerator, which is approximately inversely proportional to delay. The monitor counts are those recorded from a BF$_3$ counter continuously monitoring the neutron output of the linear accelerator.

GERMANIUM

Samples of the oxide GeO$_2$ were used. With this element an attempt was made to define the resonances better by repeating the experiment with the initial delay increased by 1 μsec, so that the two runs on each isotope interlaced, and points were obtained at 1 μsec instead of 2 μsec intervals. These runs are plotted on an expanded scale, but it is obvious that the resolution is still not good enough to separate the higher energy resonances which are probably due to two or more isotopes in some cases.

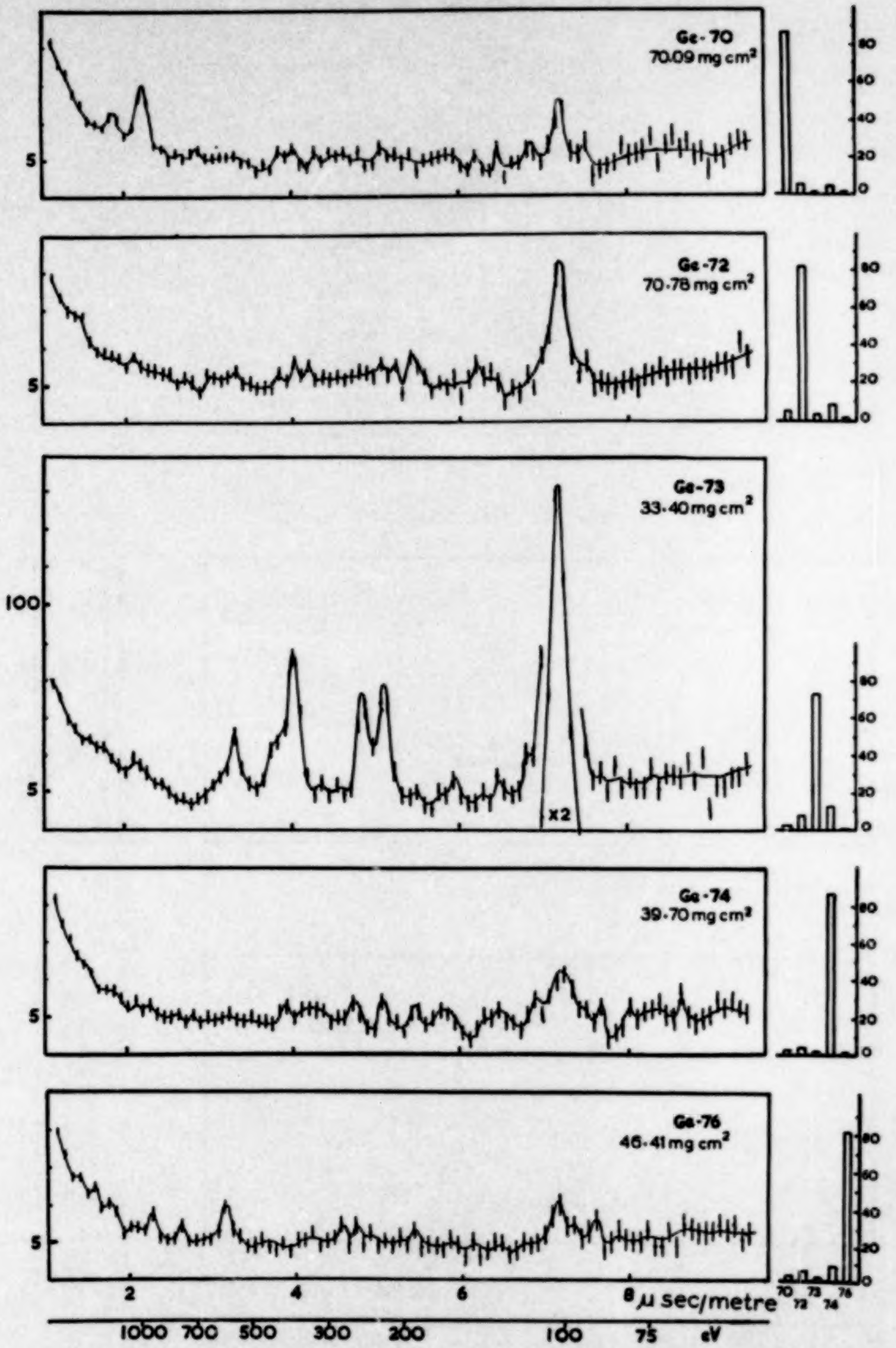

Fig. 2. Yields of γ-rays from neutron capture in Germanium samples. The histograms show the sample composition in % mg/cm²

TABLE 1 (fig. 2)

Observed Energy in eV	Mass number of Isotope
100.6 ± 2.8	73
111.1 ± 3.3	70
199.6 ± 7.6	73
221.7 ± 9.0	73
315.2 ± 14.0	73
351.7 ± 18	73, 74
471.0 ± 26	73
524.4 ± 31	76
753.0 ± 53	76
1000.0 ± 80	76
1039.0 ± 85	70
1457.0 ± 140	70

RUBIDIUM

Rubidium chloride samples were used.

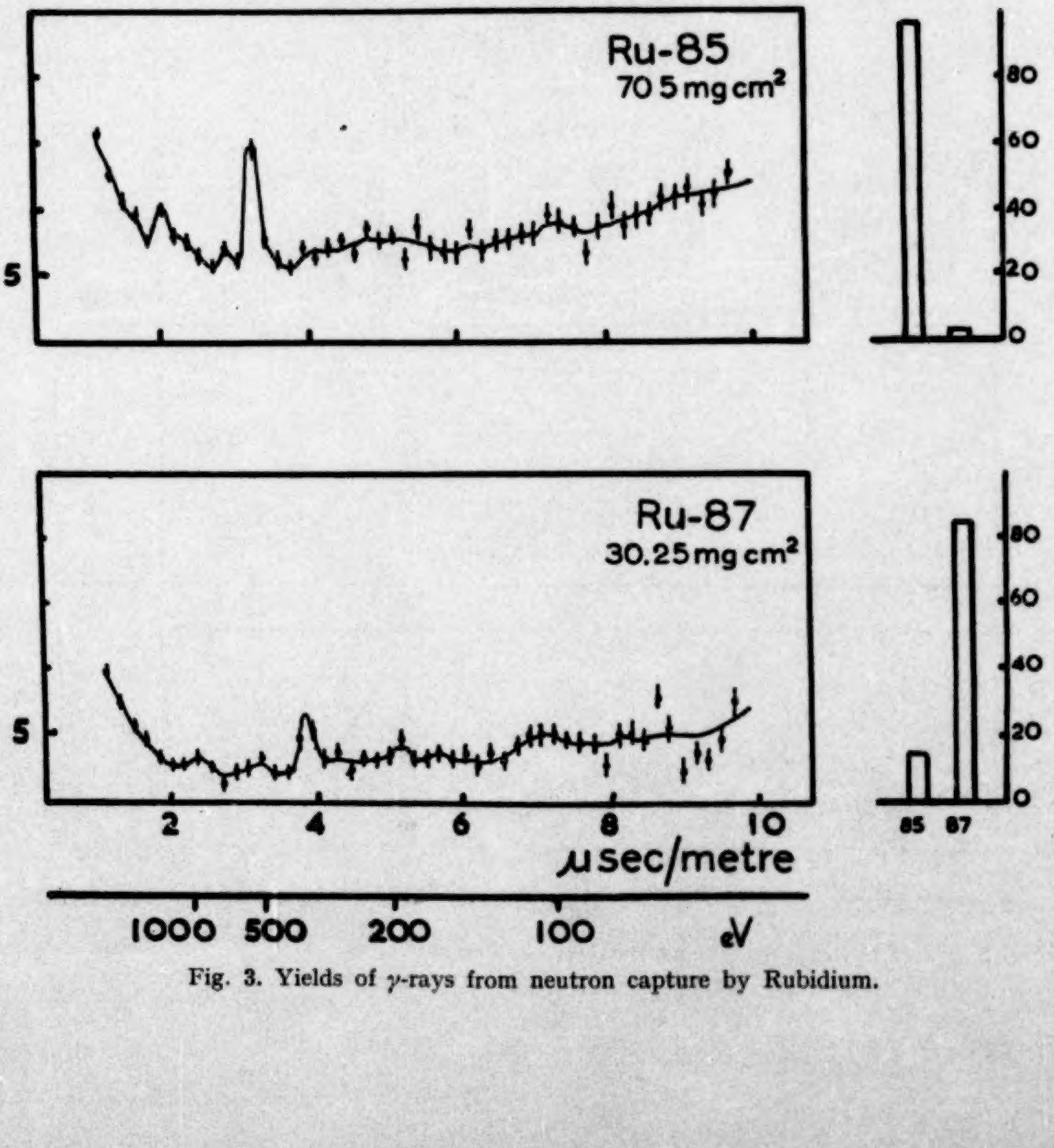

Fig. 3. Yields of γ-rays from neutron capture by Rubidium.

TABLE 2 (fig. 3)

Observed Energy in eV	Mass number of Isotope
370 ± 19	87
520 ± 30	85
1420 ± 136	85

NEODYMIUM

Neodymium oxide samples were used. With this element there was insufficient time available to do the experiment with interlaced runs, so only those resonances already reported by the Brookhaven Laboratory [2]) have been assigned. It is hoped to repeat the experiment with improved resolution with the 25 MeV linear accelerator at a later date.

TABLE 3 (fig. 4)

Observed Energy in eV	Mass number of Isotope
43.5 ± 0.9	145 †
56 ± 1.2	143 †
83 ± 2.2	145
105 ± 2.9	145
128 ± 4.1	143
158 ± 5.4	143, 148
180 ± 6.5	143
236 ± 9.4	145, 150
290 ± 12.8	148
375 ± 18.7	150

† Already assigned by Brookhaven Laboratory.

TUNGSTEN

Tungsten trioxide samples were used. The resonances already assigned by Brookhaven workers were confirmed [2]). It was only possible to do interlaced runs on two isotopes Tungsten 183 and Tungsten 184.

TABLE 4 (fig. 5)

Observed Energy in eV	Mass number of Isotope
18.7 ± 0.3	186
21.1 ± 0.32	182
27.0 ± 0.5	183
40.0 ± 0.76	183
46.03 ± 0.92	183
100.6 ± 2.8	183
112.5 ± 3.4	182
155.8 ± 5.5	183
180.4 ± 6.5	184
219.7 ± 8.8	186
259.8 ± 11.2	182

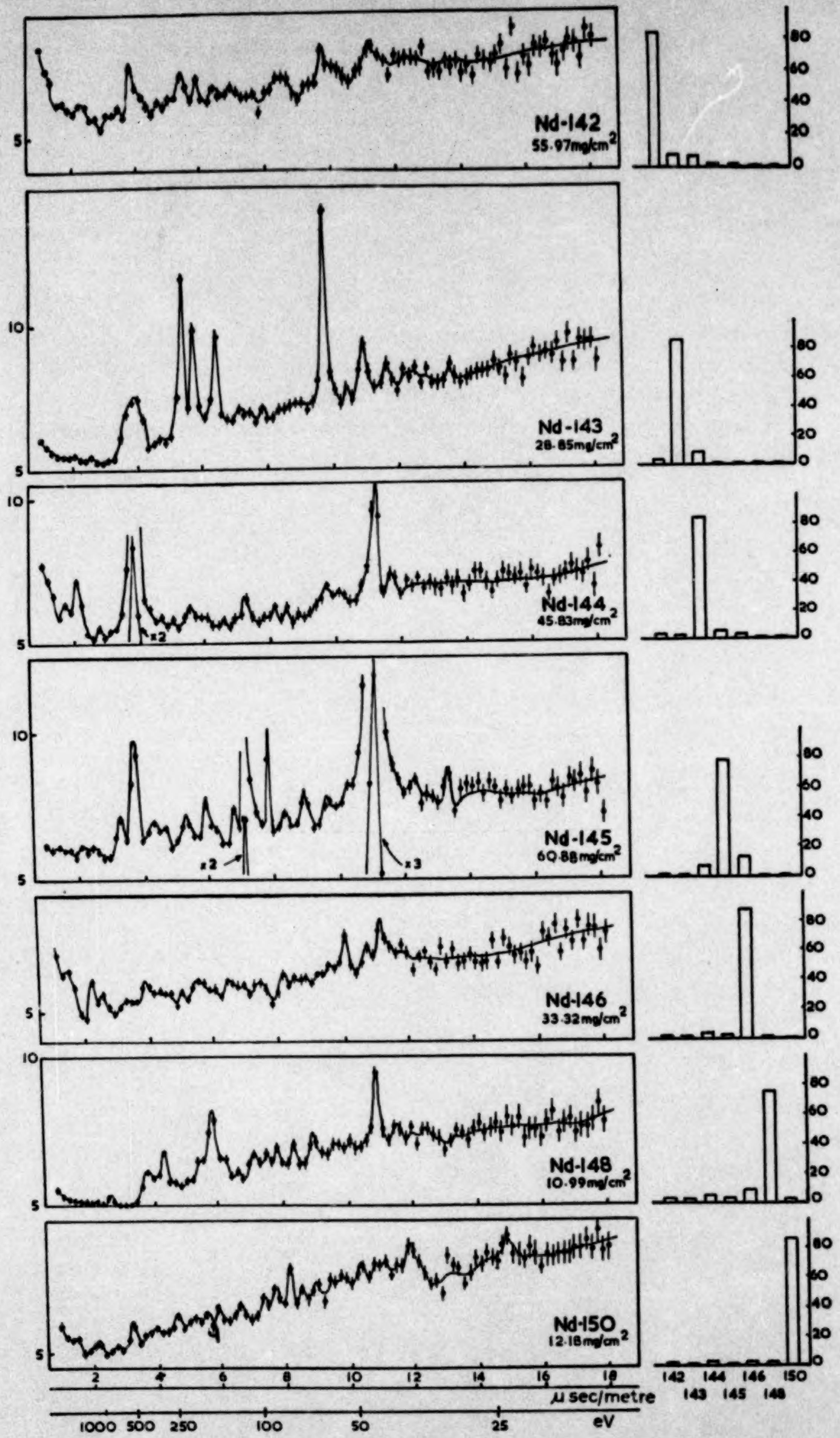

Fig. 4. Yields of γ-rays from neutron capture by Neodymium.

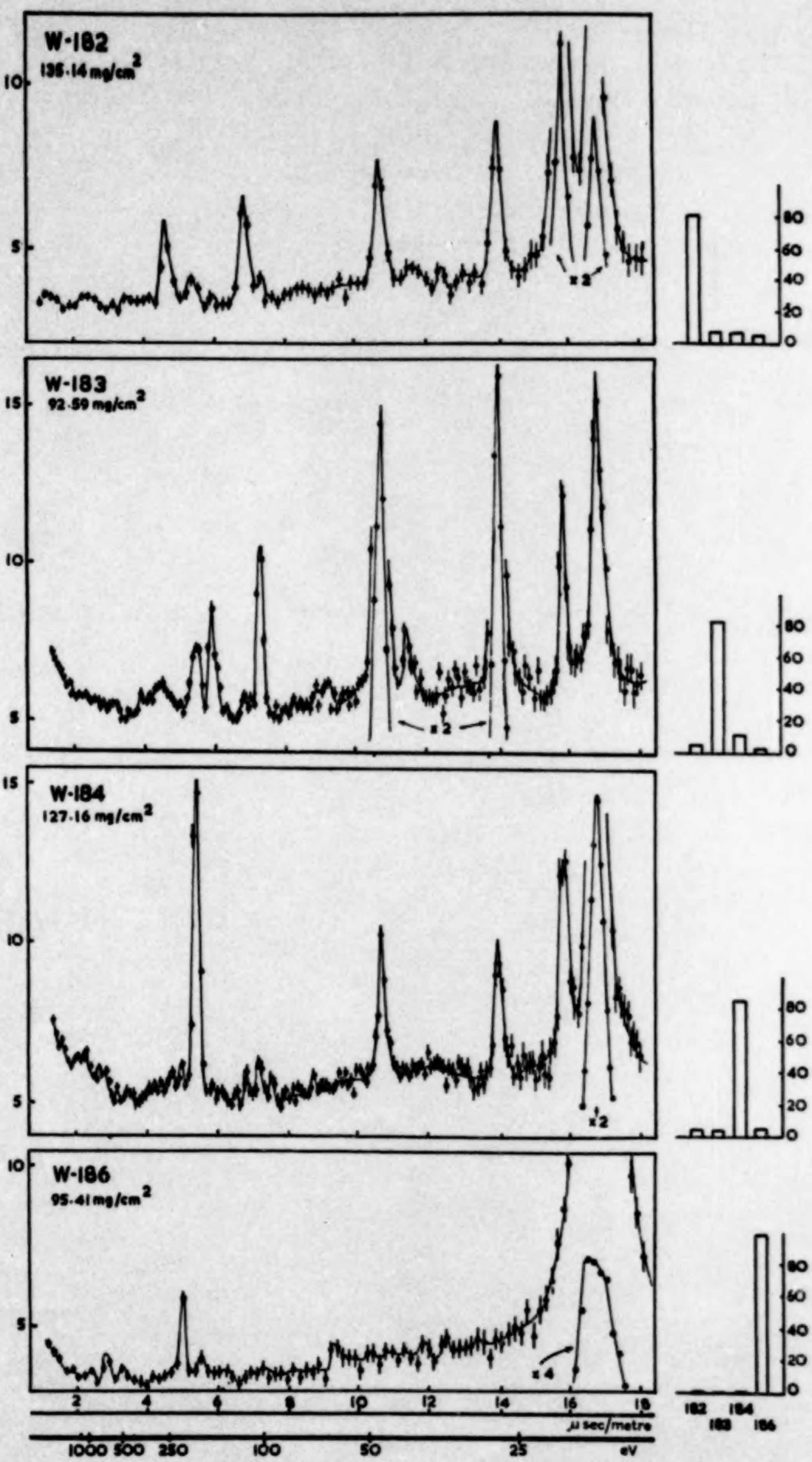

Fig. 5. Yields of γ-rays from neutron capture by Tungsten.

I would like to thank Dr. E. R. Rae for his continued interest and advice and also Dr. M. L. Smith, of the E. M. Separator Group at Harwell, for the loan of Isotopic samples.

References

1) E. R. Rae and E. M. Bowey, Journal of Nuclear Energy **4** (1957) 179
2) D. J. Hughes and J. A. Harvey, Neutron Cross Sections, BNL 325

Nuclear Physics **3** (1957) 561—570; *North-Holland Publishing Co., Amsterdam*

NEUTRON ALPHA PARTICLE ANGULAR CORRELATION IN THE REACTION ^{7}Li(d, α) AND THE GROUND STATE OF ^{5}He

F. J. M. FARLEY AND R. E. WHITE
Auckland University College, Auckland, New Zealand

Received 26 January 1957

Abstract: At a bombarding energy of 160 keV, the reaction ^{7}Li (d, α) ^{5}He is isolated by selecting the corresponding group of monoergic alpha particles with a differential detector and the angular distribution of the coincident neutrons from the disintegration of ^{5}He is then studied with a scintillation counter. The neutrons are emitted within a cone, and from the distribution through the cone it is deduced that the angular distribution function for the disintegration of ^{5}He with respect to the direction of emission of the initial alpha particle is $f(\theta) = 1+A \sin^2\theta$. The results can be fitted for $A = 0.72$ with the distribution of ^{5}He excitation energies used by Adair [10]) in interpreting data on neutron scattering by helium. The dynamics of our experiment are such that the ground state properties predominate in the results for the angular distribution and we thus confirm that the ground state has spin 3/2, since a spin of $\frac{1}{2}$ would lead to isotropy.

1. Introduction

Two reaction paths occurring in the bombardment of ^{7}Li by low energy deuterons are well established [1]). The compound nucleus ^{9}Be* breaks up either (1) to ^{8}Be*+n followed by ^{8}Be* $\rightarrow 2\alpha$; or (2) to ^{5}He+α_1, followed in about 10^{-21}s by ^{5}He $\rightarrow \alpha_2$+n. In both cases the end products are two alpha particles and a neutron, but the reactions can be distinguished by the distinctive distributions of the product particles in energy and angle. Reaction (1), which can go via a number of broad excited levels in ^{8}Be*, gives broad neutron energy groups extending up to about 13 MeV and a continuous distribution of alpha particles up to about 7 MeV. Reaction (2) on the other hand gives a monoergic group of alpha particles (α_1) of energy 7.4 MeV, with a continuum of lower energy alpha particles (α_2) and a continuous distribution of neutron energies ranging from 0.1 to 4 MeV [2, 3]). It is reaction (2) that is studied here with reference particularly to the energies released in the two stages

$$^7\text{Li} + {}^2\text{D} \rightarrow {}^5\text{He} + \alpha_1 + Q_1 \qquad \text{(a)}$$

$$^5\text{He} \rightarrow \alpha_2 + \text{n} + Q_2 \qquad \text{(b)}$$

and to the angular correlation of the neutrons with the alpha particles (α_1).

The total energy (Q_1+Q_2) released in these reactions may be obtained from the binding energy of the deuteron [4]) and the energy release in the reaction ^{7}Li(p, α)^{4}He which has been accurately determined [5]). In this way we find $Q_1+Q_2 = 15.10\pm0.02$ MeV. The division of this quantity into Q_1 and Q_2 is, however, not so clear: measurements of the range of the alpha particle group (α_1) from reaction (a) have given $Q_1 = 14.2\pm0.1$ MeV (French and Treacy [6])) in agreement with the value 14.3 MeV calculated by Livingston and Bethe [7]) from the measurements of Williams *et al.* [8]). French and Treacy's [6]) figure implies $Q_2 = 0.9\pm0.1$ MeV.

There are no direct measurements of Q_2, but indirect evidence on the mass of ^{5}He from the scattering of neutrons by ^{4}He suggests a value close to 1.0 MeV [9, 10]).

Further evidence comes from the measurements of Almquist [11]) and Moak [12]) which give $Q_2 = 0.90\pm0.07$ MeV, and 0.95 ± 0.07 MeV respectively. Ajzenberg and Lauritsen [5]) adopt a ^{5}He mass defect of 12.92 ± 0.08 MeV, which corresponds to $Q_2 = 1.0\pm0.08$ MeV.

French and Treacy [6]) confirmed the existence of reactions (a) and (b) by observing coincidences between the alpha particles α_1 and α_2. Because of the high momentum of the ^{5}He nucleus emitted in reaction (a) and the low disintegration energy Q_2, the particles α_2 leave the target in a cone of semi-angle about 12°; if the momentum brought in by the incident deuteron is neglected, the axis of the cone is at 180° to the direction of emission of the first alpha particle (α_1). French and Treacy selected the alpha particle group (α_1) by means of a differential range detector, and then studied the coincident alpha particles α_2. Although these have energy lying within the continuum of alpha particle energies from reaction (1) they were nevertheless isolated by the coincidence technique, and their energy distribution was measured. This energy distribution is related to the angular correlation of the ^{5}He disintegration with respect to the initial alpha particle α_1, and French and Treacy deduced an angular distribution function $f(\theta) = 1+A\sin^2\theta$ with $A = 1.2\pm0.1$.

Our object has been to verify this assignment by studying the neutrons from the disintegration of ^{5}He, instead of the alpha particles α_2. Because of their greater velocity the neutrons are spread over a wider cone, and therefore in this case it is possible to study the distribution of particles within the cone directly by traversing a small fast neutron detector. Once again neutrons from other reactions are excluded, and the axis of the cone is defined, by calling for coincidences with the initial alpha particle α_1. The angle of the cone of neutrons is related to the disintegration energy Q_2; and the distribution of particles within the cone gives the angular distribution function $f(\theta)$.

2. Experimental

The alpha particles α_1 from a thick lithium hydroxide target were detected at 130° to the resolved deuteron beam, (energy 160 keV), by means of a proportional counter subtending ±4.5° at the target. A pulse height discriminator allowed only the largest pulses, due to alpha particles stopping in the counter, to be accepted, with the result that the counter had differential range characteristics. A variable pressure air cell included between the target chamber and the counter allowed the selected range to be adjusted.

To calibrate the stopping power of the two mica windows the target was replaced by a source of thorium active deposit and a fixed point on the range scale at 8.78 MeV was thus obtained. Fig. 1 shows the resolution obtained: while not sufficient for a detailed study of the alpha particle group α_1, it was quite satisfactory for isolating the group and for excluding the longer range alpha particles and protons from ^{6}Li-reactions.

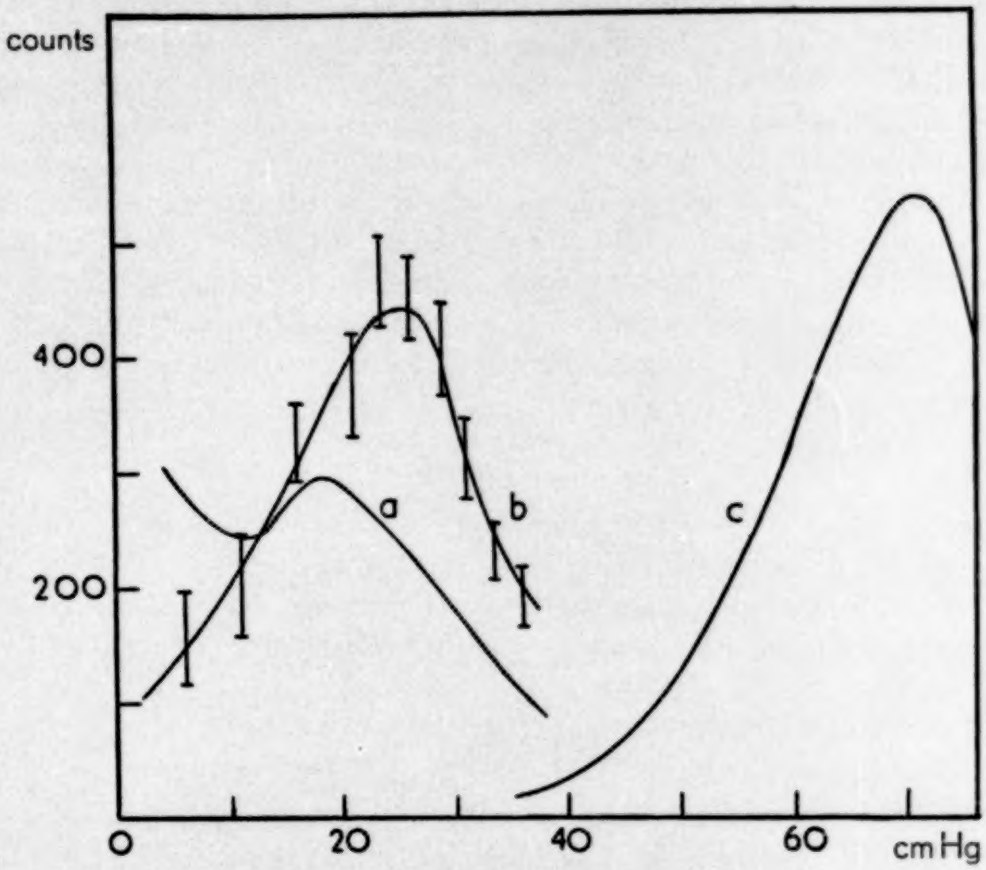

Fig. 1. Alpha particle counts versus air cell pressure.
Curve a, all alpha particles.
Curve b, alpha particles in coincidence with neutrons.
Curve c, ThC′ calibration alpha particles.

The neutrons from the disintegration of ^{5}He passed through the target backing (0.010″ copper), left the target chamber through a 0.015″ cylindrical steel wall and were detected by a scintillation counter with stilbene crystal, 1 inch diam. × ½ inch thick, subtending ±4½° at the target. This counter could be traversed through ±80° in the plane defined by the incident beam and the direction of initial alpha particle emission; zero angle was at 176° to the alpha particle counter, a correction of 4° being appropriate to allow for the momentum brought in by the incident deuteron.

The wall of the target chamber was kept thin wherever it could be struck by the coincident neutrons. About 3 % of the neutrons were scattered in the target backing and the chamber wall. The target was oriented perpendicular to the line of emission of the initial alpha particle.

A difficulty in interpreting the measurements of coincidence rate as the angle of the neutron counter is varied, is that the neutron energy and therefore the efficiency of the neutron counter varies as the distribution is traversed. The correction has been evaluated from the known neutron-proton scattering cross section and from measurements of the coincidence rate at various discriminator biases.

Coincidences between the alpha particles α_1 and the neutrons were recorded with a resolving time of 0.1 μs, and the contribution of the random coincidences was evaluated at the same time using the method of Littauer [13]). Typically with a beam current of 100 μA and a counting rate 1000/sec for alpha particles and 1500/sec for neutrons, the true and random coincidence rates were each about 0.5/sec.

3. Results

The coincidence rate was studied as a function of the pressure in the air cell with the result shown in fig. 1. This confirms the result of French and Treacy [6]) that coincidences due to the disintegration of ^{5}He are observed only when the alpha particle counter is set to record the group α_1 emitted in reaction (a). From the position of the peak relative to that of the thorium alpha particles the energy of the α_1-particles is found to be 7.36 ± 0.12 MeV. Correcting for target thickness we deduce $Q_1 = 14.15\pm0.22$ MeV in agreement with previous values.

The variation of coincidence rate with the angular position of the neutron counter was studied in runs totalling 50 h which yielded the points shown in fig. 2. The points are plotted one side of zero only, with those corresponding to negative angles marked distinctively, so that the symmetry of the experimental results about zero angle may be apparent.

4. Discussion

Before attempting to find a theoretical curve to fit the experimental points, it is necessary to consider the efficiency of the neutron counter. It has already been mentioned that the efficiency of the neutron counter varies as the ±80° angle is traversed. This is due to two effects, first to the variation of the neutron-proton scattering cross-section with energy, completely determined by the data of Adair [14]), and secondly because a fraction of the

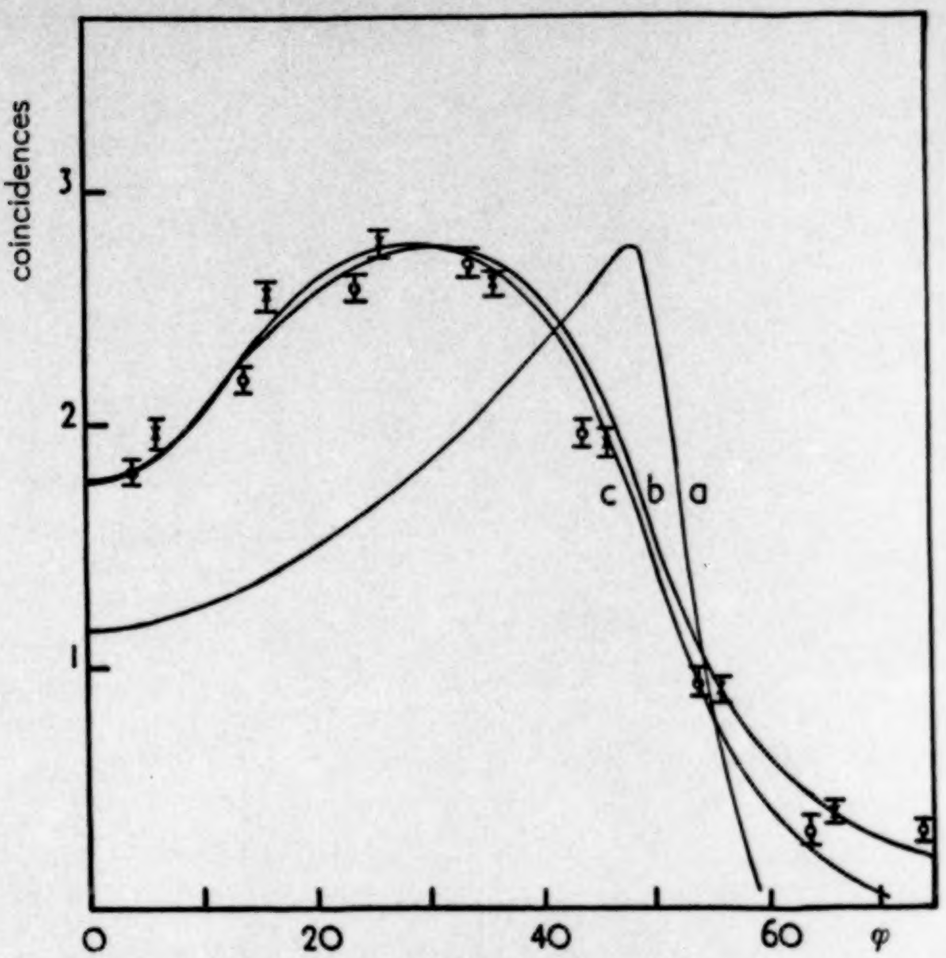

Fig. 2. Coincidences per 2.5×10^3 alpha particles versus lab. angle φ. Experimental points marked $\overline{\underline{\phi}}$ for positive values of φ, $\overline{\underline{x}}$ for negative values.
Curve a, calculated for $Q_2^0 = 1.0$ MeV, $\Gamma = 0$, $A = 0.70$.
Curve b, calculated using the neutron-alpha scattering data of Adair.
Curve c, calculated for $Q_2^0 = 0.98$ MeV, $\Gamma = 0.60$ MeV, $A = 0.70$.

proton recoil pulses are smaller than the discriminator bias and do not give a count. This fraction increases as the neutron energy is reduced. To evaluate the second effect we have

(a) calculated the pulse height spectrum to be expected when monoergic neutrons fall on a stilbene scintillator allowing for the non-linearity of the phosphor, see fig. 3;

(b) hence computed the curve of coincidence rate versus discriminator bias when the neutron counter is set at 36°: this theoretical curve fig. 4 has arbitrary scales;

(c) made measurements of coincidence rate versus discriminator bias at the same angle, and extrapolated to zero bias using the theoretical curve shape. The fit of the theoretical curve to the experimental data is shown in fig. 4.

This procedure shows that the loss of counts due to the finite working bias

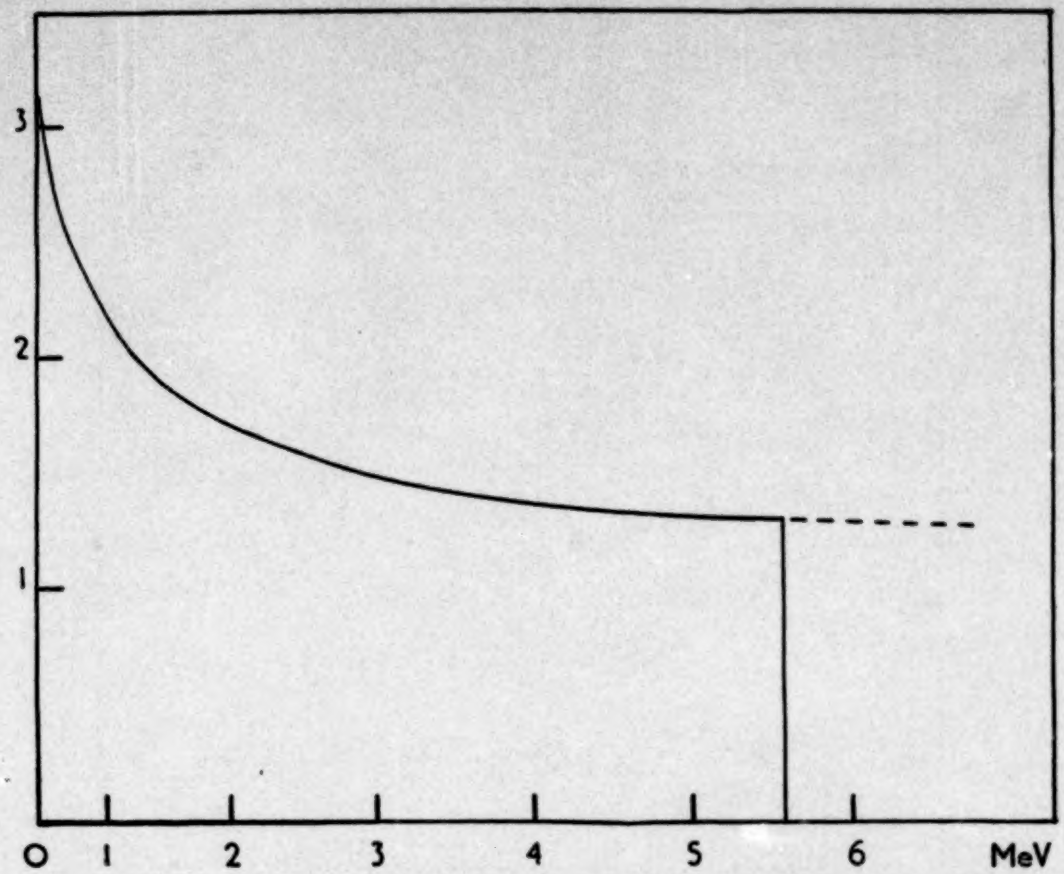

Fig. 3. Theoretical differential spectrum of recoil proton pulses from stilbene giving the number of pulses versus pulse height (arbitrary linear scale) with the corresponding proton recoil energy marked in MeV.

of 10 volts is 14±1 % at this particular angle, and the bias corresponds to a proton recoil energy of 0.35±0.02 MeV. Using the theoretical pulse height spectra we can now find the loss of counts at any other angle.

The method of calculation takes account of the spread in the energy of the neutrons incident on the phosphor due to the finite angles subtended by the counters and to the distribution of ^{5}He excitation energies.

The curve of fig. 3 is obtained from the data of Taylor *et al.* [15]) on organic phosphors. It is readily shown that the differential pulse height spectrum, that is the number of pulses versus pulse height, when monoergic neutrons are incident on a phosphor, is obtained by plotting $\mathrm{d}E/\mathrm{d}L$ versus L where L is the magnitude of the light pulse produced by a proton of energy E. The data of Taylor *et al.* gives $\mathrm{d}L/\mathrm{d}E$ versus $\mathrm{d}E/\mathrm{d}x$ where x is the proton range, and also E versus L. Combining these with the range-energy relation [16]) we compute the curve given in fig. 3. This curve gives, with arbitrary scales, the differential pulse height spectrum for monoergic neutrons of any energy provided the position of the sharp cut-off is adjusted to correspond with the maximum proton recoil energy.

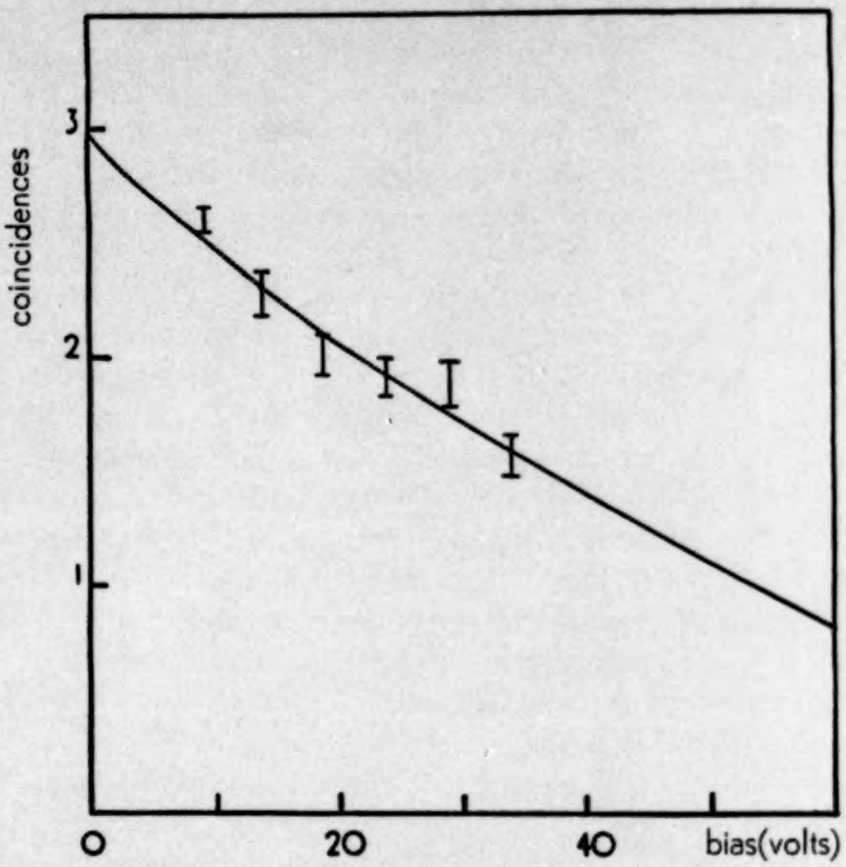

Fig. 4. Theoretical integral spectrum of recoil proton pulses at 36° fitted to the experimental points of coincidence rate versus discriminator bias.

In evaluating the correction for the loss of the smaller proton recoil pulses it has been necessary to assume a particular distribution of Q_2 values but we have checked that our results are not sensitive to small changes in this distribution. We have further checked that the possible variation of $\pm 1\ \%$ in the loss found at 36° does not appreciably affect the agreement between the experimental and theoretical curves.

In attempting to fit a theoretical curve to the experimental points of fig. 2 we recall that the distribution of neutrons over the cone is obtained from the angular distribution $f(\theta)$, of the break-up in ^{5}He space, and from the geometry of the reaction. Before comparison with the experimental points the theoretical curve is first corrected for the variation of efficiency of the neutron counter with angle (see above), and then smoothed to allow for the finite angles subtended by each detector. This yields fig. 2, curve a, which clearly does not fit the experimental points and cannot be made to fit by adjusting Q_2 because the cut-off is always too steep.

To fit the results it is necessary to allow for the finite widths of the states of ^{5}He that are excited. In effect there is a range of values for Q_2 and each contributes neutrons over a particular angular region. Each value of Q_2

below 1.6 MeV contributes a cone of neutrons with a different cut-off angle while for higher values the neutrons are distributed over the whole solid angle. This concentration of the neutrons into cones for small Q_2 values, with a resulting increase in intensity within the cones, means that these contributions predominate in the angular distribution. As this is the region of ground state excitation we see that the properties of the ground state will dominate the results.

The individual distributions for the various Q_2 values must now be appropriately weighted and combined. If we assume that the same states are excited here as in neutron scattering by helium then the required weighting factors for the Q_2 values are obtained from the variation of the scattering cross-section of helium with neutron energy. Using data derived from proton-helium scattering measurements, Adair [10]) and Dodder and Gammel [17]) have calculated this cross-section and obtained good agreement with the measurements made by Baskin *et al.* [18]). They assume that data for the ^{5}Li compound state can also be applied to ^{5}He and find that the $P_{\frac{1}{2}}$ and $P_{3/2}$ states of ^{5}He form an inverted doublet with a splitting of about 3 MeV. Using the calculated cross section curves of Adair [10]) we obtain, with $A = 0.72$, fig. 2 curve b, which is a good fit to the experimental points. Our calculated distribution is insensitive to changes in the contributions of Q_2 values above 2 MeV and therefore we cannot decide between the quite different widths assigned to the $P_{\frac{1}{2}}$ state by the above authors. This is emphasised by the fact that almost as good a fit to our results is obtained by assuming that only a single state of ^{5}He is excited. For example fig. 2 curve c, is obtained if this state is unbound by 0.98 MeV, has a width Γ of 0.70 MeV and if $A = 0.75$ These values of excitation energy and width are in good agreement with those normally assigned to the ground state [5]). Our value of $A = 0.75 \pm 0.05$ differs considerably from the value of 1.2 ± 0.1 found by French and Treacy [6]) but this is probably due to the different energies of the incident deuterons, 160 keV and 930 keV respectively.

Our results therefore confirm that the ^{5}He ground state is a $P_{3/2}$ state of negative parity as deduced by Adair [10]) and Dodder and Gammel [17]). As regards the angular correlation function $1+A\sin^2\theta$, it is possible to fit this theoretically on the assumption that a single 3/2-state of ^{5}He is involved, and that the first alpha particle α_1 is emitted isotropically with respect to the deuteron beam. The theoretical neutron-alpha particle angular correlation then depends on the spin and parity assigned to the compound nucleus ^{9}Be*. We find that the spin-parity assignments $\frac{1}{2}+$ and $\frac{1}{2}-$ both lead to $f(\theta) = 1+3\cos^2\theta$ which does not fit. A spin 3/2−state, however, formed by s-wave deuterons, and emitting a mixture of s- and d-wave alpha particles α_1 can be adjusted to fit any distribution ranging from isotropic to a pure $\sin^2\theta$: it is therefore compatible both with our result and with that of French and Treacy [6]). If the theory is generalised by allowing interference from the $\frac{1}{2}-$ state of ^{5}He then there are many more possibilities and in this case spin parity assignments $\frac{1}{2}+$ or $\frac{1}{2}-$ to the excited state of ^{9}Be are also compatible with the experimental distributions.

Our results are broadly in agreement with those recently published by Riviere [19]) but differ as regards the angular distribution function and the assignment of spin to the ^{9}Be* compound state.

5. Polarization Measurements

Polarisation effects may be present in this reaction. Theoretically if the intermediate ^{5}He state is polarised the neutrons may not be symmetrically distributed around the allowed cone. We have looked for this effect by studying the neutron-alpha particle coincidence rate as a function of the azimuth angle ϕ of the neutron cone, keeping the angle θ fixed.

Theoretically a variation of the form $\cos\phi$ can be expected, and for the $P_{3/2}$ state of ^{5}He a component of the form $\cos 2\phi$ is also possible [20]), but these can only be present if the ^{5}He sub-states are not statistically populated by the initial (d, α) reaction.

Measurements of coincidence rate were made at 45° intervals of ϕ, keeping θ fixed to obtain the maximum coincidence rate. The distribution was found to be isotropic to $\pm 3\,\%$.

Further experiments to measure polarisation effects in ^{5}He produced in another reaction are now in progress and will be reported later.

The target chamber and alpha-particle counter used in this experiment were designed by E. L. Dudding, and the accelerator was built by Dr. L. C. W. Hobbis.

We wish to thank Dr. P. B. Treacy, Dr. A. P. French, Dr. F. C. Barker and Mr. L. M. Delves for valuable discussions, and Mr. H. Naylor for his participation in the measurements. One of us, R. E. White, would like to acknowledge the assistance received from an Imperial Chemical Industries (N.Z.) Fellowship and a University of New Zealand Senior Research Fund Fellowship.

References

1) W. F. Hornyak, T. Lauritsen, P. Morrison and W. A. Fowler, Rev. Mod. Phys. **22** (1950) 291
2) H. Staub and W. E. Stephens, Phys. Rev. **55** (1939) 845
3) W. D. Whitehead, Phys. Rev. **79** (1950) 393
4) R. E. Bell and L. G. Elliott, Phys. Rev. **79** (1950) 282
5) F. Ajzenberg and T. Lauritsen, Rev. Mod. Phys. **27** (1955) 78
6) A. P. French and P. B. Treacy, Proc. Phys. Soc. A **64** (1951) 452
7) M. S. Livingston and H. A. Bethe, Rev. Mod. Phys. **9** (1937) 245
8) J. H. Williams, W. G. Sheperd and R. O. Haxby, Phys. Rev. **51** (1937) 888
9) P. Huber and E. Baldinger, Helv. Phys. Acta. **25** (1952) 435

10) R. K. Adair, Phys. Rev. **86** (1952) 155
11) E. Almquist, K. W. Allen, J. T. Dewan and T. P. Pepper, Phys. Rev. **91** (1953) 1022
12) C. D. Moak, Phys. Rev. **92** (1953) 383
13) R. M. Littauer, Rev. Sci. Instr. **21** (1950) 750
14) R. K. Adair, Rev. Mod. Phys. **22** (1950) 249
15) C. J. Taylor, W. K. Jentschke, M. E. Remey, F. S. Eby and P. G. Kruger, Phys. Rev. **84** (1951) 1034
16) H. A. Bethe, Rev. Mod. Phys. **22** (1950) 213
17) D. C. Dodder and J. L. Gammel, Phys. Rev. **88** (1952) 520
18) S. Bashkin, F. P. Mooring and B. Petree, Phys. Rev. **82** (1951) 378
19) A. C. Riviere, Nuclear Physics **2** (1956/57) 81
20) A. Simon and T. A. Welton, Phys. Rev. **90** (1953) 1036

Nuclear Physics **3** (1957) 571—584; *North-Holland Publishing Co., Amsterdam*

EMPIRICAL DETERMINATION OF NUCLEAR SHAPE FACTORS AND MOMENTS OF INERTIA

E. D. KLEMA † and R. K. OSBORN

Oak Ridge National Laboratory, Oak Ridge, Tennessee

Received 22 October 1956

Abstract: The results of certain experiments sensitive to nuclear shapes are correlated in terms of the kinematical model used previously for the correlation of nuclear ground-state properties. The data considered in the present work are the energies of the rotational levels of even nuclei, (i.e. nuclei with even numbers of protons and neutrons), the probabilities of electrodynamically-induced transitions between these levels, and the quadrupole moments of odd-mass nuclei.

The dynamics of the system represented by the model is treated purely empirically and is presumed to be characterized by a small set of well-defined physical parameters. The principal empirical conception investigated below is that of the fraction of nuclear matter which participates in collective rotational motion, and its implications for the correlation of nuclear shapes as determined from the data mentioned above. This fraction is taken to be the ratio of the number of particles outside of filled major shells (both protons and neutrons) or the number of holes, whichever is smaller, to the total number of particles in the nucleus.

The correlation obtained suggests the possibility of estimating the quadrupole moments of odd-mass nuclear ground states from the superior experimental data on neighbouring even-nuclei, and this suggestion is pursued where possible. It is found that the moments so calculated exhibit no consistent deviations from the experimental values.

1. Introduction

The concept of odd-mass nuclei as consisting of a rigidly-deformed, axially-symmetric core plus a single nucleon has been exploited in two previous papers, referred to as I ¹) and II ²), for the correlation and analysis of experimental data on nuclear ground states — spins, parities, magnetic moments, and quadrupole moments. It was intended that as many as possible of the details of the model should be determined by the experimental data themselves; hence, minimal attention was given to dynamical considerations in the course of the development and application of the model ††.

---

† Now at the University of Michigan, Ann Arbor, Michigan.

†† *Editor's note:* Readers of the authors' previous papers have probably experienced some surprise at the fact that the analysis of the data on the basis of their assumptions leads in many cases to non-zero values of the core angular momenta. Such a consequence might even be thought to throw some doubt on the consistency of these assumptions. In the present paper, the authors introduce a further assumption which may look still more hazardous. Nevertheless, in the absence of any satisfactory dynamical theory which might help to settle such doubts, the Editor thinks that the best course is to submit the results of the authors' attempt to correlate a large variety of data on the basis of clearly formulated assumptions to the judgment of the readers. It is not inconceivable that some, if not all, of these correlations could prove significant and give useful hints for a more fundamental treatment.

Nuclear ground states were constructed by superposition of core-plus-particle states which diagonalized the total system angular momentum, the space projection of the system angular momentum, the core angular momentum, the magnitude of the body projection of the core angular momentum, the system parity, and the spin-orbit interaction for the particle. The nuclear states so constructed were themselves required to be eigenfunctions of the total system angular momentum and parity with eigenvalues dictated by experiment. It was assumed that two of the components of a given nuclear ground state would be predominant; hence, in order to obtain simple, well-defined states this assumption was incorporated in a postulate that *only* two components should be employed in the construction of the nuclear state. The core-plus-particle states to be admixed, as well as the relative amplitudes of the admixture, were then largely determined by the requirement that the states selected yield nuclear magnetic moments in agreement with experiment [1]).

In order to complete the specification of the system, the core was presumed to be an axially-symmetric spheroid with the same volume as the equivalent spherical nucleus. Thus it was convenient to characterize the core shape by a single dimensionless parameter, γ, defined to be the ratio of the semi-axis of the spheroid along the symmetry axis to the radius of the equivalent sphere. It was further assumed that the mass and charge distribution in the core were uniform. Then the core shape parameter was determined by the specifications that the static and dynamic shapes of the core be of the same character (both prolate or both oblate) and that the magnitude of the core deformation be such that the core-plus-particle configurations prescribed by experimental magnetic moments yield quadrupole moments also in agreement with experiment [2]).

In this paper it is intended to exploit the above determination of core shapes for odd-mass nuclei to obtain a connection between the experimental data on the ground states of these nuclei with the data concerning the first excited states of the even nuclei obtained from odd-mass nuclei by stripping off the extra-core nucleons. The connection is, of course, immediately apparent if it is assumed that the even nucleus under consideration is indeed the core of the appropriate neighbouring odd-mass nucleus; i.e., that the extra nucleon in the latter system does not significantly polarize the core. On the basis of such an assumption, the moment of inertia of the even nucleus is completely determined in terms of the shape of the odd-mass nucleus. In turn, the energy of the 2^+ state of the even nucleus is determined by the nuclear moment of inertia, provided that the state in question is indeed one appropriate to a rigid rotator.

In order to establish a criterion as to the extent to which this central provision is realized in a given case, it is necessary at this point to invoke a modification of the model, and desirable to provide a quantitative description of that modification which is as nearly independent of the model as possible. The necessity for the modification rests upon the observation that rigid nuclear moments of inertia are altogether too large. The observation itself suggests an appropriate modification; i.e., hereafter it is to be assumed that only a fraction of the *uniformly distributed* nuclear mass participates in the collective rotation. The model-independent specification of that fraction of the total nuclear mass which does participate in the rotation is accomplished by the following definition:

k (the mass fraction) $\equiv$ the ratio of the number of particles outside of filled major shells (both protons and neutrons) or the number of holes, whichever is smaller, to the total number of nucleons in the nucleus.

If one assumes that the fractional nuclear mass, kM, where M is the mass of the nucleus, rotates as an axially-symmetric rigid rotator with uniform mass distribution about an axis at right angles to the axis of symmetry, the moment of inertia is given by

$$\Lambda_x = 1/5\, kMR_0^2\left(\gamma^2+\frac{1}{\gamma}\right), \tag{1}$$

where R_0 is the undeformed nuclear radius, here taken, as in II, to be $1.44A^{1/3}\times 10^{-13}$ cm. The energy of such a rigid rotator with angular momentum λ is given by

$$E_\lambda = \frac{\hbar^2\lambda(\lambda+1)}{2\Lambda_x}. \tag{2}$$

A criterion that a particular 2^+ first-excited state be rotational in character may be stated as follows: It is presumed that a 2^+ level of an even nucleus is rotational provided that there exists a positive real γ as the solution of the equation

$$\gamma^3-C\gamma+1 = 0, \qquad C = \frac{15\hbar^2}{E_{2^+}kA^{5/3}}, \tag{3}$$

where E_{2^+} is the energy of the level in question. This criterion may be rephrased in terms of the requirement that

$$E_{2^+}\text{ (in keV)} < \frac{1.600\times 10^5}{kA^{5/3}}. \tag{4}$$

The requirement (4) is to be compared with that invoked by Bohr and Mottelson,

$$E_{2^+} < \frac{9.22\times 10^5}{A^{5/3}}, \tag{5}$$

quoted by Temmer and Heydenburg [3]) to be "a rough criterion to be satisfied by the energy of the first excited state in order that one may expect a conventional rotational spectrum".

It is to be noted that the criterion invoked for the present investigation contains no restrictions to the region of the rare earths. Thus at this point it is to be regarded as a necessary, but not sufficient, condition that the first level be rotational in character. It remains fot the data, analyzed in the context of the present model, to provide this further restriction.

The remainder of this paper is devoted to an examination of the validity of the above proposed definition of the parameter which measures the mass fraction participating in the rotation and pursuing the implications of the concept itself.

2. Analysis of Data

The definition of k given above is model-independent in that it is completely determined in terms of the "magic numbers" and the numbers of neutrons and protons in a given nucleus. The numbers taken to be magic herein are 8, 20, 28, 50, 82, and 126. The same quantity, i.e., the mass fraction, is equally unambiguously defined within the context of the present model. From eq. (2) it is seen than an experimental moment of inertia, Λ_{xE}, may be obtained for a given even nucleus from the energy of its 2^+ rotational level according to

$$\Lambda_{xE} = \frac{2.0820}{E_{2^+}(\mathrm{MeV})} \times 10^{-48}\,\mathrm{g\ cm}^2. \tag{6}$$

Similarly, from eq. (1) a moment of inertia, $\Lambda_{x\mathrm{C}}$, may be calculated for the same nucleus if the shape factor for the core of the appropriate neighbouring odd-mass nucleus is known; i.e.,

$$\Lambda_{x\mathrm{C}} = 6.88(10^{-3}A^{5/3})\left(\gamma^2+\frac{1}{\gamma}\right) \times 10^{-48}\,\mathrm{g\ cm}^2. \tag{7}$$

Here, of course, A is the mass number of the even nucleus under consideration. Clearly, the mass fraction participating in the rotation is determined in terms of the model by the relation

$$k_{\mathrm{C}} = \frac{\Lambda_{xE}}{\Lambda_{x\mathrm{C}}}. \tag{8}$$

In table 1 the values of k and k_{C} are listed for those even nuclei whose first-excited states satisfy the criterion (4), and which have odd-mass neighbours whose magnetic and quadrupole moments have been measured. The tabulation is further restricted to include only those nuclei for which $52 \leqq Z \leqq 80$ and for which the odd-mass member of the pair is characterized according to the present model by a ground state in which the spin of the single-particle configuration is the same as the nuclear spin.

The corresponding values of the criterion parameter, C, are also listed. This parameter is called the criterion parameter since, as is seen from eq. (3), the condition that there exist a physically meaningful value of γ is equivalent to the requirement that $C \geqq 1.89$. It is this inequality which is rephrased in eq. (4). It is to be noted that if $C \geqq 1.89$, then two positive roots of eq. (3) exist. The larger of these roots has been chosen throughout, since the smaller generally implies excessive oblate distortion.

TABLE 1

Values of the mass fraction k, the criterion parameter C, and the mass-fraction parameter for the present model, k_C.

Even Nucleus	k	C	Odd-mass Nucleus	k_C
${}_{52}\mathrm{Te}_{76}^{128}$	0.06250	1.98	${}_{53}\mathrm{I}_{76}^{129}$	0.065
${}_{54}\mathrm{Xe}_{76}^{130}$	0.07692	2.23	${}_{54}\mathrm{Xe}_{77}^{131}$	0.090
${}_{54}\mathrm{Xe}_{78}^{132}$	0.06061	2.18	${}_{55}\mathrm{Cs}_{78}^{133}$	0.064
${}_{66}\mathrm{Dy}_{98}^{164}$	0.1951	4.32	${}_{67}\mathrm{Ho}_{98}^{165}$	0.204
${}_{72}\mathrm{Hf}_{108}^{180}$	0.1556	3.64	${}_{73}\mathrm{Ta}_{108}^{181}$	0.150
${}_{74}\mathrm{W}_{112}^{186}$	0.1183	3.40	${}_{75}\mathrm{Re}_{112}^{187}$	0.173
${}_{76}\mathrm{Os}_{114}^{190}$	0.09474	2.73	${}_{77}\mathrm{Ir}_{114}^{191}$	0.119
${}_{76}\mathrm{Os}_{116}^{192}$	0.08333	2.76	${}_{77}\mathrm{Ir}_{116}^{193}$	0.104
${}_{78}\mathrm{Pt}_{118}^{196}$	0.06122	2.09	${}_{79}\mathrm{Au}_{118}^{197}$	0.059
${}_{80}\mathrm{Hg}_{120}^{200}$	0.04000	2.94	${}_{80}\mathrm{Hg}_{121}^{201}$	0.058

It is desirable at this juncture to point out that no attempt has been made to compare shape factors as determined from odd-mass nuclei data with those determined from the data on even nuclei. For if we let γ_e be the shape factor defined by eq. (3) and recall the definition of C, we see that

$$\frac{\mathrm{d}\gamma_e}{\gamma_e} = -\frac{\gamma_e^3+1}{2\gamma_e^3-1}\left(\frac{\mathrm{d}k}{k}+\frac{\mathrm{d}E}{E}\right). \tag{9}$$

Thus for nearly spherical nuclei — and particularly for those with small oblate deformations — it is apparent that relative changes in either k (whose quantitative significance must be inferred with caution) or E_{2^+} will induce larger relative changes in γ_e. Conversely, however, the mass-fraction parameter, k_C, determined by the model is least sensitive to the relevant experimental data in the region of small distortions; i.e.,

$$\frac{\mathrm{d}k_C}{k_C} = -\frac{2\gamma_0^3-1}{2\gamma_0^3+1}\,\frac{\gamma_0^3-1}{\gamma_0^3+1}\,\frac{\mathrm{d}Q}{Q}, \tag{10}$$

where γ_0 is the shape factor determined from the experimental quadrupole moment, Q, as discussed in II. Furthermore, in the region of highly-distorted nuclei, TABLE

Values of the criterion parameter C. The numbers in parentheses are the

Protons \ Neutrons	68	70	72	74	76	78	80	82	84	86	88	90	92
(Te) 52	(560) 1.39	(566) 1.55	(607) 1.67	(662) 1.82	(750) 1.98	(850) 2.31							
(Xe) 54			(385) 2.23	(436) 2.28	(528) 2.23	(670) 2.18	(870) 2.21	(1380) 2.07					
(Ba) 56						(605) 1.91	(1041) 1.37	(1440) 1.31	(1600) 0.876				
(Ce) 58								(1600) 0.876					
(Nd) 60								(1572) 0.671	(695) 1.32	(455) 1.71	(300) 2.25	(128) 4.65	
(Sm) 62										(562) 1.20	(337) 1.77	(122) 4.35	(82) 5.84
(Gd) 64											(344.1) 1.54	(122.8) 3.89	(89) 4.89
(Dy) 66													
(Er) 68													
(Yb) 70													
(Hf) 72													
(W) 74													
(Os) 76													
(Pt) 78													
(Hg) 80													

$$\frac{\mathrm{d}k_\mathrm{C}}{k_\mathrm{C}} \approx -\frac{\mathrm{d}Q}{Q}. \tag{11}$$

Thus it is perhaps significant that the principal quantitative disagreement between k and k_C occurs in the region in which relatively large nuclear distortions are to be expected and in which, at the same time, there is considerable uncertainty in the measurements of quadrupole moments.

It is evident, of course, that all quantities considered herein which are model-dependent are in general quite sensitive to the nuclear radius. For example, for $\gamma_0 \approx 1$,

$$\frac{\mathrm{d}k_\mathrm{C}}{k_\mathrm{C}} \approx -2\,\frac{\mathrm{d}R_0}{R_0}, \tag{12a}$$

whereas for $\gamma_0 \approx 2$,

$$\frac{\mathrm{d}k_\mathrm{C}}{k_\mathrm{C}} \approx -0.6\,\frac{\mathrm{d}R_0}{R_0} - 0.7\,\frac{\mathrm{d}Q}{Q}. \tag{12b}$$

Clearly, therefore, for nuclei with small distortions a 15 percent decrease in

2

measured energies (in keV) of the first-excited states of the indicated nuclei.

94	96	98	100	102	104	106	108	110	112	114	116	118	120	122
(79)	(76)													
5.04	4.82													
(86.2)	(80.8)	(73)												
4.25	4.20	4.32												
	(91)	(80.6)	(80.1)											
	3.96	4.17	3.88											
			(84.1)	(78.7)										
			3.91	3.88										
					(89.0)	(90)	(93.3)							
					3.38	3.54	3.64							
						(102)	(100)	(112)	(124)					
						3.32	3.62	3.48	3.40					
								(137.22)	(154.87)	(186)	(205.74)			
								3.08	2.97	2.73	2.76			
										(316)	(329.07)	(358)	(403)	
										1.80	1.96	2.09	2.21	
											(427)	(411)	(376)	(427)
											1.75	2.17	2.94	3.43

R_0 would induce an approximately 30 percent increase in the values of k_C, which would, of course, largely destroy the apparent quantitative agreement shown in table 1.

Fig. 1 exhibits a plot of k and k_C for appropriate even and odd-mass neighbours for which the requisite experimental data are available vs A for $A \geqq 60$. The solid circles represent the values of k calculated from the definition of k. The open circles are the values obtained from eq. (8). The triangles represent nuclei whose proton number is magic, and the squares represent those whose neutron number is magic. Comparison with table 1 shows that many of the points in the figure are for nuclei which can hardly be expected to exhibit rotational spectra even in the sense of the not very definitive criterion invoked above. Nevertheless, though it is most probably not legitimate to extrapolate these calculations into this region, it was done to point out the qualitative agreement that does, in fact, exist.

Table 2 contains a listing of all first-excited-state energies and criterion parameters C for even nuclei from Te^{120} to Hg^{202}. Since there is general agreement about the positions of the energy levels as determined by various types of experiments, we have not listed references for the various numbers given. Instead, we have put down the best value known to us in each case; a number of these have not yet been published.

A study of table 2 points up the necessity for invoking further criteria to be employed in the establishment of the rotational character of states as well as delineating rather clearly what the further criteria should be. As was to be expected, no nucleus with neutron number less than 90 may reliably be regarded as having a first-excited state of rotational character. In addition, one sees that there is another sharp break in the values of C between proton numbers 76 and 78, though not as striking as that between neutron numbers 88 and 90. Thus it is henceforth presumed that k as defined above has specific application to rotational spectra only if there are at least 6 protons (or proton holes) and 6 neutrons (or neutron holes) within a given unfilled major shell.

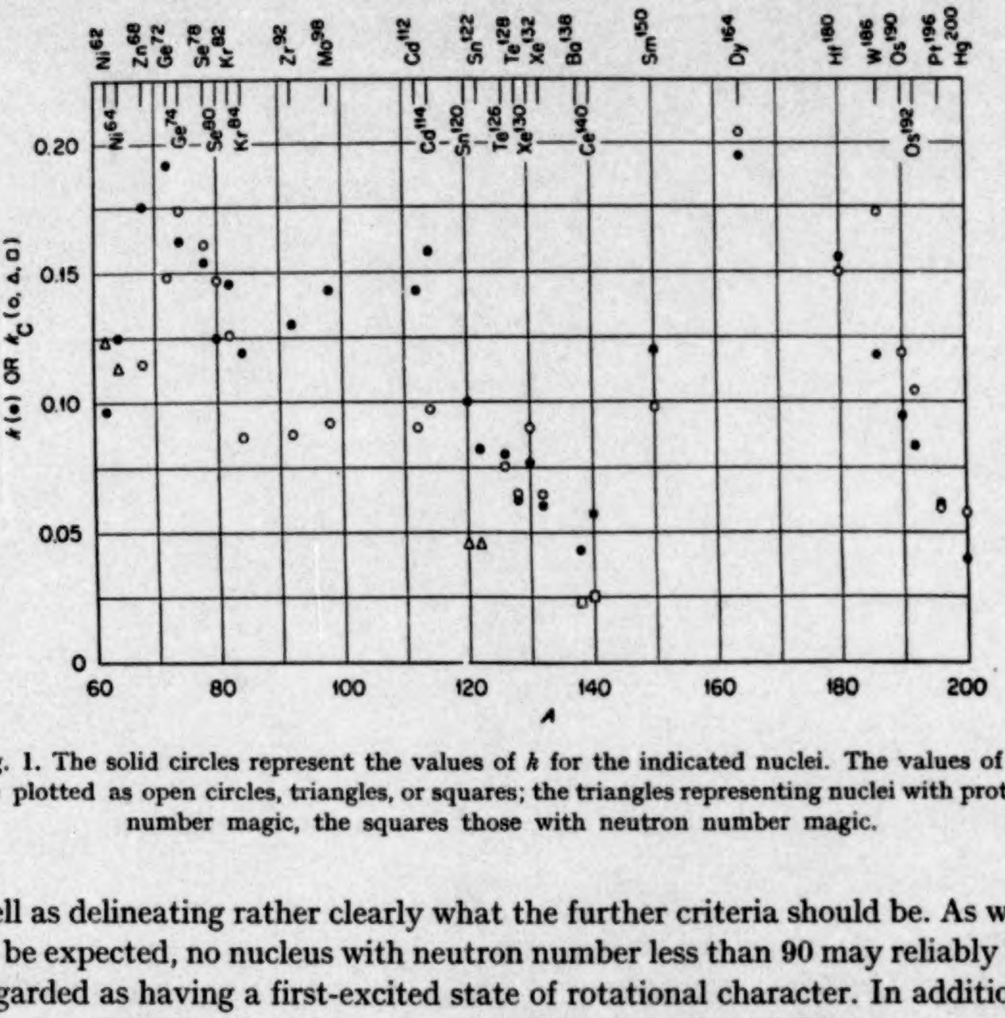

Fig. 1. The solid circles represent the values of k for the indicated nuclei. The values of k_C are plotted as open circles, triangles, or squares; the triangles representing nuclei with proton number magic, the squares those with neutron number magic.

Table 3 lists the shape parameters γ for all nuclei which satisfy the requirements on C and k as discussed above. From these values one may readily calculate the intrinsic quadrupole moments, Q_0, of these even-mass nuclei from the following relationships:

TABLE 3

Values of the shape parameter γ obtained from the measured first-excited-state energies of the listed nuclei.

Nucleus	γ	Nucleus	γ
$_{60}\mathrm{Nd}^{150}_{90}$	2.04	$_{70}\mathrm{Yb}^{170}_{100}$	1.83
$_{62}\mathrm{Sm}^{152}_{90}$	1.96	Yb^{172}	1.83
Sm^{154}	2.33	$_{72}\mathrm{Hf}^{176}_{104}$	1.67
$_{64}\mathrm{Gd}^{154}_{90}$	1.83	Hf^{178}	1.72
Gd^{156}	2.10	Hf^{180}	1.75
Gd^{158}	2.14	$_{74}\mathrm{W}^{180}_{106}$	1.65
Gd^{160}	2.08	W^{182}	1.75
$_{66}\mathrm{Dy}^{160}_{94}$	1.93	W^{184}	1.70
Dy^{162}	1.92	W^{186}	1.67
Dy^{164}	1.95	$_{76}\mathrm{Os}^{186}_{110}$	1.56
$_{68}\mathrm{Er}^{164}$	1.85	Os^{188}	1.52
Er^{166}	1.91	Os^{190}	1.42
Er^{168}	1.82	Os^{192}	1.44

$$\begin{aligned} Q_0 &\equiv \int_{\text{body}} \varrho \, \mathrm{d}\tau (3\cos^2\theta - 1) \\ &= \frac{2}{5} Z R_0^2 \left(\gamma^2 - \frac{1}{\gamma}\right). \end{aligned} \tag{13}$$

But according to the present model, the quadrupole moment of the neighbouring odd-mass nucleus constructed by adding one nucleon to a given even-mass nucleus is simply

$$Q = Q_0 e P_\mathrm{C} + \langle e_\mathrm{p} r_\mathrm{p}^2 \rangle P_\mathrm{p}, \tag{14}$$

where Q_0 is given by eq. (13), P_C and P_p are projection factors for the core and particle, respectively, and $\langle e_\mathrm{p} r_\mathrm{p}^2 \rangle$ is the mean-square radial distribution of the charge of the added particle — here taken to be $\approx 3/5 e R_0^2$. The significance and detailed construction of the projection factors have been discussed extensively in II. For the purposes of the present investigation, the relevant details of II may be summarized as follows:

a) The quadrupole moments of nuclei characterized by large deformations are predominantly determined by the shape and motion of the core; i.e.,

$$Q = Q_0 e P_\mathrm{C} \left[1 + \frac{\langle e_\mathrm{p} r_\mathrm{p}^2 \rangle P_\mathrm{p}}{e\, Q_0 P_\mathrm{C}}\right] \approx Q_0 e P_\mathrm{C}. \tag{15}$$

b) The core projection factors depend rather sensitively upon the choice of the representation in which to exhibit nuclear ground states and upon the relative amplitudes of the components selected from that representation. This sensitivity is clearly demonstrated in a comparison of the core projection factors employed herein with those derived from the hydrodynamical model for the strong-coupling situation [4]). In general, the latter are of order twice those of the former for $l+\frac{1}{2}$ nuclei with $I > 3/2$; and of order 2 to 5 times greater for the $l-\frac{1}{2}$ nuclei with $I > 3/2$. The $I = 3/2$ nuclei are characterized by about the same projection factors in both models.

The smaller the projection factor, the greater must be the static distortion to account for a given dynamic distortion; hence the present model leads to the prediction of much larger intrinsic quadrupole moments than does the strong-coupling limit of the hydrodynamical model.

TABLE 4

Calculated quadrupole moments as determined from the shape factor, γ, of even nuclei compared with the observed values of these moments.

Nucleus	Nucleus from which γ is determined	γ	Calculated Q	Observed Q
${}_{67}\mathrm{Ho}^{165}_{98}$	${}_{66}\mathrm{Dy}^{164}_{98}$	1.95	2.2	2
${}_{68}\mathrm{Er}^{167}_{99}$	${}_{68}\mathrm{Er}^{166}_{98}$	1.91	16	$\lvert 10\pm 2 \rvert$
${}_{71}\mathrm{Lu}^{175}_{104}$	${}_{70}\mathrm{Yb}^{174}_{104}$	1.76	3.0	5.9
${}_{73}\mathrm{Ta}^{181}_{108}$	${}_{72}\mathrm{Hf}^{180}_{108}$	1.75	5.8	6.2
${}_{75}\mathrm{Re}^{187}_{112}$	${}_{74}\mathrm{W}^{186}_{112}$	1.67	8.2	2.6
${}_{77}\mathrm{Ir}^{191}_{114}$	${}_{76}\mathrm{Os}^{190}_{114}$	1.42	4.2	1.25
${}_{77}\mathrm{Ir}^{193}_{116}$	${}_{76}\mathrm{Os}^{192}_{116}$	1.44	3.6	1.2

Table 4 lists the pertinent data for and the results of the calculation of quadrupole moments of odd-mass nuclei whose magnetic moments are known (the magnetic moment determines the relative amplitudes of the admixed components of the core-plus-particle states which are presumed to constitute the nuclear ground state) and which have even neighbours which satisfy the above criteria. Since the magnitudes of the measured moments probably cannot be granted more than qualitative significance, it is perhaps noteworthy that the differences between the calculated and measured moments show no apparent pattern.

The case of Er^{167} is especially interesting. Only the absolute values of the magnetic and quadrupole moments have been determined [5]). The spin of this nucleus is 7/2, and the most likely single-particle configuration is that of a single hole in the $f_{7/2}$ subshell. If this assignment is adopted, then, according to the present model, the ground state should consist of an admixture of core states — each component being characterized by an $f_{7/2}$ single particle. It is found that if the magnetic moment is presumed to be positive, the core states to be admixed must correspond to $\lambda = 4$ and 6, respectively; whereas if the magnetic moment is presumed to be negative, the appropriate core states are those with $\lambda = 2$ and 4. The presence of $\lambda = 6$ in a nuclear ground state would be completely exceptional to all previous observations. Conversely, the $\lambda = 2$ and 4 mixture is quite in line with the nature of the ground states of other $f_{7/2}$ nuclei in this region. Consequently we have assumed the negative sign for the magnetic moment. Then since the core shape factor for this nucleus is known from the energy of the first-excited state of Er^{166}, a quadrupole moment for Er^{167} is readily calculated. The value thus obtained, +16, is to be compared with the observations that $|Q| = 10 \pm 2$ [5]) and $|Q| = 10.2 \pm 3$ [6]).

The situation relative to Ho^{165} is somewhat analogous to the above in that here also only the magnitudes of the magnetic and quadrupole moments are known [7]). It is less ambiguous, however, since it is known that the signs of the moments are the same. Presumably in this region of A the quadrupole moment should be positive, thus implying a positive magnetic moment of 3.29. Since the spin is 7/2 and the expected odd-particle configuration $g_{7/2}$, this value for the magnetic moment is quite in line with those for the other nuclei in this region with like configurations. According to I the appropriate core-plus-particle ground-state configuration should consist of an admixture of $g_{7/2}$ and $d_{5/2}$ single-particle states. The entries in the various tables for Ho^{165} have been computed on the basis of the above assumptions.

The energy of the first-excited state of Yb^{174} has not been measured. However, those of Yb^{170} and Yb^{172} are known, and it is almost certain that the corresponding energy for Yb^{174} can be estimated within 5 percent. Since a 5 percent change in E_{2^+} for this nucleus leads to only a 10 percent change in the calculated quadrupole moment, this entry has been listed in table 4.

As has been remarked previously, all nuclei for which the odd particle is presumed to occupy a subshell characterized by an angular momentum differing from the measured nuclear spin have been ignored throughout the present investigation. Since, as discussed in detail in II, Eu^{153} and Yb^{173} are assumed to be members of this class, they have not been considered herein.

Finally it should be noted that the concept of a mass-fraction parameter, employed in the context of the assumption of a uniform distribution of nuclear matter and charge, has significant implications for the interpretation and correlation of different kinds of experimental information obtainable about rotational states. In particular, the interpretation of electrodynamically-induced nuclear transitions between these levels should include a dependence of the transition probability upon the parameter k, which purports to measure the fraction of nuclear matter participating in collective motion, since these probabilities depend upon the flow of charge rather than upon the static distribution of charge. In fact, the matrix element of the transition-inducing interaction should be simply proportional to *k*. The implications of this observation have been investigated in a letter 8), hereafter referred to as III, and the salient results of that investigation as well as their bearing upon the present one are summarized in table 5. The numbers in the column headed $Q_0(E)$ are the intrinsic quadrupole moments to be associated with the indicated cores (protons, neutrons) as calculated from the energies of the first-excited states of the corresponding even nuclei in accordance with eq. (2), employing the shape parameters determined from eq. (3). The quantities $Q_0(\mathrm{R})$ are intrinsic quadrupole moments obtained from measurements of

TABLE 5

Intrinsic quadrupole moments, $Q_0(E)$, $Q_0(\mathrm{R})$, and $Q_0(\mathrm{S})$, as determined from energies of first-exicted states, transition probabilities, and spectroscopic quadrupole moments, respectively. The spectroscopic moments as obtained on the basis of the hydrodynamical model are included for comparison.

Core		Even Nucleus	Odd-mass Nucleus	$Q_0(E)$	$Q_0(\mathrm{R})$	Present Model $Q_0(\mathrm{S})$	Hydrodynamical Model $Q_0(\mathrm{S})$
Protons	Neutrons						
60	90	Nd^{150}		50.4	40		
62	90	Sm^{152}	Eu^{153}	48.2	42		7
62	92	Sm^{154}		72.4	52		
64	90	Gd^{154}		42.7	46		
64	92	Gd^{156}		60.5	55		
64	94	Gd^{158}		63.8	56		
64	96	Gd^{160}		60.2	56		
66	94	Dy^{160}		51.7	41		
66	96	Dy^{162}		51.3	43		
66	98	Dy^{164}	Ho^{165}	54.0	47	51	
68	96	Er^{164}		48.7	43		
68	98	Er^{166}	Er^{167}	53.2		33	≈20
68	100	Er^{168}		47.7			
70	100	Yb^{170}		49.9	40		
70	102	Yb^{172}	Yb^{173}	50.1			11
70	104	Yb^{174}	Lu^{175}			87	14
72	104	Hf^{176}		40.9	39		
72	106	Hf^{178}		44.9	46		
72	108	Hf^{180}	Ta^{181}	47.4	46	50	14
74	106	W^{180}		41.4			
74	108	W^{182}		49.1	49		
74	110	W^{184}	Re^{185}	45.7	51		8
74	112	W^{186}	Re^{187}	43.8	50	14	7
76	110	Os^{186}		36.8	47		
76	112	Os^{188}	Os^{189}	34.2	49		≈10
76	114	Os^{190}	Ir^{191}	27.7		9	
76	116	Os^{192}	Ir^{193}	28.9		10	

cross sections for Coulomb excitation of the same first-excited states or lifetimes for their decay. The actual data, with the few exceptions noted in III, employed in this instance were Q_0's published by Bohr and Mottelson [9]) and modified, in accordance with the above discussion, by division by k. Finally, the Q_0(S)'s of the present model are intrinsic quadrupole moments for the corresponding cores calculated from the measured quadrupole moments of the indicated odd-mass nuclei in accordance with eq. (15); whereas the Q_0(S)'s of the hydrodynamical model are these same moments as predicted by the latter model in the limit of strong coupling [10]).

3. Discussion

It should be pointed out that the $Q_0(E)$'s are quite sensitive to the choice of nuclear radius. No attempt was made to adjust this parameter to achieve a "best" agreement between the $Q_0(E)$'s and the Q_0(R)'s (which do not depend upon this choice), but rather the value employed previously in II was simply retained without question. Furthermore, the determination of the Q_0(S)'s is also independent of R_0. In addition, both Q_0(R) and $Q_0(E)$ are functions (but different functions) of k, whereas Q_0(S) is not at all dependent upon the concept of a matter or charge fraction participating in collective nuclear behavior. But in contrast, the calculation of Q_0(S) is sensitive to the detailed nature of the odd-mass nuclear ground states, and in particular to the single-particle contributions to the character of these states in the context of the present model, as is evidenced by the above-mentioned sensitivity of the core projection factors to the single-particle spin and parity assignments.

Thus, considering the wide disparity in the basic physical parameters upon which these intrinsic quadrupole moments depend, it is felt that the rather good agreement among the Q_0(R)'s and the $Q_0(E)$'s (the Q_0(R)'s are proportional to the square root of the Coulomb excitation cross sections, and the uncertainty of these measurements is of the order of 30 percent [11]), and the suggestive tendency of the model to predict for odd-mass nuclei Q_0(S)'s of the same order as the other Q_0's constitutes a demonstration of at least internal consistency within the model.

It remains only to point out that there is another class of experimental data which has obvious bearing upon the question of the intrinsic quadrupole moments of odd-mass nuclei in the region of rotational spectra; namely, the measurements of the energies of and probabilities of transitions among the rotational states of these nuclei. However, the model, as conceived so far, is not readily applicable to the analysis of these data. Although the present paper deals with the consequences for the model to be derived from consideration of excited states of even nuclei, nevertheless, the simple character of the model makes it unnecessary to invoke questions of nuclear dynamics.

The energy states of the system were simply presumed to be those available to a *free* rigid rotator. Thus the intent to depart as little as possible from kinematics and empiricism was largely adhered to. However, the problem of analysing the data on the excited states of odd-mass nuclei raises in a basic way the whole question of the dynamics of the interaction of the particle with the core; hence any attempt to proceed to this analysis must entail fundamental generalizations from the present standpoint.

It is again a pleasure to acknowledge the assistance of Virginia C. Klema, who checked the calculations given above.

Appendix

Since the calculations presented in I and II were made, some new data have appeared about which it is appropriate to comment. The magnetic moment of Tm^{169} has been measured as -0.20 ± 0.03 12). This is again a case like those of W^{183} and Os^{187}, which were discussed in detail in II, of an $I = \frac{1}{2}$ nucleus whose magnetic moment cannot be correlated by any $K = 0$ configuration. Again one can correlate the moment with an odd value of λ, since μ for $(s_{\frac{1}{2}}, \lambda = 1, K = 1) = -0.64$ and μ for $(d_{3/2}, \lambda = 1, K = 1) = -0.081$. Since μ for $(d_{5/2}, \lambda = 3, K = 1) = -1.0$, one cannot correlate the moment with a $d_{5/2}$ admixture. It is interesting that in the present case of Tm^{169} λ can be a constant of the motion with $\lambda = 1$ for each component of the ground-state wave function; and indeed it seems to be in view of the correlation of the magnetic moment. This is not true in the cases of W^{183} and Os^{187}, where the admixture is $(f_{5/2}, \lambda = 3, K = 1)$ to the $(p_{\frac{1}{2}}, \lambda = 1, K = 1)$.

The quadrupole moments of K^{39} 13) and K^{41} 14) have recently been measured. They are of particular interest since they are members of the $d_{3/2}$ group, which was discussed at length in II. It is found that their quadrupole moments are successfully correlated by the methods given in II. The values of a, γ, α and γ/α for K^{39} and K^{41} are 0.786, 1.133, 0.940, 1.20 and 0.465, 1.222, 0.904, 1.35, respectively.

References

1) R. K. Osborn and E. D. Klema, Phys. Rev. **100** (1955) 822
2) R. K. Osborn and E. D. Klema, Nuclear Physics **2** (1956/57) 454
3) G. M. Temmer and N. P. Heydenburg, Phys. Rev. **99** (1955) 1609
4) Aage Bohr and Ben R. Mottelson, Mat. Fys. Medd. Dan. Vid. Selsk. **27** (1953) no. 16
5) R. J. Elliott and K. W. H. Stevens, Proc. Roy. Soc. A **219** (1953) 387
6) G. S. Bogle, H. J. Duffus and H. E. D. Scovil, Proc. Phys. Soc. A **65** (1952) 760
7) J. M. Baker and B. Bleaney, Proc. Phys. Soc. A **68** (1955) 1090
8) E. D. Klema and R. K. Osborn, Phys. Rev. **103** (1956) 833
9) Aage Bohr and Ben Mottelson, Mat. Fys. Medd. Dan. Vid. Selsk. **30** (1955) no. 1
10) Kai Siegbahn, Beta- and Gamma-Ray Spectroscopy (North-Holland Publishing Co., 1955) p. 489
11) N. P. Heydenburg and G. M. Temmer, Phys. Rev. **100** (1955) 150
12) K. H. Lindenberger and A. Steudel, Naturwiss. **42** (1955) 41
13) G. J. Ritter and G. W. Series, Proc. Phys. Soc. A **68** (1955) 450
14) C. A. Lee, B. P. Fabricand, R. O. Carlson and I. I. Rabi, Phys. Rev. **91** (1953) 1395

Nuclear Physics **3** (1957) 585—591; *North-Holland Publishing Co., Amsterdam*

ZUR THEORIE DER β-WECHSELWIRKUNG

H. KOPPE

Institut für theoretische Physik der Universität Heidelberg

Received 24 February 1957

Abstract: It is shown that non-conservation of parity in β-interaction cannot lead to an electric dipole moment of fermions, if the coupling constants are real; and that a coupling with $(1+i\gamma_5)$ leads to vanishing magnetic and electric moments of the neutrino.

1. Einleitung

Angeregt durch Überlegungen von Lee und Yang 1) haben Gerwin 2) und Wu 3) nach Abweichungen von der Spiegelsymmetrie beim β-Zerfall gesucht, und starke Effekte gefunden, die darauf hindeuten, dass neben der paritäts-erhaltenden die paritätsändernde β-Wechselwirkung in gleicher Stärke vorkommt. Lee und Yang hatten darauf hingewiesen, dass dadurch die Fermionen elektrische Dipolmomente erhalten könnten. Diese müssten jedenfalls sehr klein sein, um unterhalb der experimentellen Ausschliessungsgrenzen zu bleiben. Es stellt sich nun heraus, dass diese Schwierigkeit gar nicht besteht, sondern dass sich zeigen lässt, dass eine Nichterhaltung der Parität bei der β-Wechselwirkung nicht zu einem Dipolmoment führt, wenn die Kopplungskonstanten reell sind. Es wird weiterhin gezeigt, dass der Kopplungsansatz mit $(1+i\gamma_5)$, der durch die Experimente von Gerwin nahegelegt wird, dadurch ausgezeichnet ist, dass in diesem Falle das magnetische Moment und das Dipolmoment des Neutrinos bei beliebigen Kopplungskonstanten verschwindet.

2. Reduktion der Spinoren unter der eigentlichen Lorentzgruppe

Bekanntlich zerfällt die Spinordarstellung der orthochronen Lorentzgruppe unter der reinen Drehgruppe in die beiden Darstellungen $\vartheta_{0,\frac{1}{2}} \dot{+} \vartheta_{\frac{1}{2},0}$ vom Grade 2, d.h. es gibt zweimal zwei Linearkombinationen der Spinorkomponenten, die sich bei Raumdrehungen paarweise untereinander transformieren. Um sie zu finden, geht man davon aus, dass ein Spinor ψ bei einer infinitesimalen Drehung in der μ, ν-Ebene die Transformation †

$$\delta\psi = I_{\mu\nu}\psi = \gamma_\mu\gamma_\nu\psi \tag{1}$$

erleidet. Wie man leicht nachrechnet, bilden die sechs $I_{\mu\nu}$ zusammen mit γ_5 und 1 eine Algebra vom Grade 8. Da sie eine Subalgebra einer 4-reihigen vollständigen Matrixalgebra ist, muß sie in die direkte Summe zweier 2-reihigen vollständigen Matrixalgebren zerfallen. Die Zerfällung wird bewirkt durch die Zerlegung der Einheit im Zentrum $(1, \gamma_5)$, die die folgende Form hat:

---

† Wir setzen $ct = x_0$, $\gamma_\mu\gamma_\nu + \gamma_\nu\gamma_\mu = g_{\mu\nu}$; $\gamma_5 = \gamma_0\gamma_1\gamma_2\gamma_3$.

$$I_{\pm} = \tfrac{1}{2}(1 \pm i\gamma_5), \tag{2}$$

$$I_+ + I_- = 1, \quad I_+ \cdot I_- = 0; \quad I_{\pm}^2 = I_{\pm}. \tag{3}$$

Aus der Definition (2) folgen die für später wichtigen Beziehungen

$$i\gamma_5 I_{\pm} = I_{\pm} \cdot i\gamma_5 = \pm I_{\pm}, \tag{4}$$

$$I_+ \not{a} = \not{a} I_- \qquad (\not{a} \equiv \gamma^\mu a_\mu). \tag{5}$$

Mit Hilfe der I kann man jeden Spinor zerfällen gemäß

$$\psi = I_+\psi + I_-\psi = \psi_r + \psi_l; \qquad I_-\psi_r = I_+\psi_l = 0. \tag{6}$$

Nur beim Neutrino, bei dem I mit der Hamiltonfunktion vertauschbar ist, hat diese Zerfällung einen physikalischen Sinn: Bei den „Rechtsneutrinos" ψ_r liegt der Spin für $E > 0$ in Richtung von $\mathbf{p}$, für $E < 0$ entgegengesetzt dazu; bei den Linksneutrinos ist es gerade umgekehrt. Für die anderen Fermionen gilt das nur im extrem relativistischen Bereich; für nichtrelativistische Energieen enthalten die ψ die beiden Komponenten annähernd im Verhältnis 1 : 1.

Man erhält eine explizite Zerfällung, wenn man von der Standartdarstellung der γ ausgeht, und sie einer Ähnlichkeitstransformation mit dem Operator $Q = (1/\sqrt{2})\ (\gamma_0 + i\gamma_5)$; $Q^{-1} = Q$ unterwirft. Das gibt die Ersetzung

$$\gamma_0 \to i\gamma_5; \qquad i\gamma_5 \to \gamma_0; \qquad \boldsymbol{\gamma} \to -\boldsymbol{\gamma}.$$

In der neuen Darstellung ist γ_5 und damit I_+ diagonal und bei ψ_r resp. ψ_l verschwinden die beiden unteren resp. oberen Komponenten.

3. Die β-Wechselwirkung

Wenn zunächst Spiegelsymmetrie vorausgesetzt wird, dann ist die Wechselwirkung gegeben durch eine Linearkombination der fünf Invarianten:

$$\begin{aligned}
S &= (\overline{\mathrm{P}} \cdot \mathrm{N})(\bar{\mathrm{e}} \cdot \nu)\\
V &= (\overline{\mathrm{P}}\gamma_\mu \mathrm{N})(\bar{\mathrm{e}}\gamma^\mu \nu)\\
T &= -\sum_{\mu<\nu} (\overline{\mathrm{P}}\gamma_\mu\gamma_\nu \mathrm{N})(\bar{\mathrm{e}}\gamma^\mu\gamma^\nu \nu)\\
A &= (\overline{\mathrm{P}}\gamma_\mu \cdot i\gamma_5 \mathrm{N})(\bar{\mathrm{e}}\gamma^\mu \cdot i\gamma_5 \nu)\\
P &= (\overline{\mathrm{P}} \cdot i\gamma_5 \mathrm{N})(\bar{\mathrm{e}} \cdot i\gamma_5 \nu)
\end{aligned}$$

Wenn man die Spiegelsymmetrie aufgibt, und zunächst den durch das Experiment nahegelegten speziellen Ansatz macht, daß überall ν durch $I_+\nu$ zu ersetzen ist, dann ergibt sich zwanglos eine neue Zusammenfassung der Invarianten. Zunächst bemerkt man, daß wegen (4) z.B. die zweiten Faktoren in S und P gleich werden. Es liegt dann nahe, zur Summe resp. Differenz überzugehen, und man hat

$$\tfrac{1}{2}(S+P) = (\overline{\mathrm{P}}I_+\mathrm{N})(\bar{\mathrm{e}}I_+\nu),$$
$$\tfrac{1}{2}(S-P) = (\overline{\mathrm{P}}I_-\mathrm{N})(\bar{\mathrm{e}}I_+\nu).$$

Das gleiche ergibt sich für V and A. Schließlich gibt eine einfache Rechnung die Identität

$$\sum_{\mu<\nu}(\overline{\mathrm{P}}\gamma_\mu\gamma_\nu\mathrm{N})(\bar{\mathrm{e}}\gamma^\mu\gamma^\nu I_+\nu) = \sum_{\mu<\nu}(\overline{\mathrm{P}}\gamma_\mu\gamma_\nu I_+\mathrm{N})(\bar{\mathrm{e}}\gamma^\mu\gamma^\nu I_+\nu).$$

Unter Berücksichtigung van (3) und (4) lassen sich die I noch symmetrischer verteilen, und man kommt schließlich zu der folgenden Zusammenfassung der Invarianten, die (unter der Annahme, dass die Kopplungskonstanten reell sind) gleich in hermitisierter Form geschrieben sind †:

TABELLE 1

I	$\tfrac{1}{2}(S+P) = (\overline{\mathrm{P}}I_+\cdot I_+\mathrm{N})(\bar{\mathrm{e}}I_+\cdot I_+\nu)+(\overline{\mathrm{N}}I_-\cdot I_-\mathrm{P})(\bar{\nu}I_-\cdot I_-\mathrm{e})$
	$T = -\sum_{\mu<\nu}(\overline{\mathrm{P}}I_+\gamma_\mu\gamma_\nu I_+\mathrm{N})(\mathrm{e}I_+\gamma^\mu\gamma^\nu I_+\nu) - \sum_{\mu<\nu}(\overline{\mathrm{N}}I_-\gamma_\mu\gamma_\nu I_-\mathrm{P})(\bar{\nu}I_-\gamma^\mu\gamma^\nu I_-\mathrm{e})$
II	$\tfrac{1}{2}(S-P) = (\overline{\mathrm{P}}I_-\cdot I_-\mathrm{N})(\bar{\mathrm{e}}I_+\cdot I_+\nu)+(\overline{\mathrm{N}}I_+I_+\mathrm{P})(\bar{\nu}I_-\cdot I_-\mathrm{e})$
III	$\tfrac{1}{2}(V+A) = (\overline{\mathrm{P}}I_-\gamma_\mu I_+\mathrm{N})(\mathrm{e}I_-\gamma^\mu I_+\nu)+(\overline{\mathrm{N}}I_-\gamma_\mu I_+\mathrm{P})(\bar{\nu}I_-\gamma^\mu I_+\mathrm{e})$
	$\tfrac{1}{2}(V-A) = (\overline{\mathrm{P}}I_+\gamma_\mu I_-\mathrm{N})(\bar{\mathrm{e}}I_-\gamma^\mu I_+\nu)+(\overline{\mathrm{N}}I_+\gamma_\mu I_-\mathrm{P})(\bar{\nu}I_-\gamma^\mu I_+\mathrm{e})$

Man kann nachträglich die Voraussetzung, daß nur die Rechtsneutrinos an der β-Wechselwirkung teilnehmen, wieder fallen lassen; man muß dann nur noch die Invarianten hinzunehmen, bei denen I_+ and I_- vertauscht sind. Da man dann 10 Invarianten hat, ist das der allgemeinste Fall.

4. Berechnung der S-Matrix

Bei der Zuordnung der Graphen zu den Elementen der S-Matrix treten einige Besonderheiten auf, die zunächst nur kurz diskutiert werden sollen. Da auf Grund der Struktur von $\mathscr{H}_w$ die Leptonenlinien und die Nukleonenlinien durchlaufen, ist es zweckmäßig, die Ecken nach Art der Abb. 1 durch Kreise darzustellen. Die Berechnung der entsprechenden Anteile der S-Matrix geschieht nach dem üblichen Schema, wobei die Eckpunktoperatoren Γ aus der Tabelle 1 zu entnehmen sind. Bei der Wechselwirkung $\tfrac{1}{2}(A+V)$

---

† Es ist $(\bar{\psi}O\chi)^\dagger = (\bar{\chi}O^\dagger\psi)$ wenn man formal setzt $\gamma^\dagger = \gamma$ und folglich $\gamma_s{}^\dagger = \gamma_s$, $(I_+)^\dagger = I_-$. Vgl. Schweber und Bethe, Mesons and Fields, Band 1. S. 20.

kommt z.B. in jede Ecke der Operator $I_-\gamma I_+$, bei $\frac{1}{2}(A-V)$ dagegen in die Nukleonenecken der Operator $I_+\gamma I_-$.

Bei den Wechselwirkungen der Gruppen I und II sind die Verhältnisse komplizierter. Bei $\frac{1}{2}(S+P)$ kommt z.B. an den Ecken, bei denen ein Neutrino und ein Neutron absorbiert wird, in beide Fermionenecken ein I_+, dagegen an den Ecken, an denen neutrale Teilchen emittiert werden, ein I_-. Wir nennen die Ecken der ersten Art die „schwarzen" (schraffierte Kreise), die der zweiten Art die „weißen". Dabei müssen längs jeder Fermionenlinie die schwarzen und die weißen Ecken abwechseln. Ein Selbstenergiegraph eines Elektrons sieht also so aus, wie es in Abb. 2 dargestellt ist, während der entsprechende Graph mit einer nichtüberkreuzten inneren Leptonenlinie nur bei den Wechselwirkungen der Gruppe III möglich ist.

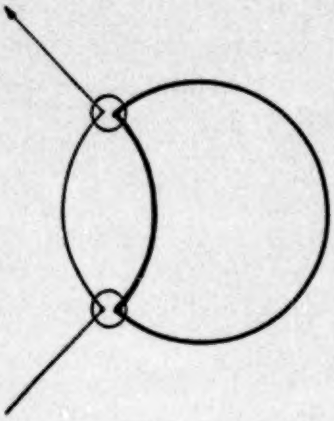

Fig. 1

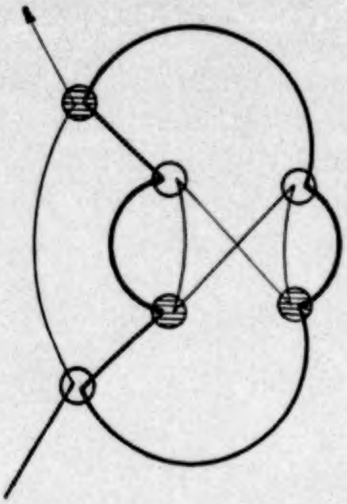

Fig. 2

5. Das elektrische Dipolmoment

Um das durch die Wechselwirkung bedingte magnetische Zusatzmoment (Paulimoment) oder elektrische Dipolmoment eines Fermions zu berechnen, betrachten wir die Graphen mit zwei äußeren Fermionenlinien und einer äußeren Photonenlinie. Jeder solche Graph definiert einen Vertex-Operator $\Lambda(p,\ p',\ e)$, der von den Impulsen des ein- und auslaufenden Fermions und dem Polarisationsvektor e des Photons vom Impuls $k = p'-p$ abhängt. Wir entwickeln in eine Potenzreihe nach k, und greifen die in k linearen Terme heraus:

$$\Lambda(p,p',\ e) = \cdots i\lceil k\lceil e\, M(p^2)+\gamma_5\lceil k\lceil e\, N(p^2)+\cdots \tag{7}$$

Dann ist $M(m^2)$ resp. $N(m^2)$ der Beitrag des Graphen zum magnetischen Zusatzmoment, resp. elektrischen Dipolmoment.

Die folgende Beweisführung beruht auf einigen strukturellen Eigenschaften der Λ, die etwas näher betrachtet werden sollen. Jeder Graph besteht aus einer durchlaufenden Fermionenlinie und geschlossenen Fermionenpolygonen, die miteinander durch β-Wechselwirkung und beliebigen Mengen von inneren Bosonenlinien (Photonen und Mesonen) verbunden sind, und wo irgendwo eine äußere Photonenlinie angreift. Unter Λ verstehen wir den Operator, der zwischen den Ecken steht, an denen die äußeren Linien angreifen. Für den Graphen der Abb. 3a sieht Λ z.B. folgendermaßen aus (wenn wir als β-Wechselwirkung $S+P$ wählen, annehmen, daß das einlaufende Teilchen ein Elektron ist, und alle für das Folgende unwesentlichen numerischen Faktoren weglassen):

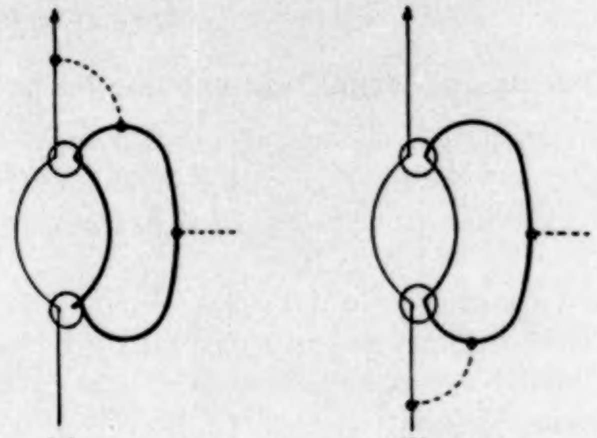

(*a*) (*b*)

Fig. 3

$$\Lambda = \int \left[\gamma^{\mu} \frac{1}{\not{p}_1 - m} I_+ \frac{1}{\not{p}_2 - m} I_-\right] \cdot \mathrm{Spur}\left(I_- \frac{1}{\not{p}_3 - M} \not{e} \frac{1}{\not{p}_4 - M} \gamma_{\mu} \right.$$
$$\left. \times \frac{1}{\not{p}_5 - M} I_+ \frac{1}{\not{p}_6 - M}\right) \cdot \frac{1}{k'^2} \Pi\delta \cdot \mathrm{d}p_1 \cdots \mathrm{d}p_6 \mathrm{d}k'. \tag{8}$$

Dabei ist $\Pi\delta$ das Produkt der δ-Funktionen für die einzelnen Ecken.

Zu jedem Graphen gibt es einen topologisch Inversen (Vgl. Abb. 3). Wenn wir den zugehörigen Vertexoperator mit $\Lambda'(p, p', e)$ bezeichnen, dann gilt (vgl. Anhang 1)

$$\Lambda'(p,\ p',\ e) = \gamma_0 \tilde{\Lambda}(\hat{p}',\ \hat{p},\ \hat{e})\gamma_0. \tag{9}$$

Dabei ist $\hat{p}$ der Vektor, der aus p durch eine räumliche Inversion entsteht, und ~ bedeutet, daß die Reihenfolge der γ's umzukehren ist. Wendet man das wieder auf die in k linearen Terme an, dann geht wegen der Vertauschung von p und p' zunächst in $-k$ über, und wir erhalten

$$\Lambda'(p,\ p',\ e) = \cdots \gamma_0(-i\hat{\not{e}}\hat{\not{k}}M(p^2) - \gamma_5\hat{\not{e}}\hat{\not{k}}N(p^2))\gamma_0 \cdots.$$

Nun antikommutieren $\not{e}$ und $\not{k}$ wegen $e_{\mu}k^{\mu} = 0$. Außerdem ist $\gamma_0\gamma_5\gamma_0 = -\gamma_5$ und

$$\gamma_0 \hat{\not{a}} \gamma_0 = \not{a} \tag{10}$$

sodaß man schließlich erhält:

$$\Lambda'(p_1 p', e) = \cdots i \lceil k \lceil e \, M(p^2) - \gamma_5 \lceil k \lceil e \, N(p^2) \ldots \cdot \qquad (11)$$

Für einen symmetrischen Graphen ist $\Lambda' = \Lambda$, und deshalb nach (7) und (11) $N(p^2) = 0$; er liefert also keinen Betrag zum Dipolmoment. Für unsymmetrische Graphen liefern die beiden zueinander inversen gerade entgegengesetzte Beiträge, die sich bei der Summation über alle Graphen wegheben. Es kann also kein elektrisches Dipolmoment auftreten.

6. Das magnetische Moment des Neutrinos

Es soll jetzt gezeigt werden, dass eine Beschränkung der Wechselwirkung auf Rechtsneutrinos unabhängig von sonstigen Annahmen zum Verschwinden des magnetischen und elektrischen Momentes des Neutrinos führt.

Wir beschränken uns zunächst auf die β-Wechselwirkung und die elektromagnetische Wechselwirkung. Dann zeigen die Vertex-Graphen für ein Neutrino die Besonderheit, dass die erste und letzte Wechselwirkung auf der durchlaufenden Fermionenlinie eine β-Wechselwirkung sein muss. Folglich fängt der Faktor in Λ, der von der durchlaufenden Fermionenlinie herrührt, mit einem I_- an (Erzeugung des auslaufenden Neutrinos) und hört mit einem I_+ auf (Vernichtung des einlaufenden Neutrinos). Wegen (3) gilt also

$$\Lambda = I_- \Lambda I_+$$

und speziell für die in k linearen Glieder

$$i \lceil k \lceil e \, M + \gamma_5 \lceil k \lceil e \, N = I_-(i \lceil k \lceil e \, M + \gamma_5 \lceil k \lceil e \, N) I_+ = (i \lceil k \lceil e \, M + \gamma_5 \lceil k \lceil e \, N) I_- I_+ = 0,$$

d.h. das Paulimoment und das elektrische Dipolmoment verschwinden. Diese Schlussweise gilt nicht mehr, wenn man Rechts- und Linksneutrinos mischt, weil dann z.B. auch am Anfang der durchlaufenden Linie ein I_+ stehen kann.

Dagegen verschwindet das magnetische Moment des Neutrinos auch unter Berücksichtigung beliebiger anderer Wechselwirkungen, vorausgesetzt, dass man diese so abändert, dass nur Rechtsmesonen entstehen können. Dann muss der Feldoperator des Neutrinofeldes in allen Wechselwirkungen in der Kombination $I_+ \nu$ oder $\bar{\nu} I_-$ stehen, und der der durchlaufenden Linie entsprechende Faktor enthält unter allen Umständen vorn ein I_- und am Schluss ein I_+.

Anhang

BEZIEHUNG ZWISCHEN INVERSEN GRAPHEN

Man erhält den Ausdruck für Λ', wenn man in dem Integral für Λ 1.) p und p' vertauscht, 2.) die Reihenfolge aller γ umkehrt, und 3.) I_+ und I_- vertauscht (oder allgemeiner γ_5 durch $-\gamma_5$ ersetzt).

Da Spuren gegen eine Umkehrung der Reihenfolge der γ invariant sind, braucht man die Reihenfolge nur in dem Faktor umzukehren, der der durchlaufenden Linie entspricht. Da ein Operator C, $C^2 = 1$, $C\tilde{\gamma}C = \gamma$ existiert, wird die zweite Bedingung erfüllt, wenn man Λ durch $C\tilde{\Lambda}C$ ersetzt. Praktisch bedeutet das, dass es gleichgültig ist, auf welcher Stufe der Rechnung man die Umkehrung der Reihenfolge vornimmt, und man kann an Stelle von $C\tilde{\Lambda}C$ einfach $\tilde{\Lambda}$ schreiben, wenn man unter der Wirkung von $\tilde{}$ die Umkehrung der Reihenfolge aller γ versteht. Jetzt bilden wir $\gamma_0\tilde{\Lambda}\gamma_0$. Die γ_0 wirken zunächst nur auf die γ, die ausserhalb der Spuren stehen, und verwandeln hier γ_5 in $-\gamma_5$, $\lceil a$ in $\widehat{\lceil a}$ (wobei $\hat{}$ die Rauminversion bedeutet), und die γ^μ die in irgendwelchen Eckenoperatoren stehen, in γ_μ. Wir unterwerfen jetzt alle Vektoren einer räumlichen Inversion, und ersetzen die $\widehat{\lceil a}$, die jetzt in den Spuren auftreten, gemäss (10) durch $\gamma_0\lceil a\gamma_0$ und die γ_μ durch $\gamma_0\gamma^\mu\gamma_0$. Multipliziert man jetzt die γ_0 in den Spuren weg, dann stehen wieder die $\lceil a$ da, die Indizes an den freien γ sind heraufgeschoben worden, und alle γ_5 durch $-\gamma_5$ ersetzt, so dass schliesslich die gewünschte Umordnung von Λ in $\Lambda' = \gamma_0\Lambda\gamma_0$ erreicht ist.

Literatur

1) T. D. Lee und C. N. Yang, Phys. Rev. **104** (1956) 254
2) R. Garwin, L. Ledermann und M. Weinrich, Phys. Rev. **105** (1957) 1415
3) C. S. Wu, E. Ambler, R. W. Haywood, D. D. Hoppes and P. R. Hudson, Phys. Rev. **105** (1957) 1413

Nuclear Physics **3** (1957) 592—597; *North-Holland Publishing Co., Amsterdam*

INVARIANCE PROPERTIES AND IDENTITIES BETWEEN RENORMALIZATION CONSTANTS

A. PETERMANN

CERN *Theoretical Study Division at the Institute for Theoretical Physics, University of Copenhagen*

Received 7 February 1957

Abstract: The invariance of a given mixture of meson fields under the Stueckelberg transformation — of which the Foldy transformation is a special case — is first briefly recalled. Then, if one requires, for this mixture, the invariance under the charge renormalization group, identities between the renormalization constants are found which are the counterparts, in meson theory, of the well-known Ward identity in quantum electrodynamics.

1. Introduction

The general transformation given by Stueckelberg and the author [1]) contains the Foldy transformation [2]) as a very special case; it reflects an invariant property of the Lagrangian of a fermion field in interaction with a mixture of scalar, pseudoscalar, and pseudovector fields. In the second section of the present paper the Stueckelberg transformation will be recalled together with the transformation properties which the various fields must have to make the Lagrangian invariant. In the third section the resulting quantized theory is examined, and it is required to be invariant under the charge renormalization group [3]). Whereas the choice of the various normalization constants Z_i is a priori entirely free, the Stueckelberg transformation restricts this choice, and the constants are thus bound to satisfy identities of the same type as the Ward identity of quantum electrodynamics. An example in perturbation theory is finally given.

2. The Stueckelberg Transformation

As a starting point one considers the Lagrangian $L(u^\dagger, u, A_\alpha, \phi_5, \phi_{\alpha 5}, \phi_0)$, functional of the classical fields $A_\alpha, \phi_5, \phi_{\alpha 5}, \phi_0, u^\dagger, u$, and splits it in the following way:

$$L(u^\dagger, u, A_\alpha \ldots) = L^{(u)} + L^{(\text{free})}, \tag{2.1}$$

with the definition

$$\begin{aligned} L^{(u)} &= \int \frac{1}{2i} [(u^\dagger \partial_\alpha)\gamma^\alpha u - u^\dagger \gamma^\alpha (\partial_\alpha u)] + h \int u^\dagger u \phi_0 \\ &\quad + e \int u^\dagger \gamma^\alpha u A_\alpha + f \int u^\dagger \gamma_5 \gamma^\alpha \phi_\alpha{}^5 + g \int u^\dagger \gamma_5 u \phi^5 \\ &= L^{(u0)} + L^{(\text{int})}; \end{aligned} \tag{2.2}$$

$L^{(\text{free})}$ being the Lagrangian for the free electromagnetic and meson fields, and $L^{(u0)}$ the Langrangian for the free Fermi field. The $L^{(u)}$ part of (2.1) obviously represents the part of the Lagrangian bilinear in $u^\dagger$, u. In (2.2) the following notations have been used: h, e, f and g are coupling constants; ϕ_0, ϕ_5, and $\phi_{\alpha 5}$ are scalar, pseudoscalar, and pseudovector fields, respectively, A_α the electromagnetic potentials; $\phi_5 = \|g^{ik}\|\,\phi^5$.

Stueckelberg studied the group of transformations which leaves invariant the bilinear part $L^{(u)}$ of the Lagrangian L. This group is generated by the three infinitesimal parameters $\delta\tau_0$, $\delta\lambda_0$, $\delta\lambda_5$ defined, with full spinor indices, by

$$\begin{gathered} \delta u^A = \delta\Gamma^A_B u^B; \qquad \delta u^\dagger_A = -u^\dagger_B \delta\Gamma^{\dagger B}_A; \\ \delta\Gamma = \frac{3i}{4}\gamma_0\delta\tau_0 + e\gamma_0\delta\lambda_0 + if\gamma^5\delta\lambda_5; \qquad \gamma^A_{0B} = -i\delta^A_B. \end{gathered} \tag{2.3}$$

The conclusion concerning the $\delta\tau_0$ transformation is that it means only a change in the normalization of the metrics, and is thus irrelevant for our purpose here.

For $\delta\lambda_0$ one finds that it represents a change in the ordinary electromagnetic gauge.

The $\delta\lambda_5$ part is discussed as follows: If the transformation (2.3) is performed, keeping $\delta\tau_0 = 0$ and $\delta\lambda_0 = 0$, the variation of the Lagrangian $L^{(u)}$ is

$$\begin{aligned} \delta L^{(u)} = {} & \frac{1}{2i}\{(u^\dagger if\gamma^5\delta\lambda_5\gamma\partial)u + (u^\dagger\gamma\partial)if\gamma^5\delta\lambda_5 u \\ & \qquad - u^\dagger if\gamma^5\delta\lambda_5(\gamma\partial u) - u^\dagger(\gamma\partial if\gamma^5\delta\lambda_5 u)\} \\ & - hiu^\dagger if\gamma^5\delta\lambda_5 u\phi_0 - iu^\dagger if\gamma^5\delta\lambda_5 uh\phi_0 \\ & - iu^\dagger uh\delta\phi_0 + 2gu^\dagger if\delta\lambda_5 u\phi^5 \\ & + gu^\dagger\gamma^5 u\delta\phi_5 + fu^\dagger\gamma_\alpha\gamma^5 u\delta\phi_5{}^\alpha. \end{aligned} \tag{2.4}$$

It is zero if the following conditions are fulfilled:

$$\delta\phi_5{}^\alpha = \partial^\alpha\delta\lambda_5, \tag{2.5a}$$

$$\delta g\phi_5 = -2fh\phi_0\delta\lambda_5, \tag{2.5b}$$

$$\delta h\phi_0 = +2fg\phi^5\delta\lambda_5. \tag{2.5c}$$

These three equations express the infinitesimal Stueckelberg transformations for the potentials. The integrated form leads, for the potentials, to the following dependence on the gauge λ_5:

$$\begin{aligned} h\phi_0 &= a_0\cos(2f\lambda_5) + b_5\sin(2f\lambda_5), \\ g\phi_5 &= -a_0\sin(2f\lambda_5) + b_5\cos(2f\lambda_5), \\ \phi_{\alpha 5} &= \varphi_{\alpha 5} + \partial_\alpha\lambda_5, \end{aligned} \tag{2.6}$$

a_0, b_5, and $\varphi_{\alpha 5}$ being arbitrary functions independent of λ_5. Thus, the Lagrangians generated by the scalar, pseudoscalar, and pseudovector potentials related by (2.6) are equivalent. The restricted Foldy transformation is that leading from the gauge $\lambda_5 = 0$ (pure ps coupling) to that where $\lambda_5 = -g(2mf)^{-1}\varphi_5$ (pv coupling + non-linear terms in the field φ_5); the arbitrary functions are chosen to satisfy $a_0 = -m$; $b_5 = g\varphi_5$; $\varphi_{\alpha 5} = 0$.

3. Identities for the Renormalization Constants

The charge renormalization group, in the form discussed by Bogoljubov and Sirkov, shows the physical equivalence oi two different sets of fields and coupling constants:

$$u^{\dagger(1)},\ u^{(1)},\ \phi_0{}^{(1)},\ \phi_5{}^{(1)},\ \phi_{\alpha 5}^{(1)}\cdot\ f^{(1)},\ g^{(1)},\ h^{(1)}; \tag{3.1}$$

$$\begin{gathered}
u^{\dagger(2)} = Z_2^{\frac{1}{2}} u^{\dagger(1)}; \quad u^{(2)} = Z_2^{\frac{1}{2}} u^{(1)}; \quad \phi_0{}^{(2)} = Z_s^{\frac{1}{2}} \phi_0{}^{(1)}; \\
\phi_5{}^{(2)} = Z_{\mathrm{ps}}^{\frac{1}{2}}\, \phi_5{}^{(1)}; \quad \phi_{\alpha 5}^{(2)} = Z_{\mathrm{pv}}^{\frac{1}{2}} \phi_{\alpha 5}^{(1)}; \quad f^{(2)} = Z_2{}^{-1} Z_{\mathrm{pv}}^{-\frac{1}{2}} Z_f f^{(1)}; \\
g^{(2)} = Z_2{}^{-1} Z_{\mathrm{ps}}^{-\frac{1}{2}} Z_g g^{(1)}; \quad h^{(2)} = Z^{-1} Z_s^{-\frac{1}{2}} Z_h h^{(1)};
\end{gathered} \tag{3.2}$$

where the Z_i's are arbitrary numbers.

Both sets (3.1) and (3.2) describe the same physical particles with the same interaction effects between them, and no restrictions exist a priori concerning the choice of the different normalization constants Z_i, which can be chosen quite independently of each other.

But, if one requires for this system of fields the invariance under the Stuckelberg transformation, one has to examine the compatibility of the joint transformations (2.3) [with $\delta\tau_0 = \delta\lambda_0 = 0$] and (2.5a—c) with (3.1) and (3.2). More precisely the character of transformation of the different fields under the Stueckelberg transformation is postulated to hold in both ways of description (3.1) and (3.2).

If one writes (2.3) [with $\delta\tau_0 = \delta\lambda_0 = 0$] and (2.5a—c) in the system 2 of (3.2), one has

$$\delta u^{(2)} = if^{(2)} \gamma^5 u^{(2)} \delta\lambda_5{}^{(2)}; \quad \delta u^{\dagger(2)} = if^{(2)} u^{\dagger(2)} \gamma^5 \delta\lambda_5{}^{(2)}, \tag{3.3a}$$

$$\delta h_0{}^{(2)} \phi_0{}^{(2)} = +2f^{(2)} g^{(2)} \phi^{5(2)} \delta\lambda_5{}^{(2)}, \tag{3.3b}$$

$$\delta g^{(2)} \phi_5{}^{(2)} = -2f^{(2)} h^{(2)} \phi_0{}^{(2)} \delta\lambda_5{}^{(2)}, \tag{3.3c}$$

$$\delta\phi_{\alpha 5}^{(2)} = \partial_\alpha \delta\lambda_5{}^{(2)}. \tag{3.3d}$$

Using (3.2) to convert (3.3a—d) into the system 1, one gets the transformation law for the gauge λ_5 as well as certain relations between the Z_i's.

It is worth emphasizing at this point that the Z_i's are supposed to be numbers independent of the gauge λ_5, and that one may write, for instance, $\delta(Z_{\mathrm{pv}}^{\frac{1}{2}} \phi_{\alpha 5}) = Z_{\mathrm{pv}}^{\frac{1}{2}} \delta\phi_{\alpha 5}$. The case where the Z_i's are functionals of λ_5 offers a quite different degree of complexity and will not be discussed here.

This statement being made, one starts with (3.3d) which yields

$$Z_{\mathrm{pv}}^{\frac{1}{2}}\,\delta\phi_{\alpha 5}^{(1)} = \partial_\alpha \delta\lambda_5^{(2)}.$$

But in the system 1 one is allowed to write

$$\delta\phi_{\alpha 5}^{(1)} = \partial_\alpha \delta\lambda_5^{(1)}.$$

Thus,

$$\delta\lambda_5^{(2)} = Z_{\mathrm{pv}}^{\frac{1}{2}}\,\delta\lambda_5^{(1)}. \tag{3.4}$$

which is the law of transformation of the so-called mesic gauge λ_5. Furthermore, (3.3a) is written, according to (3.2), as

$$Z_2^{\frac{1}{2}}\,\delta u^{(1)} = iZ_2^{-1}\,Z_{\mathrm{pv}}^{-\frac{1}{2}}\,Z_f f^{(1)}\gamma^5 Z_{\mathrm{pv}}^{\frac{1}{2}}\,\delta\lambda_5^{(1)}\,Z_2^{\frac{1}{2}}\,u^{(1)}$$

or

$$\delta u^{(1)} = iZ_2^{-1}\,Z_f f^{(1)}\gamma^5 u^{(1)}\,\delta\lambda_5^{(1)}; \tag{3.5}$$

(3.4) has been used. As (3.3a) yields, in the system 1,

$$\delta u^{(1)} = if^{(1)}\gamma^5 u^{(1)}\,\delta\lambda_5^{(1)},$$

the comparison with (3.5) shows that

$$Z_2^{-1}Z_f = 1. \tag{3.6}$$

From (3.3b) and again (3.2),

$$\begin{aligned} Z_s^{\frac{1}{2}}\,\delta\phi_0^{(1)} = {} & +2Z_2^{-1}\,Z_{\mathrm{pv}}^{-\frac{1}{2}}\,Z_f f^{(1)}\,Z_2^{-1}\,Z_{\mathrm{ps}}^{-\frac{1}{2}}\,Z_g g^{(1)} \\ & \times (Z_2^{-1}\,Z_s^{-\frac{1}{2}}\,Z_h h^{(1)})^{-1}\,Z_{\mathrm{ps}}^{\frac{1}{2}}\,\phi_5^{(1)}\,Z_{\mathrm{pv}}^{\frac{1}{2}}\,\delta\lambda_5^{(1)}, \end{aligned}$$

or

$$\delta\phi_0^{(1)} = +2Z_g\,Z_h^{-1}\,g^{(1)}\,f^{(1)}\,h^{(1)-1}\,\phi_5^{(1)}\,\delta\lambda_5^{(1)},$$

(3.6) being used. This can be compared with the equivalent transformation in the system 1

$$\delta\phi_0^{(1)} = +2g^{(1)}\,f^{(1)}\,h^{(1)-1}\,\phi_5^{(1)}\,\delta\lambda_5^{(1)}.$$

This imposes the further condition

$$Z_g = Z_h. \tag{3.7}$$

With the aid of (3.4), (3.6) and (3.7), it is seen that (3.3c) is true in the system 2 as well as in the system 1, thus giving no more restriction for the constants Z_i.

Now, summarizing the restrictions that the invariance under the Stueckelberg transformation imposes to the a priori arbitrary constants of the renormalization group, one can say that

$$Z_2 = Z_f \text{ and } Z_g = Z_h$$

are two Ward-like identities to be satisfied in any system of fields which must be invariant under the transformation (2.3), (2.5a—c).

Moreover, the transformation law of the gauge λ_5 ought to be similar to that of the pseudovector field.

As a practical example one can investigate the S-matrix generated by the interaction Lagrangian (2.2). Performing the Stueckelberg transformation, the radiative corrections due to the electromagnetic field A_α remain independent of the gauge λ_5. Thus the numbers Z_i due to the electromagnetic corrections have a clear meaning. For instance, Z_f is the renormalization constant arising from the electromagnetic corrections to the interaction of the Fermi field described by $L^{(u0)}$ of (2.2) with a pseudovector field. Then it is interesting to check, to the first order of a perturbation expansion in the fine structure constant at least, that the imperative conditions (3.6) and (3.7) are fulfilled.

To this end one has first to consider the trace of the first order electromagnetic correction to the scattering of the Fermion by a pv field, which will lead to Z_f:

$$f\alpha\gamma_\alpha S_F \gamma_\mu \gamma_5 S_F \gamma_\alpha . \tag{3.8}$$

Here S_F is the fermion Green function derived from $L^{(u0)}$. It is essential that the mass be put in the interaction Lagrangian; for otherwise the assumption made concerning the invariance of the Z_i's under the λ_5 transformation is no longer justified: these new Z_i's would be gauge-variant and satisfy different relations.

Now, in (3.8) the matrix γ_5 can be put to the right without any change of sign, taking into account the anticommutation properties of S_F. The expression on the left of γ_5 is

$$f\alpha\gamma_\alpha S_F \gamma_\mu S_F \gamma_\alpha .$$

Thus the part of the matrix element (3.8), relevant to our purpose, reduces to $fZ_1\gamma_\mu\gamma_5$, where the renormalization constant Z_1 is, at this order, that of quantum electrodynamics. The wave function renormalization, Z_2, is also obviously that of quantum electrodynamics. The Ward identity for Z_1 and Z_2 then completes the proof of the identity (3.6) to the first order in α.

To check (3.7) to this order, one has to write the traces of the matrix elements proportional to α for the scattering of the Fermion by a scalar and a pseudoscalar field.

They yield respectively

$$h\alpha\gamma_\alpha S_F 1 S_F \gamma_\alpha , \tag{3.9}$$

$$g\alpha\gamma_\alpha S_F \gamma_5 S_F \gamma_\alpha . \tag{3.10}$$

Z_h is the constant coefficient of h in (3.9), whereas Z_g will be the constant coefficient of $g\gamma_5$ in (3.10). It is immediate, owing to the anticommutation property of γ_5 with both S_F and γ_α, that $Z_h = Z_g$ to this order.

For the higher orders the identities (3.6) and (3.7) can be shown to hold generally, thus confirming that these relations, here derived independently from the perturbation method, are satisfied in the power series in α.

The author is grateful for Dr. Källén's criticisms of the manuscript and for many discussions during the development of this work.

References

1) E. C. G. Stueckelberg and A. Petermann, Helv. Phys. Acta **26** (1953) 499
2) L. L. Foldy, Phys. Rev. **84** (1951) 168
F. J. Dyson, Phys. Rev. **73** (1948) 929
3) E. C. G. Stueckelberg and A. Petermann, Helv. Phys. Acta **24** (1951) 317. Cf. also N. N. Bogoljubov and D. V. Sirkov, Nuovo Cimento **10** (1956) 845

Nuclear Physics **3** (1957) 598—605; *North-Holland Publishing Co., Amsterdam*

TWO-COMPONENT THEORY OF THE NEUTRINO AND K-MESON DECAYS COMPRISING TWO NEUTRINOS

S. ONEDA

Theoretical Physics Department, University of Manchester †

Received 20 March 1957

Abstract: The K-meson decays comprising two neutrinos are investigated by using a two-component theory of the neutrino. The results are closely connected with the question whether the conservation of fermion numbers is valid or not. They will also give some information on the character of the primary weak interactions.

1. Introduction

Recently Yang and Lee [1]) have suggested that the law of conservation of parity may be violated for the weak interactions. Some interesting experiments proposed by these authors have already shown that parity is not conserved in weak interactions — at least in the neutrino processes. In the first place, Wu *et al.* [2]) have confirmed the existence of parity non-conserving terms in the β-decay of oriented Co^{60} nuclei. Moreover, Ledermann *et al.* [3]) have found a correlation between the direction of the μ-meson and the electron involved in the $\pi \rightarrow \mu \rightarrow e$ decay, which necessarily implies that these decay interactions are not invariant under inversion. In this connection, Landau [4]), Salam [5]) and Yang and Lee [6]) have independently proposed a theory which tries to relate the violation of parity-conservation to the vanishing mass of the neutrino. The Dirac equation for the zero-mass particle splits into two independent pairs of equations. So long as we uphold the conservation of parity, we cannot confine ourselves to a single pair of equations, since both pairs transform into each other as a result of space inversion. If, however, as stressed by Landau [4]), we restrict our attention to combined inversions — simultaneous inversion under parity and particle-antiparticle conjugation —, we arrive at the new possibility of describing a neutrino by a single pair of equations. In this theory the neutrino is always polarised in the direction of its motion. The polarisation of the anti-neutrino is correspondingly reversed. Thus, the neutrino cannot be a truly neutral particle. The purpose of this paper is to point out that this two component theory of the neutrino also gives interesting results for the K-meson decays comprising two neutrinos. We know already that various decay modes occur for the K-meson. In addition to the decay modes into pions, $K \rightarrow 2\pi$ and

---

† On leave of absence from the Institute of Theoretical Physics, University of Kanazawa, Japan.

$K \to 3\pi$, we have also lepton modes $K \to \mu+\nu$, $\mu+\nu+\pi$ and $e+\nu+\pi$. Most probably, all weak interactions which comprise leptons would be neutrino processes. The hypothesis that the neutrino is the source of all weak lepton interactions seems the best to explain the non-occurrence of many processes, not observed experimentally so far, and which otherwise could easily take place. However, even from this restricted stand-point, the following two neutrino processes would occur:

(I) $K^0 \to 2\nu$

(II) $K^+ \to \pi^+ + 2\nu$
$K^0 \to \pi^0 + 2\nu$.

Experimentally it does not seem to have been settled whether these reactions do take place or not. The two-component theory of the neutrino gives several interesting predictions on these processes. The results depend closely on whether the attractive postulate of the conservation of fermion numbers (lepton numbers as well as baryon numbers) does hold or not. Thus, a careful experimental analysis of these processes would be enlightening.

2. K-Meson Decays Comprising two Neutrinos

We use for the two-component neutrino the conventional four-component formalism given by Yang and Lee [6]). $\psi(\nu)$ and $\psi^c(\bar{\nu})$ denote the neutrino and its anti-particle field, respectively. The two-component conditions are

$$\gamma_5 \psi = -\psi, \ \gamma_5 \psi^c = \psi^c.$$

This theory allows us to construct only the following covariant expressions from the $\psi(\nu)$ and $\psi^c(\bar{\nu})$ (we write $\bar{\psi} \equiv \psi^* \gamma_4$):

Four vector with respect to rotation

$$\bar{\psi}\gamma_\mu \psi = \tfrac{1}{2}\bar{\psi}\gamma_\mu (1-\gamma_5)\psi, \tag{1}$$

Scalar with respect to rotation

$$\bar{\psi}\psi^c = \tfrac{1}{2}\bar{\psi}(1+\gamma_5)\psi^c. \tag{1'}$$

Thus the forms of interaction for two-neutrino processes reduce to very simple ones. We discuss here in detail only the case that the K-meson has spin zero, because this choice seems to be most favoured by the present experiments. The extension to the spin-one K-meson can be done easily.

2.1. $K^0 \to 2\nu$ DECAY

(A) $K^0 \to \nu + \bar{\nu}$.

This decay is absolutely forbidden in the two-component theory of the neutrino, if the K-meson has spin zero. In the rest system of the K^0-meson, the ν and $\bar{\nu}$ are emitted in opposite directions, while their spins are both parallel to the momentum of the ν. This is impossible for the spin-zero K-meson. Thus $\pi^0 \rightarrow \nu+\bar{\nu}$ is also absolutely forbidden in this theory.

Another way of looking at the above result is as follows. Taking into account (1), the general form of the interaction
$K^0(p) \rightarrow \nu(q_1)+\bar{\nu}(q_2)$ would be

$$\varphi_K(p)(gq_{1\alpha}+fq_{2\alpha})\bar{\psi}(q_1)\gamma_\alpha\psi(q_2)+\text{c.c.}. \tag{2}$$

Here p, q_1 and q_2 are the energy-momentum four vectors of the K-meson and the ν and $\bar{\nu}$. (Of course, $p = q_1+q_2$). g and f are scalars which are dependent on the mechanism by which the interaction (A) occurs. Using the equation of motion of the neutrino with zero mass, the expression (2) vanishes. It should be noted that this selection rule arises only for an initial boson of spin zero. For bosons of higher spin the decay (A) would occur unless some other selection rule operates.

(B) $K^0 \rightarrow \nu+\nu$ or $\bar{\nu}+\bar{\nu}$.

From (1′) the general form of interaction for this process is given by

$$g\varphi_K(p)\bar{\psi}(q_1)\psi^c(q_2)+\text{c.c.} \tag{3}$$

g in (3) is the quantity similar to g and f in (2). Thus the two neutrino or anti-neutrino emissions is possible for any value of the spin of the initial meson unless we introduce a new selection rule. The life-time of this decay may be shorter than that of the corresponding decays of the K-meson such as $K \rightarrow \mu+\nu$ and $K \rightarrow \mu(e)+\nu+\pi$ because the available phase space volume is more favourable.

2.2. $K^+ \rightarrow \pi^+ + 2\nu$ DECAY

(C) $K^+(p) \rightarrow \pi^+(q)+\nu(q_1)+\bar{\nu}(q_2)$
$K^0 \rightarrow \pi^0+\nu+\bar{\nu}$.

We construct the most general form of this interaction, choosing p, q_1 and q_2 as independent four-vectors.

$$\varphi_K(p)\varphi_\pi^*(q)\{gp_\alpha+f\varepsilon_{\alpha\beta\lambda\sigma}p_\beta q_{1\lambda}q_{2\sigma}\}\times\bar{\psi}(q_1)\gamma_\alpha\psi(q_2)+\text{c.c.}. \tag{4}$$

$\varepsilon_{\alpha\beta\lambda\sigma}$ is 1 if α, β, λ, σ is an even permutation of 1, 2, 3, 4; it is -1 if it is odd, and zero if two subscripts are equal. If the interaction (C) is a primary interaction, the term containing $\varepsilon_{\alpha\beta\lambda\sigma}$ in (4) corresponds to a primary interaction which contains derivates of the fermion wave functions. This would be an unpleasant feature for a primary interaction. So we may discard this term if (4) is a primary interaction. On the other hand, as will be discussed in section 3, if this decay occurs through the intermediary of simpler primary interactions (such as usual weak Fermi interactions or Yukawa type weak interactions) the number of the independent four vectors decreases to two, say p and $q = p-(q_1+q_2)$ because $\nu(q_1)$ and $\nu(q_2)$ are emitted from the same vertex (see figs. 1 and 2). In this case the $\varepsilon_{\alpha\beta\lambda\sigma}$

term in (4) does not appear. So, after all, we put $f = 0$ in (4). g is a scalar which is, in general, a function of $p^2 = M_K^2$, $q^2 = m_\pi^2$, $(p_\alpha q_\alpha)$, and the masses of particles which occur in any intermediate stage of our process (C).

The energy spectrum of the π^+-meson in the rest system of the K$^+$-meson is given, except for irrelevant factors, by

$$W(E)\mathrm{d}E \propto g^2 E(E+2m_\pi)\sqrt{E(E+2m_\pi)}\mathrm{d}E, \tag{5}$$

where E is the kinetic energy of the secondary π^+-meson, whose maximum value, E_{max}, is about 127 MeV. The energy distribution in this case is an increasing function of E and has its maximum value at $E = E_{\mathrm{max}}$. Note that this is near to the kinetic energy of the π^+-meson in the $K^+ \to \pi^+ + \pi^0$ decay.

(D) $K^+(p) \to \pi^+(q) + \nu(q_1) + \nu(q_2)$ (or $\pi^+ + \bar{\nu} + \bar{\nu}$)
$K^0 \to \pi^0 + \nu + \nu$ (or $\pi^0 + \bar{\nu} + \bar{\nu}$).

By following the same arguments as for (C), we get the following general form of interaction:

$$g' \varphi_K(p) \varphi_\pi^*(q) \bar{\psi}(q_1) \psi^c(q_2) + \text{c.c.} \tag{6}$$

where g' is the effective coupling constant similar to g in (5). In contrast to the case (C), we need not restrict the number of independent four vectors in getting the form (6). The energy spectrum of the π^+-meson is

$$W(E)\mathrm{d}E \propto g'^2 \sqrt{E(E+2m_\pi)}(E_{\mathrm{max}}-E)\mathrm{d}E \tag{7}$$

which reaches a maximum value near $E \approx 46$ MeV and which vanishes at both $E = 0$ and $E = E_{\mathrm{max}}$. The latter fact can be simply explained since at $E = E_{\mathrm{max}}$ both neutrinos are emitted in the opposite direction to the π^+-meson and such a state is not available for either $\nu + \nu$ or $\bar{\nu} + \bar{\nu}$ emission. On the other hand, as is indicated by eq. (5), such a state is favoured for $\nu + \bar{\nu}$ emission. The spectra (5) and (7) are thus seen to have quite different shapes.

2.3. THEORETICAL IMPLICATIONS

The detection of the existence of $K^0 \to 2\nu$ would not be so easy. There are, however, several helpful circumstances:

(i) The production of K^0-mesons can only occur in association with some other strange particle (say, a hyperon). This is very helpful in determining the K^0-production.

(ii) There may exist other neutral modes including only neutral pions, $K^0 \to \pi^0 + \pi^0$ and $K^0 \to \pi^0 + \pi^0 + \pi^0$. The branching ratios of these decays in comparison with the observable mode $K^0 \to \pi^+ + \pi^-$ would be decided by the transformation properties of these weak interactions in isobaric spin space. The tentative one which makes $K^+ \to \pi^+ + \pi^0$ first forbidden is $\Delta I = \pm\frac{1}{2}$.

(iii) If the $K^0 \to 2\nu$ process occurs, its transition probability would be fairly larger than that of the following processes: $K^0 \to \pi^0 + 2\nu$, $K^0 \to e^{\pm}(\mu^{\pm}) + \nu + \pi^{\mp}$, $K^0 \to 3\pi^0$ and $K^0 \to \pi^0 + \pi^0 + \gamma$ etc.

This argument of phase space volume seems also to be supported by the experimental fact that the abundance of the $K^+ \to \mu^+ + \nu$ mode is larger than that of $K^+ \to \mu^+(e^+) + \nu + \pi^0$ and $K^+ \to \pi^+ + \pi^+ + \pi^-$. So $K^0 \to 2\nu$ will be a predominant mode next to $K^0 \to \pi^+ + \pi^-$ (and probably $K^0 \to \pi^0 + \pi^0$) if it does occur. So it would be possible to settle the question of the existence of this decay. This is important because of the following conclusions.

(a) If the K-meson has *spin zero* and if the mode of decay $K^0 \to 2\nu$ is confirmed, in the two-component theory of the neutrino this *unequivocally* means that the tentative conservation law of fermion numbers is violated.

(b) If the conservation law of fermion numbers is true, we need not introduce any new selection rule for the spin-zero K-meson, to forbid the $K^0 \to 2\nu$ decay.

These conclusions could also be checked by the analysis of the energy spectrum of the π^+-meson in the $K^+ \to \pi^+ + 2\nu$ decay, because it has a different shape according to the scheme $K^+ \to \pi^+ + \nu + \bar{\nu}$ or $K^+ \to \pi^+ + \bar{\nu} + \bar{\nu}$ (or $\pi^+ + \bar{\nu} + \bar{\nu}$). Thus we may tell whether the conservation of fermion numbers is valid. Unfortunately, there are quite a number of processes in which the K^+-meson gives rise to a single positively charged secondary particle. In the rest-system of the K^+-meson, the kinetic energies of the secondary charged particle are as follows (in the three-body decay cases the maximum values are given):

$K^+ \to \pi^+ + \pi^0$	$E(\pi^+) \approx 108.5$ MeV
$K^+ \to \mu^+ + \nu$	$E(\mu^+) \approx 152$ MeV
$K^+ \to \pi^+ + \pi^0 + \pi^0$	$E_{\max}(\pi^+) \approx 53$ MeV
$K^+ \to \mu^+ + \nu + \pi^0$	$E_{\max}(\mu^+) \approx 133$ MeV
$K^+ \to e^+ + \nu + \pi^0$	$E_{\max}(e^+) \approx 228$ MeV
$K^+ \to \pi^+ + 2\nu$	$E_{\max}(\pi^+) \approx 127$ MeV.

Great care must be taken to separate the last process from the others. Of course, these processes may be identified by tracing through to the secondary π^0, π^+ and μ^+-decays. In the first stage, it might be more feasible to check the possible existence of either the $K^+ \to \pi^+ + \nu + \bar{\nu}$ or $K^+ \to \pi^+ + \nu + \nu$ (or $\pi^+ + \bar{\nu} + \bar{\nu}$) decays by searching for the π^+-mesons with energies corresponding to the maximum probabilities of the above decay modes. These are $E(\pi^+) \approx 127$ MeV for $K^+ \to \pi^+ + \nu + \bar{\nu}$ and $E(\pi^+) \approx 46$ MeV for $K^+ \to \pi^+ + \nu + \nu$ (or $\pi^+ + \bar{\nu} + \bar{\nu}$). The abundance of these modes, $K^+ \to \pi^+ + 2\nu$, would be comparable with that of the $K^+ \to \pi^0 + e^+(\mu^+) + \nu$ decays etc., provided there is no selection rule.

In the energy spectra (5) and (7), the effective coupling constants g and g' are, strictly speaking, not constant and can contain the scalar $p_\alpha q_\alpha = M_K(E+m_\pi)$. However, even if we take into account this fact, the characteristic feature of the energy spectra would not change and would be quite useful to distinguish the two different possibilities. In fact, in the lowest order calculations for the specific models considered in the next section, these statements can be justified.

3. The Primary Weak Interactions

As discussed before, the present complicated situation respecting the weak interactions could possibly be explained in terms of the two simplest classes of primary interactions:

(E) Universal Fermi interaction between four fermions

(F) Universal boson-fermion interaction of the Yukawa type
($\pi \to \mu+\nu$, $K \to \mu+\nu$, hyperon decays etc.).

The orders of magnitude of the coupling constants, $f \approx 10^{-49}$ erg cm^3 for (E) and $g^2/4\pi \approx 10^{-15}$ for (F), are essentially the same. Clearly we cannot explain the whole weak interactions in terms of only class (F) since we have the $\mu \to e+2\nu$ decay. From the standpoint that only these classes of interactions (E) or (F) are primary weak interactions, such decays as $K \to \pi + 2\nu$ will occur by the intermediary of the strong baryon-meson interactions and of the weak interaction (E) or (F).

The coupling constants of (E) and (F) are so small that they cannot appear more than once (see fig. 1 and 2). Thus the two neutrinos under consideration must be emitted from the same weak vertex. This fact was used in 2.2. That is, in fig. 2 the complicated contributions from the intermediate states can be expressed in terms of the energy-momentum vectors of the K-meson and the π-meson only. The weak vertex under consideration has interesting properties. All other vertices must represent strong interactions which conserve the strangeness quantum number. Thus the strangeness quantum number of the baryon-meson part of the weak interactions

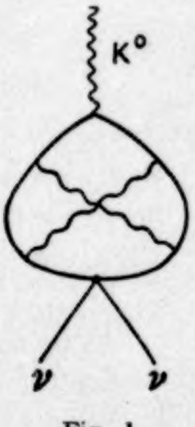

Fig. 1

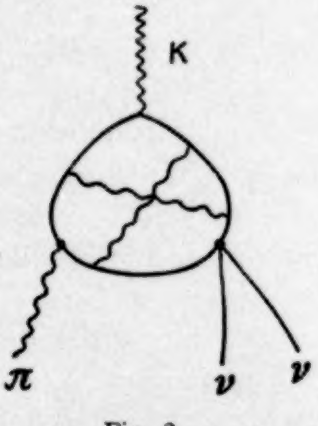

Fig. 2

comprising two neutrinos (figs. 1 and 2) must be the same as that of the decaying K-meson under consideration. Thus the primary weak vertex which is responsible for the decays of K^+ and K^0 (not $\overline{K}^0$) comprising two neutrinos is[†]

for (E):

$$\text{(G)}\quad \begin{array}{l} N+\bar{\Lambda}^0 \to 2\nu, \quad P+\bar{\Sigma}^+ \to 2\nu, \quad N+\bar{\Sigma}^0 \to 2\nu \\ \bar{\Xi}^-+\Sigma^- \to 2\nu \quad \bar{\Xi}^0+\Sigma^0 \to 2\nu; \end{array}$$

for (F):

$$\text{(H)}\quad K^0 \to 2\nu.$$

Thus we get:

(*c*) *If the K-meson has spin zero and if the tentative conservation law of fermion numbers is true* we cannot construct the elementary interaction (H). So the class of interactions (F) cannot contribute to the decay $K^+ \to \pi^+ + \nu + \bar{\nu}$. Thus if we have no (G)-type interactions, $K^+ \to \pi^+ + \nu + \bar{\nu}$ would not occur under the above assumptions.

On the contrary for K-mesons of higher spin, or under violation of the conservation law of fermion numbers, both (G) and (H) may contribute to the processes under consideration. The simplest intermediations are, for example,

$$K^0 \to P+\bar{\Sigma}^+ \to 2\nu, \; K^+ \to P+\bar{\Sigma}^0 \to N+\pi^+ +\bar{\Sigma}^0 \to \pi^+ + 2\nu$$
$$K^+ \to K^0 + \pi^+ \to \pi^+ + 2\nu \text{ etc.}$$

(d) *If the K-meson has spin zero and if the conservation of fermion numbers is valid* (the $K^0 \to 2\nu$ decay is forbidden), and if further $K^+ \to \pi^+ + \nu + \bar{\nu}$ is confirmed by the experiments on the energy spectrum of the secondary π^+-meson, we shall have a definite proof that Fermi-type interactions[††] (G) are only responsible for this process, provided the two-component theory of the neutrino and our standpoint concerning the primary weak interactions (E) and (F) are true.

This again leads to the alternative hyperon decays into two neutrinos by the universal Fermi interaction (G). The life-time of, e.g., $\Sigma^+ \to P + \nu + \bar{\nu}$ would be of the order 10^{-8} sec, which could not be excluded by the present experimental evidence. The energy spectrum of the secondary proton would also give interesting information on the two-component theory of the neutrino and the conservation law of fermion numbers.

[†] The description in terms of (K_1^0, K_2^0) instead of $(K^0, \overline{K}^0)$ give the same conclusion as regards the $K^0 \to 2\nu$ decay.

[††] The same type of argument can also be applied to other K-meson decays comprising leptons. For instance, if $K^+ \to \pi^+ + \pi^+ + e^- + \gamma$ happens to be observed, this will also lead to the conclusion that the class of interactions (E) such as $N + \bar{\Sigma}^+ \to e^- + \nu$ etc. is contributing whereas the class (F) is not, because the K^- which can contribute to the $e^- + \nu$ decay has a different strangeness quantum number from the K^+. These points will be discussed in a subsequent note.

I would like to express my thanks to Professor L. Rosenfeld for telling me about Landau's and Salam's unpublished work, and also for his helpful discussions. I am indebted to Professor C. N. Yang for sending me his papers before publication. Stimulating discussions on the parity problems with Dr. J. Werle and Dr. M. Umezawa are greatly appreciated. Thanks are also due to tne University of Manchester for the award of an I.C.I. Fellowship.

References

1) T. D. Lee and C. N. Yang, Phys. Rev. **104** (1956) 254
2) C. S. Wu, E. Ambler, R. W. Hayward, D. D. Hoppes and R. P. Hudson, Phys. Rev. **105** (1957) 1413
3) R. L. Garwin, L. M. Lederman and M. Weinrich, Phys. Rev. **105** (1957) 1415
4) L. Landau, Nuclear Physics **3** (1957) 127
5) A. Salam, to be published
6) T. D. Lee and C. N. Yang, Phys. Rev. **105** (1957) 1671

Nuclear Physics **3** (1957) 606—611; *North-Holland Publishing Co., Amsterdam*

SPACE-TIME REFLECTIONS AND ISOBARIC SPIN

J. C. TAYLOR

Imperial College of Science and Technology, London

Received 20 March 1957

Abstract: An 8-component spinor representation of the extended Lorentz group is identified with the proton-neutron doublet. Electromagnetic interactions break invariance under Schwinger time-reversal but not Wigner time-reversal. This is analogous to the way in which weak interactions break parity invariance. A similar representation can be assigned to the Λ-particle, if it is a parity doublet.

1. Introduction

One of the lessons of the recent discovery [1]) that neutrino interactions break parity invariance may be that physicists have not been bold enough in their choice of representations of the extended Lorentz group (i.e., the group including space and time-reflections). There is a certain irreducible representation of the group which, it is suggested, can be identified with the proton-neutron doublet; thus affording the explanation of isobaric spin. The electromagnetic interaction would then break some invariance law — in fact, invariance under time-reversal. But this need no longer disturb us, since it is only analogous to the way neutrino interactions (and probably all weak interactions) break space-reflection invariance.

The analogy between photons and neutrinos goes further. First consider the neutrino. Although it destroys invariance under the usual space-reflection operator, S, invariance under the operation

$$S' = S \times \text{charge conjugation } (C)$$

may well be preserved, as has been noted by Yang and Lee [2]), and by Landau [3]). Whether or not this is actually so will be determined by experiment. In the meantime, we shall assume invariance under S'. The beauty of this, as stressed by Landau [3]), is that there is then a perfectly proper sense in which parity invariance is *not* broken at all. The odd phenomena observed by Wu and Garwin and their collaborators [1]) are then ascribed simply to the fact that no charged particle can be in an eigenstate of the parity operator, S'.

Consider now time-reversal invariance, and the photon. Two distinct time-reversal operators are known, Schwinger time-reversal, which we shall call T, and Wigner time-reversal, T'. Pauli [4]) has studied these two operations, and shown that $T' = T \times C$. There is an obvious parallel with S and S'.

The representation proposed for the nucleon doublet uses a Schwinger-type operator, T. The photon must break invariance under T; but, in analogy with the case of the neutrino, invariance under T' will be preserved.

The unusual representation proposed has $ST = TS$, instead of $ST = -TS$ as is usual for fermions. This is assumed, not only for nucleons, but for all baryons. In this scheme, a place can be found for the Λ-particle as a parity doublet. For the other known baryons and the mesons, one has to resort to a compound model, as suggested for instance by Sakata [5]).

2. Space-Reflection and the 2-Component Neutrino

In this section, the operator S' for the neutrino is described; so that it can later be compared with the time-reversal operators.

The Lagrangian for the 2-component neutrino is [2])

$$\begin{aligned} &i\phi^*\left(\frac{\partial\phi}{\partial t}+\sigma_k\frac{\partial\phi}{\partial x_k}\right)-i\left(\frac{\partial\phi^*}{\partial t}+\frac{\partial\phi^*}{\partial x_k}\sigma_k\right)\phi \\ &-i\left(\frac{\partial\phi}{\partial t}+\frac{\partial\phi}{\partial x_k}\sigma_k{}^{\mathrm{T}}\right)\phi^*+i\phi\left(\frac{\partial\phi^*}{\partial t}+\sigma_k{}^{\mathrm{T}}\frac{\partial\phi^*}{\partial x_k}\right). \end{aligned} \tag{1}$$

(The superscript $^{\mathrm{T}}$ denotes the transposed matrix). This is invariant under the operation

$$S': \qquad t \to t, \qquad x_k \to -x_k, \qquad \phi \to \sigma_2\phi^*,$$

because

$$\sigma_2\sigma_k\sigma_2 = -\sigma_k^{\mathrm{T}}.$$

As explained in the introduction, the usual parity operator, S, for any field apart from the neutrino, can be replaced by $S' = S \times C$; and then it is quite possible that all fields and their interactions are invariant under the operations S'. For the electromagnetic field,

$$S': \qquad A_0 \to -A_0,\ A_k \to A_k,\ F_{ij} \to -F_{ij},\ F_{0k} \to F_{0k}, \tag{2}$$

which is strange looking but quite consistent with Maxwell's equations.

We wish to bring out one other point about the neutrino interactions. Take for instance the muon decay interaction

$$A(\bar{\psi}_\mu\gamma_\alpha\psi_e)(\phi^*\sigma_\alpha\phi)+B(\bar{\psi}_\mu\gamma_\alpha\gamma_5\psi_e)(\phi^*\sigma_\alpha\phi).$$

(Here ϕ is the neutrino field, and $\sigma_0 = 1$.) Recent experiments indicate that $A = B$. If this is so, both the electron and the muon interact with the neutrino via their components

$$(1+\gamma_5)\psi \tag{3}$$

only. By taking a representation in which γ_5 is diagonal, one sees that these are just the two components of ψ which transform the same as ϕ under proper homogeneous Lorentz transformations [†]. We shall want to bear expression (3) in mind when we consider the interaction of photons with nucleons.

3. Time-Reversal

In this section, we review the generally accepted facts about time-reversal. According to Schwinger 6), we should not expect the Lagrangian in quantum field theory to be invariant under time-inversion, but rather

$$T,\ T': \qquad L \to L^{\mathrm{T}}. \tag{4}$$

(Here, the superscript $^{\mathrm{T}}$ denotes the transposed Hilbert-space operator.) This is connected with the fact that the commutation relations change sign under T. Therefore, T is not a unitary operator: in fact, it is anti-unitary in the sense of Wigner 7),

$$\langle A|B\rangle \to \langle B|A\rangle.$$

For a spin $\frac{1}{2}$ field, Schwinger's time-reversal operator is

$$T: \qquad \psi \to V\psi^{\mathrm{T}}, \tag{5}$$

where

$$V^*V = 1, \qquad V^{-1}\gamma_0 V = -\gamma_0, \qquad V^{-1}\gamma_i V = \gamma_i. \tag{6}$$

T produces the transformation (4), provided that the Lagrangian is antisymmetrised in the usual way (like the Lagrangian in (1)).

An alternative time-reversal, and historically the oldest, is Wigner's

$$T': \qquad \psi \to W^*\psi^{*\mathrm{T}}, \qquad \psi^* \to \psi^{\mathrm{T}} W, \tag{7}$$

where

$$W^*W = 1, \qquad W\gamma_0 W^{-1} = \gamma_0^{*\mathrm{T}}, \qquad W\gamma_i W^{-1} = -\gamma_i^{*\mathrm{T}}. \tag{8}$$

The notation is that $*$ denotes the Hermitian conjugate, $^{\mathrm{T}}$ denotes the transpose of a γ-matrix, and the transpose in Hilbert-space of a field operator (i.e. it has nothing to do with its spinor suffix). The γ-matrices satisfy $\gamma_0^2 = 1$, $\gamma_1^2 = \gamma_2^2 = \gamma_3^2 = -1$. T′ also produces the transformation (3). According to Pauli, $T' = TC$; and so T and T' are related in the same way as S and S'.

The ordinary parity operator will also be wanted:

$$S: \qquad \psi \to U\psi, \tag{9}$$

where

$$U^*U = 1, \qquad U^{-1}\gamma_0 U = \gamma_0, \qquad U^{-1}\gamma_i U = -\gamma_i. \tag{10}$$

The important properties of S, T and T' are

$$ST = -TS, \tag{11}$$

[†] This hypothesis implies that β-decay goes through a mixture of scalar, tensor and pseudoscalar couplings only.

$$T'^2 = -1, \qquad (ST')^2 = -1. \tag{12}$$

To prove (11), note that equations (6) and (10) determine the commutation relations of U and V with every element of the Dirac algebra, and therefore with each other. A particular choice is $U = \gamma_0, V = \gamma_0\gamma_5$, for which $UV = -VU$; and this equation is therefore true generally. For equation (12), observe that, under T'^2, $\psi \to W^* W^T \psi$. But $W^* W^T$ is invariant under a unitary transformation of the γ-matrices, and can be shown to be -1 in a particular representation. Thus the first of equation (12) is verified. The proof of the second is similar. The vital point about (12) is that the value of T'^2 is unaltered on multiplying W by a phase factor. The commutation relation between S and T', on the other hand, is altered by a phase factor in S.

Finally, we put on record that the neutrino, with the Lagrangian (1), has no operator T, but does have a T',

$$T': \qquad \phi \to \sigma_2 \phi^{*T}.$$

4. The Unusual Representations

Consider a spinor field for which the reflection operators satisfy

$$ST = TS, \qquad S^2 = 1, \qquad T^2 = -1. \tag{13}$$

According to (11), no 4-component spinor has these properties. But (13) may be satisfied with an 8-component spinor, χ and

$$\begin{aligned} S: &\qquad \chi \to \tau_3 \gamma_0 \chi, \\ T: &\qquad \chi \to \tau_2 \gamma_0 \gamma_5 \chi^T, \end{aligned} \tag{14}$$

Here the τ's are a new set of Pauli matrices.

The representation defined by (13) and (14) is irreducible in the following sense. In a spinor representation of the *homogeneous* Lorentz group, $ST = \pm TS$ and the only irreducible representation with $ST = TS$ has $S = T$ [8]). When $S = T$, however, it is impossible to construct an invariant equation of motion for a spinor particle with mass. It is assumed, therefore, that, for the *inhomogeneous* group, (14) defines an irreducible representation, at least when the mass is non-zero. A more rigorous discussion of this point would require a proper account of the place of representation of the extended inhomogeneous Lorentz group in quantum field theory. So far as I know, this has never been undertaken.

Accepting, then, the representation (13), the Lagrangian for χ must be invariant under S and T (or rather, must transform according to (4) under T): and so must be invariant under unitary transformations in the τ-space. Thus we identify χ with the proton-neutron field, and τ-space with isobaric spin space.

Suppose the interaction with the electromagnetic field to break invariance under T. The current may then contain τ_3, which is a "pseudo-scalar" for time-reversal. Thus τ_3 is to be identified with the isobaric spin matrix normally denoted by that symbol. In fact, the current is known to contain the combination

$$(1 + \tau_3).$$

We can offer no explanation for this particular combination, but the analogy with (3) may not be accidental. (Remember, γ_5 is a pseudoscalar, just as τ_3 is a time-reversal "pseudo-scalar".)

We now show that time-reversal invariance is restored on passing from T to T'. In fact, if we require, instead of (13),

$$ST' = T'S, \qquad S^2 = 1, \qquad T'^2 = -1, \tag{15}$$

then these equations can be satisfied by an ordinary 4-component spinor; thus,

S: $\quad \psi \to \gamma_0 \psi$,

T': $\quad \psi \to W^* \psi^{*\mathrm{T}}$.

Evidently, then, on replacing T by T', the representation defined by (13) becomes reducible, and the nucleon doublet splits up into two separate particles; and so the electromagnetic interaction no longer breaks any invariance rule. This is analogous to the neutrino interaction, which breaks invariance under S; while the invariance is restored on changing over from S to S'.

According to (14), the proton and neutron have opposite parity. This is no contradiction. We may say either that all charged particles have opposite parity to neutral ones, or that all charged baryons and mesons (apart from the muon) have opposite parity to neutral ones. In either case the parity difference is unobservable.

It would be nice to find representations corresponding to the other known isobaric multiplets. We assume all baryons correspond to representations with $ST = TS$. The Λ is the simplest particle to consider next. According to this scheme, it has to be an 8-component quantity.

We suggest for the Λ-particle a representation in which

$$ST = TS, \qquad S^2 = -1, \qquad T^2 = 1.$$

The S and T operators then differ from (14) by factors of i only. However, if we now change from T to T', we *cannot* in this case find a reducible representation, because of (12). Rather, for

$$ST' = T'S, \qquad S^2 = -1, \qquad T'^2 = 1,$$

we must take

S: $\quad \chi \to i\tau_3\gamma_0\chi$,

T': $\quad \chi \to \tau_2 W^* \chi^{*\mathrm{T}}$.

In this case, therefore, the doublet does not split into two separate particles when T is replaced by T'; and so the electromagnetic field cannot interact with some components and not with others. The particle is a genuine parity doublet, and the degeneracy between its two components is removed only by the weak interactions, which break S as well as T invariance.

Michel [9]) has already suggested that the unusual representations ($T'^2 = 1$, for spinors) of Wigner time-reversal could be used to describe parity doublets.

The remaining baryons and mesons cannot be interpreted as irreducible representations of the extended Lorentz group. Therefore, we suppose that they are compounds of nucleons and Λ-particles, according to the scheme, for example, of Sakata [5]). Consequently, K-mesons and Σ-particles, as well as the Λ-particle, should be parity doublets.

We may summarise our proposals as follows.

Baryons have $ST = TS$;
Photons break T-invariance, but not T'-invariance;
Leptons have $ST = -TS$;
Neutrinos break S-invariance, but not S'-invariance.

This scheme is not claimed to be unique or final. It is also incomplete, in so far as the weak interactions of baryons are not mentioned. It is hoped, however, to indicate how our new knowledge of the neutrino may help us to understand isobaric spin.

I am deeply indebted to Professor Michel and Dr. Shaw for the opportunity to see their unpublished writings [8, 9]); and to Professor Abdus Salam and Dr Shaw for valuable conversations.

References

1) T. Lee and C. Yang, Phys. Rev. **104** (1956) 254
C. Wu *et al.*, Phys. Rev. **105** (1957) 1413
R. Garwin *et al.*, Phys. Rev. **105** (1957) 1415
2) T. Lee and C. Yang, Phys. Rev. **105** (1957) 1671
3) L. Landau, Nuclear Physics **3** (1957) 127
4) W. Pauli, in Niels Bohr and the Development of Physics (Pergamon Press, London, 1955)
5) S. Sakata, Prog. Th. Phys. (to be published)
6) J. Schwinger, Phys. Rev. **82** (1951) 914
7) E. Wigner, Gött. Nachr. (Math. Naturw. Klasse) (1932) 256
8) R. Shaw, Thesis (Cambridge, 1955) (unpublished)
9) L. Michel, Seminar notes (Paris, 1956) (unpublished)

Nuclear Physics **3** (1957) 612—623; *North-Holland Publishing Co., Amsterdam*

SOME REMARKS ON SELF-ACCELERATION AND SIMILAR EFFECTS IN QUANTUM FIELD THEORY

K. WILDERMUTH AND K. BAUMANN

CERN *Theoretical Study Division at the Institute for Theoretical Physics,*
University of Copenhagen

Received 1 February 1957

Abstract: Some examples of the appearance of self-acceleration effects in quantum field theory are examined. As opposed to the situation in classical theory, it turns out that whenever there are self-acceleration solutions, there are no solutions free from self-acceleration. In order to avoid self-acceleration, the structure of the theory has to be changed fundamentally. The principal change consists in the introduction of acausality.

1. Introduction

During the last few years, the physical reasons for the occurrence of electron self-acceleration in electrodynamics have been investigated in a number of papers [1–8]. It turns out that in order to compensate for the infinitely large positive mass of the electromagnetic field for a point electron, a negative mechanical mass of the electron has to be introduced. Thus the electromagnetic radiation force acts as self-accelerating instead of damping force.

In classical theory the runaway-solutions could be excluded by requiring a physically reasonable motion, i.e. a constant velocity, for the particles at infinity, when all interactions between the particles have vanished. In this paper we shall discuss the extent to which these considerations (especially as presented in ref. [8])) must be modified in the quantal treatment.

At the very beginning one statement is possible. In quantum field theory we can never switch off the interaction between the particles and the vacuum fluctuations of the field. Therefore we may suppose that each particle state finally drops into a runaway state. This means, for example, that even free electrons are always self-accelerated [†]. Therefore, in our opinion, quantum electrodynamics in its present form presumably does not contain any reasonable solutions even for free particles.

Similar effects occur in other field theories which we shall briefly discuss after the treatment of quantum electrodynamics.

2. Quantum electrodynamics

2.1. DIAGONALIZATION OF THE HAMILTONIAN

We shall consider a simplified version of quantum electrodynamics which, however, maintains those features of the exact theory essential to the treatment of the self-acceleration. We consider a non-relativistic electron interacting with the dipole part of the electromagnetic field. This is an approximation to reality only for motions of the electron for which the distance of the electron from the origin is small compared to the wavelength of the electromagnetic waves. Therefore our description of the influence of short waves is not in agreement with that of quantum electrodynamics — not even in a qualitative way†. Furthermore we do not consider vacuum polarization effects which also have a strong influence on the short-wave behaviour. Since the influence of the short waves ($\lambda \ll 10^{-11}$ cm) is important for the magnitude of self-acceleration, we cannot expect to attain even approximative quantitative agreement with complete quantum electrodynamics as regards self-acceleration effects. On the other hand, our example has in common with quantum electrodynamics those qualitative features which lead to self-acceleration for a negative mechanical mass of the electron, namely the possibility of emission of an arbitrarily high number of field quanta.

[†] This was already stated by Steinwedel [7]).

The version of quantum electrodynamics we are considering has been applied by van Kampen [9]) to a calculation of light scattering phenomena, and we can use his results. Van Kampen has shown that it is possible to work out the exact solutions in this case. This is of vital importance for our purpose, for it is well known that one cannot get the runaway solutions by an expansion in powers of the coupling constant [7, 8, 10]).

As the detailed calculations can be found in van Kampen's paper, we shall only write down the results which will be used later on. We start from the Hamiltonian ††

$$H = \frac{1}{2m_0}(\mathbf{P} - e\mathbf{A}(\mathbf{R}))^2 + \frac{1}{8\pi}\int (\mathbf{E}^2 + (\mathrm{rot}\,\mathbf{A})^2)\,\mathrm{d}\tau - \mathbf{K}(t)\cdot\mathbf{R} \tag{1}$$

where we have added a position-independent external force term which will be useful for the following physical discussion. **R**, **P**, and m_0 are the position, canonical momentum, and mechanical mass of the electron, **A** the electromagnetic potential, and **E** the electric field strength.

From (1) we have

$$m_0\ddot{\mathbf{R}} = \mathbf{K}(t) + e\mathbf{E} + e[\dot{\mathbf{R}}, \mathrm{rot}\,\mathbf{A}] \tag{2}$$

or in non-relativistic approximation

$$m_0\ddot{\mathbf{R}} = \mathbf{K}(t) + e\mathbf{E}. \tag{2'}$$

Expanding **A** and **E** in dipole waves with amplitudes $\mathbf{q}_n$, $\mathbf{p}_n$ ($\mathbf{p}_n$ canonically conjugate to $\mathbf{q}_n$) we get

† For example, the contribution of short waves to the zero-point oscillations of the electron after quantization is not described correctly.

†† Throughout this work we put $c = \hbar = 1$.

$$H = \frac{1}{2m_0}\mathbf{P}^2 - \frac{1}{m_0}\mathbf{P}\cdot\sum\varepsilon_n\mathbf{q}_n + \frac{1}{2m_0}\left(\sum\varepsilon_n\mathbf{q}_n\right)^2 + \tfrac{1}{2}\sum(\mathbf{p}_n^2+\nu_n^2\mathbf{q}_n^2) - \mathbf{K}(t)\mathbf{R} \tag{3}$$

as an approximation to (1) for small **R**, and

$$m_0\ddot{\mathbf{R}} = \mathbf{K}(t) - \sum\varepsilon_n\dot{\mathbf{q}}_n. \tag{4}$$

By writing

$$\varepsilon_n = \delta_n\nu_n\sqrt{\frac{4e^2}{3L}} \tag{5}$$

(where L is the radius of the normalization sphere) we also include the case of an extended electron; for an extended electron δ_n approaches zero as $n \to \infty$, whereas $\delta_n = 1$ for a point-electron. Eq. (3) represents our final model Hamiltonian, which can be treated exactly.

Now a canonical transformation

$$\begin{aligned} \mathbf{p}_n - \mathbf{K} &= \mathbf{p}'_n, & \mathbf{q}_n &= \mathbf{q}'_n + \frac{\varepsilon_n}{m\nu_n^2}\mathbf{P}', \\ \mathbf{P} &= \mathbf{P}', & \mathbf{R} &= \mathbf{R}' + \sum\frac{\varepsilon_n}{m\nu_n^2}\mathbf{p}'_n, \end{aligned} \tag{6}$$

where

$$m = m_0 + \sum\left(\frac{\varepsilon_n}{\nu_n}\right)^2 \tag{7}$$

is the total classical mass of the electron (without contributions from zero point oscillations), removes the second term in (3), thus decoupling the field and particle variables. By an orthogonal transformation †

$$\mathbf{q}'_n = \sum X_{nl}\mathbf{q}_l'', \qquad \mathbf{p}'_n = \sum X_{nl}\mathbf{p}_l'' \tag{8}$$

the Hamiltonian can be represented as a sum of oscillator terms in these variables:

$$H = \frac{1}{2m}\mathbf{P}'^2 + \tfrac{1}{2}\sum(\mathbf{p}_n''^2 + k_n^2\mathbf{q}_n''^2) - \mathbf{K}\cdot\mathbf{R}' - \tfrac{1}{2}\mathbf{K}^2\sum\frac{\varepsilon_n^2}{m^2\nu_n^2}. \tag{9}$$

According to van Kampen the k_n's are, in the point electron limit, determined by the equation

$$\tan Lk = k/\varkappa, \qquad \varkappa = 3m/2e^2. \tag{10}$$

Since in the transition to the point electron the electromagnetic mass, $\Sigma(\varepsilon_n/\nu_n)^2$, becomes greater than the total mass of the electron, m_0 has to become negative (in the point limit it becomes $-\infty$). Then the quadratic forms in the decoupled field variables in (9) are no longer positive definite.

---

† The X_{nl}'s have been evaluated by van Kampen 9)).

As a consequence of this one k_n^2 becomes negative, i.e. eq. (10) has two imaginary eigenvalues

$$k_0 = \pm i\varkappa. \tag{11}$$

These eigenvalues are responsible for the self-acceleration, as we shall see in a moment. From (9) we have

$$\mathbf{p}_n'' = \dot{\mathbf{q}}_n'', \qquad k_n^2 \mathbf{q}_n'' = -\dot{\mathbf{p}}_n''. \tag{12}$$

The classical solutions of these equations are

$$\mathbf{q}_n'' = \mathbf{a}_n \sin (k_n t + \varphi_n). \tag{13}$$

They describe oscillations of the electron produced by the standing electromagnetic waves.

For $\mathbf{p}_0''$, $\mathbf{p}_0''$ we obtain

$$\mathbf{q}_0'' = \mathbf{a}_0 \, \mathrm{e}^{\pm \varkappa t}, \qquad \mathbf{p}_0'' = \mathbf{b}_0 \, \mathrm{e}^{\pm \varkappa t}. \tag{14}$$

For large t this gives for the undashed coordinates

$$\mathbf{R} \propto \mathrm{e}^{\varkappa t}, \tag{15}$$

which is just the self-acceleration solution. Therefore $\mathbf{q}_0''$, $\mathbf{p}_0''$ describe the action of the self-accelerating radiation force.

2.2. DISCUSSION OF THE STABLE SOLUTIONS OF CLASSICAL THEORY

Now we consider the case where an oscillating external force is slowly switched on and off. The examination of this case yields some insight into the forces acting on the mechanical mass of the electron. First, we can see from it why, in spite of the negative mechanical mass, there are also solutions without self-acceleration in the classical theory of a point electron. Secondly, it shows the essential physical difference with respect to self-acceleration between classical physics and quantum theory.

If there is no radiation field at the beginning, we have in the classical case

$$\mathbf{q}_n''(0) = \mathbf{p}_n''(0) = 0 \tag{16}$$

and therefore by virtue of eq. (12) for arbitrary times t

$$\mathbf{q}_n''(t) = \mathbf{p}_n''(t) = 0. \tag{17}$$

For the self-acceleration-free case we get by eq. (14) analogously to (17) for all t's

$$\mathbf{q}_0''(t) = \mathbf{p}_0''(t) = 0.$$

Using eq. (6) and (8) we get

$$\begin{aligned} m_0 \ddot{\mathbf{R}} &= \mathbf{K}(t) + e\mathbf{E} = \mathbf{K}(t) - \sum \varepsilon_n \dot{\mathbf{q}}_n \\ &= \mathbf{K}(t) - \sum \frac{\varepsilon_n^2}{m \nu_n^2} \mathbf{P}' \\ &= \mathbf{K}(t) \left(1 - \sum \frac{\varepsilon_n^2}{m \nu_n^2}\right) \end{aligned} \tag{19}$$

or by (8)

$$m_0 \ddot{\mathbf{R}} = \mathbf{K}(t) \frac{m_0}{m}. \tag{20}$$

From this we see that the force acting on the mechanical mass of the electron is opposite to the external force for negative m_0 (see also ref. [8])). This means that self-acceleration will take place unless a definite phase relation exists between external force and electrical field strength. This phase relation depends in general on the given initial conditions, and is essentially determined by the electromagnetic proper field of the electron, which has therefore a stabilizing effect †.

Now in quantum theory it is impossible to fulfil such a phase condition. For the uncertainty relation prevents e.g. the electromagnetic vacuum fluctuations from being zero. Therefore in quantum theory one cannot avoid the self-acceleration by choosing appropriate boundary conditions [7]) — not even for free electrons. If we omit the terms responsible for the self-acceleration, as proposed by van Kampen [9]), an essential structural change in the theory is produced. This will be seen later.

2.3. INSTABILITY OF THE SOLUTIONS IN QUANTUM THEORY

Let us consider the oscillations of an electron produced by the electromagnetic vacuum fluctuations. Using (6) and (8) we get

$$\langle(\mathbf{R}-\mathbf{R}')^2\rangle = \sum \left(\frac{\varepsilon_l}{m v_l^2}\right)^2 \langle \mathbf{p}_l'^2\rangle = \sum_{l=0}^{\infty} B_l^2 \langle \mathbf{p}_l''^2\rangle, \tag{21}$$

where [9]) ††

$$B_l^2 = \frac{2e^2}{3m^2} \frac{2\cos^2\eta_l}{k_l^2 L} \tag{22}$$

and

$$B_0^2 = \frac{2}{m}\left(\frac{2e^2}{3m}\right)^2. \tag{22a}$$

The contributions (22) to $\langle(\mathbf{R}-\mathbf{R}')^2\rangle$ yield a spreading of the electron position of the order 10^{-10} cm ††† if the infra-red divergence is cut off, e.g.

---

† Of course this difficulty does not appear for positive m_0. In this case we get damped oscillations, until the stationary phase relation between external force and electron motion has been reached.

†† The $\cos\eta_l$ approach zero for $l \to \infty$ (even for a point-electron) thus effecting convergence for high momenta. The reason is that the electromagnetic field has to accelerate an infinitely heavy mechanical mass in the point-electron case. If one does not bear in mind the proper field of the electron (that is, if one puts $m = m_0$) one gets $\cos\eta_l = 1$, and (21) does not converge for high momenta.

††† As it is well known, this is reduced to 10^{-11} cm by considering relativistic effects.

by binding the electron to a nucleus. As a time measure for the destruction of the initial state we may consider the time which passes, until the self-acceleration oscillator has also produced a smearing of the order 10^{-10} cm.

Let us choose a representation which is diagonal in the q'' so that p'' equals $-i\partial/\partial q''$. Then we get the following Schrödinger equation for the self-acceleration oscillator with imaginary frequency †:

$$H_s\psi = \tfrac{1}{2}(p_0{}^2-\varkappa^2 q_0{}^2)\psi = -\tfrac{1}{2}\left(\frac{\partial^2}{\partial q_0{}^2}+\varkappa^2 q_0{}^2\right)\psi = E\psi. \tag{23}$$

Here we have restricted ourselves to one dimension for simplicity. The potential is not increasing, but decreasing with increasing q_0 (repulsive potential). Therefore (23) has a continuous eigenvalue spectrum $-\infty<E<\infty$. The eigenfunctions are the parabolic cylinder functions (see also Steinwedel [7])). As they are not very handy, we shall use WKB-solutions instead of them. It is easy to show that they coincide with the exact solutions for $|q_0| \to \infty$. For $E > 0$ they are

$$\psi_E(q_0,t) = \left(\frac{E}{\varkappa}\right)^{\frac{1}{4}}\left(\tfrac{1}{2}\varkappa q_0{}^2+\frac{E}{\varkappa}\right)^{-\frac{1}{4}} \\ \times \mathrm{e}^{\pm i\frac{E}{\varkappa}\left[\frac{1}{\sqrt{2}}\frac{\varkappa q_0}{\sqrt{E}}\sqrt{1+\frac{\varkappa^2 q_0{}^2}{2E}}+\ln\left(\frac{1}{\sqrt{2}}\frac{\varkappa q_0}{\sqrt{E}}+\sqrt{1+\frac{\varkappa^2 q_0{}^2}{2E}}\right)\right]}\,\mathrm{e}^{-iEt}. \tag{24}$$

The plus sign in the exponent describes a wave running in the positive q_0 direction, the minus sign one in the negative q_0 direction. As is well known the WKB-solutions are valid as long as the change in wavelength is small compared with the relative change in potential energy, which means $E/\varkappa \gg 1$ in our case.

By superposition of functions (24) we can describe a wave-packet concentrated round the origin with a half-width b at time $t = 0$, and running in the positive q_0 direction with a momentum K. For $q_0 \to \infty$ the shape of such a packet is

$$\psi(q_0,t)\sim\frac{q_0{}^{-\frac{1}{2}}\,\mathrm{e}^{\frac{i}{2}\varkappa q_0{}^2}\,\mathrm{e}^{i\frac{K^2}{2\varkappa}\left(\ln\frac{2\varkappa q_0}{K}-\varkappa t\right)}}{\left[\frac{\varkappa}{b}-i\left(\ln\frac{2\varkappa q_0}{K}-\varkappa t-1\right)\right]^{\frac{1}{2}}}\ \exp\left\{\frac{-\frac{K^2}{2\varkappa}\left(\ln\frac{2\varkappa q_0}{K}-\varkappa t\right)^2}{\frac{\varkappa}{b}-i\left(\ln\frac{2\varkappa q_0}{K}\varkappa t-1\right)}\right\}. \tag{25}$$

This has a maximum for

---

† Observe that H_s is hermitian, that is, p_0 and q_0 are hermitian operators.

$$q_0 = \frac{K}{2\varkappa} e^{\varkappa t}, \tag{26}$$

provided $K^2/\varkappa \gg 1$, where K^2 is approximately twice the energy of the wave packet. Therefore (25) is a wave packet with its centre moving according to eq. (26). On the other hand, (26) represents the classical solution describing a particle (in q_0 space) starting at $t = 0$ with a momentum K at the origin. Therefore (25) has a reasonable behaviour according to the correspondence principle.

Because of this we calculate approximately the time t_z for which $B_0^2\langle p_0''^2\rangle \approx (10^{-10}\text{ cm})^2$ by describing q_0 and p_0 classically, taking account of the uncertainty principle by choosing $p_0''\, q_0'' = 1$ for $t = 0$.

From (14) we have

$$\begin{aligned} q_0'' &= a_0\, e^{\varkappa t} + b_0\, e^{-\varkappa t}, \\ p_0'' &= \varkappa(a_0\, e^{\varkappa t} - b_0\, e^{-\varkappa t}). \end{aligned} \tag{27}$$

Thus for $t = 0$,

$$\varkappa(a_0^2 - b_0^2) = 1. \tag{28}$$

For large t, that is $\varkappa t \gg 1$, the negative exponent terms can be neglected. In order to keep $q_0''(t)$ and $p_0''(t)$ as small as possible for $\varkappa t \gg 1$ we have to choose $b_0 = 0$. For in this case a_0^2 takes on its minimum value. Then

$$\langle(\mathbf{R}-\mathbf{R}')^2\rangle_s \equiv B_0^2 p_0^2 \approx 3\frac{2}{m}\,\frac{2e^2}{3m}\, e^{\frac{3m}{e^2}t}. \tag{29}$$

This is equal to $(10^{-10}\text{ cm})^2$ for $t_z \approx 10^{-23}$ sec; the value $(10^{-8}\text{ cm})^2$ corresponds to $t_z \approx 10^{-22}$ sec. Thus t_z is much shorter than the characteristic t's of quantum electrodynamic processes (10^{-8} to 10^{-15} sec.) Therefore in our theory any electronic state would be destroyed immediately by self-acceleration.[†]

Of course the quantitative results will be changed strongly in the complete quantum electrodynamics,[††] but the qualitative situation should remain unchanged. This means that also in the framework of this theory there will be no stable electron state provided $m_0 < 0$.

We shall briefly discuss the wave function of a self-acceleration state. For simplicity we consider the case of an electron coupled to only one oscillator, and restrict ourselves to one coordinate. The generalization to many oscillators and to three dimensions is straightforward.

The Hamiltonian is now

[†] In our considerations for $t = 0$ the momentum $p_0 = a_0\varkappa = \sqrt{\varkappa}$ is not large compared with $\sqrt{\varkappa}$ (eq. 26)); consequently there is no pronounced correspondence between the classical and the quantal picture. However, an exact treatment should not change the order of magnitude of t_z.

[††] E.g., the electron-velocity cannot be greater than c. Thus the electron needs at least 0.3×10^{-20} (0.3×10^{-18}) sec for passing 10^{-10} (10^{-8}) cm. Already at $t = 0$ we have $B_0 p_0 > c$.

$$H = \frac{1}{2m} P^2 + \frac{1}{2m_0} (\varepsilon q')^2 + \tfrac{1}{2}(p'^2 + \nu^2 q'^2), \qquad m = m_0 + (\varepsilon/\nu)^2. \tag{30}$$

Self-acceleration takes place only if $(\varepsilon/\nu)^2 > m$. It is useful to choose a representation diagonal in p'. Then the Schrödinger-equation is

$$\left\{\frac{1}{2m} P^2 + \frac{1}{2} \frac{\nu^2 m}{m_0} \left(- \frac{\partial}{\partial p'^2} + \frac{m_0}{\nu^2 m} p'^2 \right)\right\} \psi = E\psi. \tag{31}$$

Here the variables are already separated so that $p' = p'' = p$ and $q' = q'' = q$, and we have for $p' \to \infty$

$$\psi \sim e^{iP'R'}\, p^{-\frac{1}{2}}\, e^{\frac{i}{2}\frac{p^2}{\varkappa'}}\, e^{\frac{i}{2}\varkappa' \xi^2 \left(\ln \frac{2\xi p}{\varkappa'} - \varkappa' t\right)} \times \left[\frac{1}{\varkappa' b} - i\left(\ln \frac{2p}{\varkappa' \xi} - \varkappa' t - 1\right)\right]^{-\frac{1}{2}} \exp \left\{ \frac{-\frac{1}{2}\varkappa' \xi^2 \left(\ln \frac{2p}{\varkappa'\xi} - \varkappa' t\right)^2}{\frac{1}{\varkappa' b} - i\left(\ln \frac{2p}{\varkappa'\xi} - \varkappa' t - 1\right)} \right\}, \qquad \varkappa' = (\nu^2 m/m_0)^{\frac{1}{2}}, \tag{32}$$

where ξ is the initial position in q'-space of the centre of the wave packet, and b the initial width in p'-space. (32) is expressed in the electron coordinate space by writing

$$R' = R - \frac{\varepsilon}{m\nu^2} p. \tag{33}$$

Using (32), (33) we may construct a wave packet in R-space. Then only for

$$R \approx \frac{\varepsilon}{m\nu^2} p \tag{34}$$

is there no destructive interference. On the other hand (32) is different from zero only for

$$p \approx \tfrac{1}{2}\varkappa' \xi\, e^{\varkappa' t}. \tag{35}$$

Thus we have the correct correspondence to classical theory with respect to the R-dependence.

With the aid of the wave function (32) one may calculate for large t the time which passes until a new light quantum is emitted. As it should be, the calculation yields an emission probability proportional to exp $(2\varkappa' t)$.

If we have infinitely many radiation oscillators, the self-acceleration solution is multiplied by an infinite number of zero-point oscillations. The coordinates p' and p'' are connected by a rotation. Therefore these more complicated wave functions behave qualitatively like (32), e.g.

$$R \propto e^{\varkappa t}, \quad \varkappa = 3m/2e^2. \tag{36}$$

Also in this case the emission probability for light quanta increases like exp $(2\varkappa t)$.

2.4. CONSEQUENCES OF DROPPING THE RUNAWAY TERM

As pointed out by van Kampen [9]), the self-acceleration phenomena can be avoided by simply omitting the imaginary oscillation term in the Hamiltonian. However, while in classical physics this only corresponds to an omission of the unphysical solutions of our basic equations, it means in quantum theory a change in the basic equations themselves which is a structural change of the theory. Obviously the uncertainty relations, which of course also hold for the self-acceleration variables, would prevent us from constructing states ψ with $p_0\psi = q_0\psi = 0$ in the unchanged theory.

It can easily be shown that the field operators $\mathbf{A}'$, $\mathbf{E}'$, obtained by dropping the runaway term in the expansion of $\mathbf{A}$ and $\mathbf{E}$, fulfil the commutation relations †

$$\left[A_i'(\mathbf{r}),\ -\frac{1}{4\pi}E_k'(\mathbf{r}')\right] = i\delta_{ik}\delta(\mathbf{r}-\mathbf{r}') \\ -3i\varkappa\, \mathrm{e}^{-\varkappa(r+r')}(\delta_{ik}-\bar{r}_i\bar{r}_k-\bar{r}_i'\bar{r}_k'+\bar{\mathbf{r}}\cdot\bar{\mathbf{r}}'\bar{r}_i\bar{r}_k') \tag{37}$$

where $\bar{\mathbf{r}} = \mathbf{r}/r$, $\bar{\mathbf{r}}' = \mathbf{r}'/r'$.

The commutator is no longer a δ-function, but is spread over an area of 10^{-13} cm. This means that a finite extension is introduced again for the interaction of light-quanta and electron. Therefore the theory is made acausal, i.e. spacelike measurements influence each other if their distance is $\leqq 10^{-13}$ cm.

These results should not change fundamentally in an exact quantum-electrodynamical treatment. The acausality introduced into the theory by dropping the self-acceleration might be of a much smaller range, because according to perturbation theory the electron self-energy diverges only logarithmically with decreasing radius.

The occurrence of self-acceleration can also be interpreted energetically. In quantum electrodynamics one adds a term $-\delta m \int \psi^* \psi \mathrm{d}\tau$. This term compensates the self-energy of the electron and makes its total mass equal to m_e. Now we consider a state in which a superposed electromagnetic field interferes partially destructively with the proper field of the electron — in our example such an interference is effected by the radiation field in the neighbourhood of the self-accelerated electron (cf. ref. [7]) and [8])) if we assume that $\delta m = +\infty$ as is indicated by the first few terms of a perturbation expansion.†† In such a case the expectation value of the energy may become negative. Because of Lorentz invariance there is then no state of lowest energy. Therefore an electron of positive energy will drop into states of lower and lower energy — by emission of light quanta — because the manifold of these states is infinitely greater than that of the physically reasonable states. It is even to be expected that the vacuum will break down by pair emission. As we have seen formerly, one would have to change fundamentally the structure of the theory in order to prevent these effects.

---

† These commutation relations are not translation-invariant. This is connected with the expansion of the quantities round the origin.

†† According to our considerations it is then doubtful whether the δm-term can be calculated exactly instead of by perturbation theory. For in order to define it we have to assume the existence of eigenfunctions of the Hamiltonian corresponding to plane electron waves. But if the energy density is not positive definite, self-acceleration-free states cannot exist. In general, any power series solution of the theory will diverge, if only there are self-acceleration solutions which cannot be expanded in powers of e, as is well known [10]).

It should be noted that the renormalization of mass, as performed in our model theory, is equivalent to a renormalization of the cross-section for the scattering of light by electrons (cf. ref. [9])). Furthermore it may be added that this theory in its exact form (3) or (9) has not any reasonable solutions. However, by neglecting the self-acceleration term in (9), i.e. changing the theory at small distances, one gets excellent agreement with experience e.g. for light scattering. This throws some light on the question why the exact quantum electrodynamics yields so excellent agreement with experience, in spite of the fact that probably it has no reasonable solutions.

3. Non-relativistic Scalar Meson-theory

Considerations analogous to the preceding ones can be applied to a nucleon coupled to a scalar meson field. In the non-relativistic limit the Hamiltonian is

$$H = \frac{\mathbf{P}^2}{2m_0} + g\varphi(\mathbf{R}) + \frac{1}{8\pi}\int \{\dot{\varphi}^2 + (\mathrm{grad}\,\varphi)^2 + \mu^2\varphi^2\}\,\mathrm{d}\tau \tag{38}$$

in standard notation. The operator (38) was diagonalized by McVoy and Steinwedel [11]). Also in this case the inertia of the static field is positively infinite, so that again the mechanical mass has to equal to $-\infty$, i.e. the energy density of the matter field becomes negative. Thus we get self-acceleration. Omission of the self-acceleration terms again yields non-local commutation relations †

$$[\varphi(\mathbf{r}),\ \dot{\varphi}(\mathbf{r}')/4\pi] \rightarrow i\delta(\mathbf{r}-\mathbf{r}') + i\mu_0(r')\{4\pi\mathbf{h}(\mathbf{r}) \cdot \int \mathbf{h}v_0\,\mathrm{d}\tau - v_0(\mathbf{r})\}, \tag{39}$$

where [11])

$$u_0(r) = \frac{\sqrt{6}}{4\pi}\left(\frac{\mu+\varkappa}{2\mu^2-\varkappa(\varkappa+\mu)}\right)^{\frac{1}{2}} \mathbf{e}\cdot\mathrm{grad}\,\frac{\mathrm{e}^{-\varkappa r}}{r},$$

$$v_0(\mathbf{r}) = \sqrt{6}\left(\frac{\mu+\varkappa}{2\mu^2-\varkappa(\varkappa+\mu)}\right)^{\frac{1}{2}} \mathbf{e}\cdot\mathrm{grad}\,\frac{\mathrm{e}^{-\varkappa r}-\mathrm{e}^{-\mu r}}{r},$$

$$\mathbf{h}(\mathbf{r}) = -\frac{g}{4\pi\sqrt{m}}\,\mathrm{grad}\,\frac{\mathrm{e}^{-\mu r}}{r},$$

$$\varkappa = \mu\left(\frac{\alpha}{2} + \sqrt{\alpha + \frac{\alpha^2}{4}}\right), \quad \alpha = \frac{3m}{\mu g^2} + \tfrac{1}{2}.$$

The self-acceleration constant $\varkappa$ is of the order of the mesic mass μ. Therefore eq. (39) are non-local over distances of the order of the range of the nuclear forces. Thus the modification is much more serious than in quantum electrodynamics, and meson-theory is not even approximately a local theory after omitting the self-accelerating features. The nucleon gets an extension of the order of the range of the nuclear forces.

---

† The commutation relations (39) are not translation-invariant for the same reason as in the case of the relations (37).

Again the transition to the relativistic treatment will change the results quantitatively but not qualitatively.

Finally we mention briefly the meson pair theory of Wentzel 12), which was much discussed recently 13, 14, 15). Here the scattering of a meson by an infinitely heavy nucleus is considered. The interaction has the form 15),

$$H_{\mathscr{I}} = g\int \mathrm{d}\tau \mathrm{d}\tau' U(r)\phi(r)U(r')\phi(r');$$

$\phi(\mathbf{r})$ is a scalar meson field, $U(\mathbf{r})$ is a smearing function describing the non-local interaction between nucleus and meson field. In the limit of a point interaction g has to become negative (attractive potential) in order to yield a non-zero cross section. As a consequence of this negative interaction energy mesons are emitted permanently. Simultaneously the meson density at the origin increases exponentially. This produces an increasing negative interaction energy so that energy is conserved. Because of the mesic vacuum-fluctuations this effect cannot be prevented in quantum-theory without reintroducing an extended interaction. The role of the negative mechanical mass of the previous examples is here taken over by the negative interaction energy. The quantitative treatment is completely analogous to that of the previous examples.

4. Final Remarks

Our considerations indicate that field theories get unphysical features as soon as the Hamiltonian becomes indefinite as a consequence of renormalization.† Then the Hamiltonian gets negative eigenvalues. These eigenvalues have no lower limit for invariance reasons. In this case self-acceleration and related effects appear.††

Furthermore it has turned out that such effects can only be prevented by changing the structure of the theory, and not simply by selecting the physical reasonable solutions by boundary conditions as in classical theory.

We did not discuss the additional difficulties in connection with charge renormalization (indefinite metrics 18)); it is possible 19) that these difficulties do not occur in quantum electrodynamics.

Finally we want to mention a point of view which in some respect also covers the theories with indefinite metrics (Lee's model). All the theories we considered, as well as Lee's model, have one point in common: If we fix the constants of the theories (for instance rest mass, coupling constant) and then make the transition from interactions of finite range to point-interactions, the cross sections tend to zero[9, 11, 18]). In order to get formally finite cross sections, the constants of the theories have to be changed in a way which brings in unphysical features. In the case of quantum electrodynamics and scalar meson theory infinite negative mechanical masses have to be introduced, in meson pair theory a negative interaction, and in Lee's model [18]) an imaginary coupling constant.

---

† This probably always happens when the mass has to be renormalized by an infinite amount because negatively infinite energies have to be introduced to compensate for the positively infinite energies and vice versa, as discussed in section 2.

†† From a physical point of view the situation is quite similar to that in the linear integral equation theories of Bopp 16) and Stueckelberg 17). There the singularities are also removed by introducing compensating negative energy densities.

The authors want to thank Professor Niels Bohr for his hospitality and Professor Møller, Dr. Källén, and Professor Wightman for criticism of the manuscript and discussions during the development of this work.

References

1) W. Wessel, Z. f. Physik **110** (1938) 625; Ann. Phys. **43** (1943) 565
2) F. Bopp, Ann. Phys. **42** (1942) 573; Z. Naturforsch. **1** (1946) 53
3) D. Bohm and M. Weinstein, Phys. Rev. **74** (1948) 1789
4) H. McManus, Proc. Roy. Soc. A **195** (1948) 323
5) C. J. Eliezer, Rev. Mod. Phys. **19** (1947) 147
6) G. Morpurgo, Nuovo Cimento **9** (1952) 808
7) H. Steinwedel, Fortschr. Physik **1** (1953) 7
8) K. Wildermuth, Z. Naturforsch. **10a** (1955) 450
9) N. G. van Kampen, Mat. Fys. Medd. Dan. Vid. Selsk. **26** (1951) no. 15
10) H. J. Bhabha, Phys. Rev. **70** (1946) 759
11) K. McVoy and H. Steinwedel, Nuclear Physics **1** (1956) 164
12) G. Wentzel, Helv. Phys. Acta **15** (1942) 111
13) G. Morpurgo and B. F. Touschek, Nuovo Cimento **10** (1953) 1681
14) W. Thirring, Helv. Phys. Acta **28** (1955) 344
15) E. Arnous, Journ. Phys. Rad. **17** (1956) 107
16) F. Bopp, Ann. Phys. **42** (1942) 573
17) E. C. G. Stueckelberg, Helv. Phys. Acta **17** (1944) 3
18) G. Källén and W. Pauli, Mat. Fys. Medd. Dan. Vid. Selsk **30** (1955) no. 7
19) G. Källén, Some remarks on the so-called "ghost states" in field theory, unpublished

BOOK REVIEWS

H. Kopfermann, *Kernmomente*, Zweite neubearbeitete und erweiterte Auflage (Akademische Verlagsgesellschaft, Frankfurt am Main. 1956. xvi-462 pages. 54 DM)

The development of radio-wave and microwave methods with their many ingenious variations has changed the face of high-resolution spectroscopy. The second edition of Prof. Kopfermann's well-known monograph is practically a new book, which will worthily take the place of its predecessor. Nobody will object to the author's decision to retain in this edition the full treatment of optical techniques of hyperfine structure which formed the backbone of the previous one: it would be difficult to surpass the excellence of this presentation, which bears the mark of the master. The same qualities distinguish the treatment of the new methods: the essential ideas are introduced in a simple and elegant manner, by appealing to the correspondence between quantal and classical features; this allows the reader to get a thorough grasp of the essentials without being hampered by technical complications and yet without sacrificing in any way the accuracy of the physical description; and the rigorous quantal calculations which follow are made much more transparent by the preliminary correspondence treatment. From the methodical point of view, we find here a striking illustration of the fundamental significance — too often underestimated by writers of textbooks on quantum mechanics — of the correspondence argument.

The problem of the arrangement of such a varied and abundant subject matter has received a solution which is perhaps not absolutely perfect, but certainly very ingenious: the methods are classified according to the state of aggregation in which the investigated substances are taken: free atoms, molecules, liquids or solids. In this frame, all theoretical and experimental aspects of the vast field of research find their place rather neatly in well-ordered succession. The book — besides being the indispensable *vade-mecum* of the specialist — thus acquires enhanced value as a systematic guide for advanced research students.

The last part of Prof. Kopfermann's treatise is devoted to a discussion of the empirical material on the basis of the current models of nuclear structure. This is perhaps not as authoritative, nor as complete, as the rest, but it gives at any rate a very clear and up-to-date account of the various aspects of the question, in which even the specialist will find something to learn.

The lengthy list of misprints at the end is probably more indicative of care than of negligence; there are, however, some (trivial) misprints which are not listed: the name of Zeeman, for instance, is on some pages capriciously supplied with a superfluous 'n'. It is desirable that the German publishers should respect *all* the recommendations of the International Union of Physics concerning symbols and units (see this journal **1** (1956) 539): in particular, when dealing with vectors, they ought to discard those clumsy arrows and brackets and go over to the Clarendon type and simple product symbols. With the neater typography which would result from the adoption of these recommendations, their standard of production would compare with that of the best American publishers.

L. R.

T. G. Cowling, *Magnetohydrodynamics* (Interscience tracts on physics and astronomy, No. 4) (Interscience Publishers Inc., New York. 1957. viii-115 pages. Paper cover $1.75, hard cover $3.50)

This new addition to the 'Interscience tracts' fully upholds the high standard of excellence set by the preceding ones (see this journal **2** (1956/57) 109). Prof. Cowling's masterly exposition of all the aspects of a subject of rapidly increasing importance everywhere brings out the essential points; and he does not miss either the numerous opportunities which the subject offers of exercising his renowned (and sometimes redoubted) critical acumen. Besides the main applications to astrophysics and geomagnetism, the few relevant laboratory experiments up to 1955 are described and illustrated; it was too late to include the latest developments, which open such exciting prospects: but as a basis for the study and furtherance of this new line of investigation, the present booklet appears at the right moment. It should be a best-seller.

L. R.

APPEAL TO CONTRIBUTORS

Among the factors delaying the appearence of a paper, the most serious is the unsatisfactory presentation of the typescript. An appeal is made to contributors to follow the simple rules and conventions laid down in the instruction sheet which has already been widely distributed and copies of which are available on request from the publishers or the members of the Editorial Board. Attention is called in particular to the writing of formulae. Authors are especially requested *not* to typewrite formulae, but to write them in long hand, very carefully, since the compositor cannot guess the meaning of a symbol which is not legible. In future, the Editor will be forced to return unsatisfactory typescripts to the authors for the necessary material improvements.

It frequently happens that after a paper has been communicated, the author sends substantial corrections or alterations. Since the publisher and printer spare no effort to achieve prompt publication, such late alterations often arrive after the paper has already been set, and inflict on them much unnecessary trouble and cost. Contributors should realise that a too hasty writing-up of a paper thus defeats the prospect of a quick publication.

Editor and publisher trust that the authors will not shun the slight trouble which the careful preparation of the typescript entails and thank them in advance for their cooperation.

JUST OUT

QUANTUM MECHANICS

by

H. A. KRAMERS

Late-Professor of Theoretical Physics, University of Leiden
Translated by D. TER HAAR, *Clarendon Laboratory - Oxford*

This book is an English translation of the well-known pre-war monograph on Quantum Theory.
The author was closely connected with Niels Bohr's institute from 1912 until 1926, during which period quantum theory was developed, to a large extent by the Copenhagen school, into essentially its present form. Among Kramers' own contributions to this development one may mention the so-called W-K-B method, the symbolic method for calculating intensities of spectral lines, the derivation of the wave equation for a relativistic electron (independent of and practically simultaneous with Dirac's derivation), and the idea of mass renormalisation. As a consequence, the presentation of quantum theory in the present textbook is more lively and less stereotyped than in most texts on the subject and often sheds light on details which are usually overlooked. Also, there are in this monograph a number of those mathematical gems which were so typical of Kramers.

6×9″, xvi +496 pages

Guilders 45.— (90 s.)

CONTENTS:

I. *Quantum theory of free particles.*
II. *Non relativistic quantum theory of bound particles.*
III. *The non-relativistic treatment of the many-body problem.*
IV. *Transformation theory.*
V. *Perturbation theory.*
VI. *The spinning electron.*
VII. *The exclusion principle.*
VIII. *Electromagnetic radiation.*

Sole distributors for U.S.A.: Interscience Publishers, Inc. - New York
NORTH-HOLLAND PUBLISHING COMPANY-AMSTERDAM
Send your order to your bookseller or directly to the publisher

N·H P·C